The University Of Sheffield.

Evolutionary development of the plant spore and pollen wall

A thesis submitted by

Simon Wallace

for the degree of Doctor of Philosophy

Department of Animal and Plant Sciences

August 2013

Acknowledgements

I am very grateful to my supervisors, Prof. Andrew Fleming, Prof. David Beerling and Prof. Charles Wellman, for their support and encouragement throughout this project.

I would like to express my gratitude to Bob Keen, Heather Walker and Marion Bauch for their invaluable assistance and advice in D59 lab; my postgraduate colleagues, Dr Hoe Han Goh, Dr Xiaojia Yin, Dr Adam Hayes, Dr Chloé Steels, Supatthra Narawatthana, Rachel George, Amin Adik, Dr Jen Sloan, Bobby Caine, Thomas Harcourt, Julia Van Campen, Sam Amsbury, Jenn Dick, Dr Phakpoom Phraprasert, Ross Carter, Dr Kate Allinson, Dr Janine Pendleton, Dr Brian Pedder, Faisal Abuhmida, Doreen Mkuu, Sam Slater, Dr Joe Quirk, Dr Lyla Taylor and Dr Claire Humphreys for their support and banter during my time in Sheffield; and to all my other friends in the Department of Animal and Plant Sciences.

Many thanks also go to Dr Steve Rolfe for offering his expertise and time with regards to microarray analysis; James Mason for his generous help with Raman microspectroscopy; Prof. Mike Burrell for his general laboratory advice and guidance; Dr Steve Ellin for his assistance in preparing palynological samples; Chris Hill and Svet Tzokov for sharing their electron microscopy expertise; and Dr Katie Field and Dr Timmy O'Donoghue and other members of the Beerling lab for their jollity and support.

Special thanks go to Dr Caspar Chater for his unstinting and generous support, advice and friendship. Enormous thanks also go to various collaborators and correspondents; Dr Andrew Cuming, Dr Yasuko Kamisugi, Scott Schuette, Prof. Roy Brown and Prof. Ralf Reski.

I gratefully acknowledge the Natural Environment Research Council (NERC) for funding my PhD studentship. I also would like to acknowledge my undergraduate tutors, Dr Richard Lindsay and Dr John Rostron whose love of the natural world assured me that quitting a career in insurance to enrol at university was a good decision.

Finally, I would like to dedicate this thesis to my parents who I am very lucky to have in my life.

Abstract

The origin of land plants required aquatic green algal ancestors to evolve a number of key adaptations that enabled them to overcome physiological difficulties associated with survival in the harsh subaerial environment. One of these key adaptations was the development of a durable spore wall structure, containing a sporopolleninous exine layer, to withstand attrition, desiccation and exposure to UV-B radiation. All land plants (embryophytes) possess such walled spores (or their homologue pollen). However, the spore/pollen wall became more complicated over time, via a series of additional developmental steps, as it began to serve an increasing number of functions.

A significant amount of study has been conducted with regards to the molecular genetics of pollen wall development in the angiosperm, *Arabidopsis thaliana* (L.), particularly with respect to the exine layer and sporopollenin biosynthesis. However, research into the molecular genetics of spore wall development in basal plants has thus far been extremely limited. In this thesis, the results of a fully replicated microarray analysis at early and mid stages of sporogenesis in the free-sporing model moss *Physcomitrella patens*, have allowed up and down regulated genes to be compared with those known to be involved in pollen wall development, therefore facilitating the identification of candidate genes likely to be involved in the development of the spore wall. Additionally, by way of a gene knock-out experiment with *P. patens*, this study demonstrates that the *MALE STERILITY 2* (*MS2*) gene, which is involved in wall development in the pollen of *A. thaliana*, is highly conserved and has a similar function in *P. patens*. However, the moss homologue of *MS2* is shown to be unable to recover functionality in *A. thaliana* indicating that the *MS2* gene, although conserved, has evolved in angiosperms as their pollen walls have increased in complexity.

Portions of this thesis have been published in peer-reviewed journals. The references for these publications are as follows:

Wallace S, Fleming A, Wellman CH, Beerling DJ. 2011. Evolutionary development of the plant spore and pollen wall. *AoB Plants*, plr027 doi:10.1093/aobpla/plr027.

O'Donoghue M, Chater C, Wallace S, Gray JE, Beerling DJ, Fleming AJ. 2013. Genome-wide transcriptomic analysis of the sporophyte of the moss *Physcomitrella patens*. *Journal of Experimental Botany*, **64(12):** 3567-3581.

Contents

List of figures

Page

Chapter 4

Chapter 5

List of tables

Page

Chapter 5

List of appendices

Page

List of abbreviations/acronyms

ATP	Adenosine-5'-triphosphate
BDMA	Benzyldimethylamine
BSA	Bovine serum albumin
CaMV	Cauliflower mosaic virus
cDNA	Complementary deoxyribonucleic acid
CDS	Coding DNA sequence
CIAP	Calf intestinal alkaline phosphatase
cm	Centimetre
Col-3	Columbia-3
CTAB	Cetyltrimethyl ammonium bromide
DIG	Digoxigenin
DNA	Deoxyribonucleic acid
dNTP	Deoxynucleotide Triphosphate
EDTA	Ethylenediaminetetraacetic acid
EST	Expressed sequence tag
FP	Forward primer
FT-IR	Fourier transform infrared spectroscopy
g	Gram
GFP	Green fluorescent protein
GUS	Beta-Glucuronidase
HEPES	4-(2-hydroxyethyl)-1-piperazineethanesulfonic acid
JTT	Jones-Taylor-Thornton
KOD	*Thermococcus kodakaraensis*
Kv	Kilovolt
LB	Luria-Bertani
LOESS	Locally weighted polynomial regression
M	Molar
mg	Milligram
mJ	Millijoules
ml	millilitre
mm	millimetre

mM	Millimolar
M-MLV RT	Moloney murine leukemia virus reverse transcriptase
mRNA	Messenger ribonucleic acid
msec	Millisecond
MUSCLE	Multiple sequence comparison by log-expectation
NJ	Neighbour joining
nM	Nanomolar
PCA	Principle component analysis
PCR	Polymerase chain reaction
PEG	Polyethylene glycol
PHD	Plant homeo domain
PRM-B	Protoplast regeneration medium-bottom layer
PRM-L	Liquid protoplast regeneration medium
PRM-T	protoplast regeneration medium-top layer
RNA	Ribonucleic acid
RNAi	RNA interference
RNase	Ribonuclease
RO	Reverse osmosis
RP	Reverse primer
rpm	Revolutions per minute
RT-PCR	Reverse transcription polymerase chain reaction
SAIL	Syngenta arabidopsis insertion library
SD	Standard deviation
SDS	Sodium dodecyl sulfate
SEM	Scanning electron microscope
SNP	Single nucleotide polymorphism
SOC	Super Optimal broth with Catabolite repression
Sq-RT-PCR	Semi-quantitative reverse transcription polymerase chain reaction
SSC	Saline-sodium citrate
TAE	Tris acetate/EDTA
TAIR	The arabidopsis information resource
TBLASTN	Protein-nucleotide 6-frame translation basic local alignment search tool
T-DNA	Transferred DNA

TE	Tris/EDTA
TEM	Transmission electron microscope
TF	Transcription factor
TGR	Targeted gene replacement
U	Unit
UDP	Uridine diphosphate
UV	Ultraviolet
V	Volt
v/v	Volume to volume
WLCL	White-line-centred-lamellae
w/v	Weight to volume
µF	Microfaraday
µg	Microgram
µl	Microlitre
µM	Micromolar

CHAPTER 1. **General introduction**

1.1 Introduction

The colonisation of land by plants in the Palaeozoic was a highly significant event in Earth's history, both from an evolutionary point of view and because it fundamentally changed the ecology and environment of the planet (Beerling 2007). Land plants evolved to form crucial components of all modern terrestrial ecosystems through evolutionary adaptations involving changes in anatomy, physiology and life cycle (Waters 2003; Menand *et al*. 2007; Cronk 2009). Key adaptations include rooting structures, conducting tissues, cuticle, stomata, and sex organs such as gametangia and spores/pollen.

Development of a durable spore wall is essential for terrestrialisation as it enables the spore to withstand physical abrasion, desiccation and UV-B radiation (Wellman 2004). As part of their life cycle, sexually reproducing embryophytes manufacture either spores, or their more derived homologues pollen. The major component of the spore/pollen wall proposed to be of primary importance in enabling resistance to the conditions described above is the highly resistant biopolymer sporopollenin (Ito *et al*. 2007; Cronk 2009).

It seems reasonable to hypothesize that colonisation of the land by plants was not possible prior to the evolution of the sporopollenin spore wall, and this adaptation is considered to be a synapomorphy of the embryophytes. Additionally, spore walls are not present in the hypothesised embryophyte antecedents, the green algae (Wellman 2004). However, the production of sporopollenin is highly likely to be preadaptive as it is present in a number of different algal groups such as the charophyceans which have been proposed as the sister group to the embryophytes. In certain charophyceans, sporopollenin occurs, but is located in an inner layer of the zygote wall (Graham 1993). Phylogenetic studies and fossil evidence have shown that the most basal living land plants are the paraphyletic 'bryophytes' (Kenrick and Crane 1997; Qiu *et al*. 2006) (Fig. 1.1). They comprise the liverworts, mosses and hornworts, and their phylogenetic position should allow us to further elaborate the evolutionary changes which facilitated the conquest of the land by plants (Rensing *et al*. 2008). The moss *Physcomitrella patens* is the first 'bryophyte' genome to be

sequenced. This genome, through comparisons with angiosperm genomes, is proving to be a valuable tool in experimental studies which attempt to reconstruct genome evolution during the colonisation of land (Reski and Cove 2004; Quatrano *et al*. 2007; Rensing *et al*. 2008).

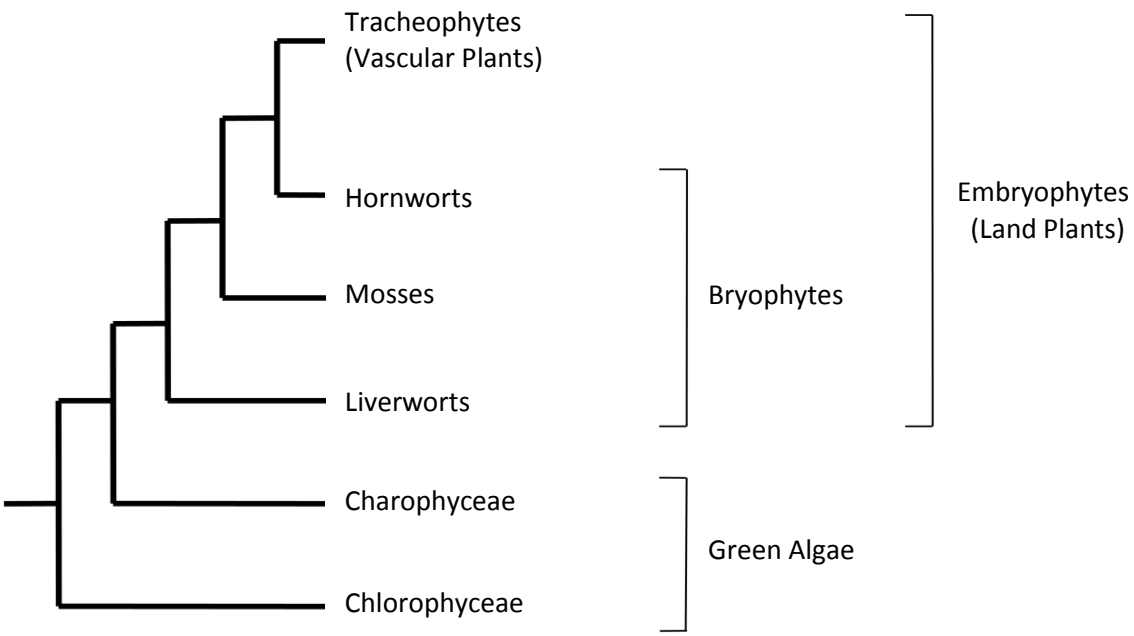

Figure 1.1. Phylogenetic tree for land plant evolution derived from analysis by Qui *et al.* (2006). The bryophytes are a paraphyletic group comprising three separate lineages. Together with the vascular plants (which include the angiosperms), bryophytes form the embryophytes which have a sister group relationship to the green algae.

1.2 Spore/pollen wall structure and development

The spore/pollen walls of embryophytes have multiple layers and components which are laid down in a regulated manner during spore/pollen development. Layers containing the macromolecule sporopollenin, collectively known as the exospore, are the component enabling the resistance of the spore/pollen wall to numerous environmental factors which make life on land challenging. Sporopollenin is highly resistant to physical, chemical and biological degradation procedures. Consequently its precise chemical composition, structure and biosynthetic route has not yet been ascertained (Meuter-Gerhards *et al*. 1999). Traditional convention asserts that sporopollenin is a polymer of carotenoid esters (Cronk 2009). However, modern

purification, degradation and analytical techniques have shown that it is comprised of polyhydroxylated unbranched aliphatic units with small quantities of oxygenated aromatic rings and phenylpropanoids (Ahlers *et al*. 1999; Domínguez *et al*. 1999). The inner intine layer, or endospore, constitutes the non-sporopolleninous component of spore/pollen walls and is associated with polysaccharide metabolism, primarily consisting of cellulose and pectin (Hess 1993; Suárez-Cervera *et al*. 2002). The intine can be subdivided into two commonly inconspicuous layers, the exintine and the endintine.

1.2.1 Sporogenesis

Sporogenesis is the process in which haploid spores are formed from the diploid sporophyte and facilitates the transition from the sporophyte generation to the gametophyte generation (Cronk 2009). The process takes place in sporangia, or microsporangia, where initially central cells develop an archesporial cell identity which is different to that of the cells of the sporangium wall. The archesporial cells give rise to sporogenous cells (spore mother cells or sporocytes) which undergo mitosis. The number of mitotic cell divisions determines the eventual number of sporogenous cells and therefore ultimately the number of spores/pollen grains. After mitosis the sporogenous cells undergo meiotic cell division which produces four distinct haploid cells or microspores, joined together in a tetrad. It is at this tetrad stage where the sporopolleninous layers of the microspore wall begin to develop. The microspores eventually separate and mature to form free spores/pollen grains (Cronk 2009; Hill 1996).

1.2.2 Modes of sporopollenin deposition in spore and pollen walls

The basic mechanisms involved in the formation of the spore wall, and the deposition of sporopollenin in the exospore/exine, have been illuminated by numerous ultrastructural studies performed on extant and fossil species across the plant kingdom (Paxson-Sowders *et al*. 2001). Blackmore and Barnes (1987) proposed a number of sporopollenin deposition processes apparent in the spore wall. Firstly, they recognised the role of white-line-centred-lamellae (WLCL) in this process. The accumulation of sporopollenin on an array of WLCL is regarded as being the most primitive method of sporopollenin deposition and has been identified in a number of algal groups and most, if not all, embryophytes (Wellman 2004). These lamellae

materialise at the plasma membrane with sporopollenin polymerising out onto either side of the white line. They accumulate in a variety of ways to form the spore/pollen wall (Blackmore and Barnes 1987; Blackmore *et al*. 2000; Wellman 2004).

Another mode of exospore/exine formation involves the deposition of sporopollenin from the surrounding cells of the tapetum. Transmission electron microscopy (TEM) has shown that the tapetal cells in many embryophytes possess a highly active secretory system containing lipophilic globules which are thought to contain the precursors of sporopollenin and are deposited onto the surface either directly contributing to the exospore/exine or forming extra-exosporal layers commonly referred to as the perispore, or perine (Piffanelli *et al*. 1998). Blackmore et al. (2000) suggested that a tapetal contribution to the spore wall can take place in a variety of ways including the addition to the layers formed by the WLCL or directly onto WLCL. Studies of pollen wall formation in angiosperms highlight the role that the tapetal cells play in supplying nutrients and lipid components to developing microsporocytes and microspores (Scott *et al*. 1991; Ariizumi *et al*. 2004; de Azevedo Souza *et al*. 2009). Interestingly, the most basal extant land plants (liverworts) lack a tapetum, which is acquired in mosses and vascular plants, where it appears to function much like the anther tapetum in angiosperms, and is primarily associated with perine formation. Therefore, basal land plants which do not possess a tapetum consequently do not develop a perine layer (Blackmore and Barnes 1987; Polevola 2012). Ubisch bodies (or orbicules), small granules of sporopollenin mostly occuring on the innermost walls of secretory tapeta in various land plant groups, have been observed in some bryophytes and lycophytes, and given this, Pacini *et al*. (1985) have proposed that the secretory tapetum is the earliest type.

An alternative deposition process involves centripetal accumulation of sporopollenin onto previously formed layers. Blackmore *et al*. (2000) noted that exospore formation may be achieved by sporopollenin accumulation below a pre-existing layer, either by WLCL accumulation, or by the deposition of granular or unstructured sporopollenin. A further mode of deposition is observed in seed plants where sporopollenin accumulates within a pre-patterned cell surface glycocalyx referred to as the primexine (Blackmore and Barnes 1987; Blackmore *et al*. 2000; Wellman 2004) which is essentially an exine precursor.

1.2.3 Spore wall development in bryophytes

Spore wall development has been studied in all three of the traditional bryophyte groups (reviewed in Brown and Lemmon 1988, 1990). In the majority of liverworts, immediately after meiosis, a polysaccharide wall (the spore special wall) is laid down outside of the plasma membrane (Brown and Lemmon 1985). In many liverworts this spore special wall seems to function as a primexine in which the pattern of exospore ornamentation is established (Brown and Lemmon 1993). However, in some liverworts exospore ornamentation appears to be determined by exospore precursors produced by the diploid sporocyte prior to meiosis and formation of the haploid spores (Brown *et al*. 1986). The exospore develops centripetally (Brown and Lemmon 1993) based on WLCL formed outside of the spore cytoplasm. At completion the entire exospore comprises of sporopollenin deposited on WLCL. At maturity the lamellate structure thus formed is clearly discernible and is highly characteristic of the liverwort exospore. Liverworts lack a tapetum and there is therefore no input from this source. The innermost layer of fibrillar intine is the final wall layer to be formed (Brown and Lemmon 1993).

Studies of spore wall development in hornworts are limited. As with liverworts, a spore special wall is formed after meiosis and functions as a primexine in which the exospore is set down. It was initially thought that the exospore formed in the absence of WLCL, but Taylor and Renzaglia (unpublished) have recently demonstrated their presence (W. A. Taylor, University of Wisconsin-Eau Claire, USA, pers. comm. 2011). Recent analyses of *Phaeomegaceros fimbriatus* has shown that the mature spore wall has a thin perine-like outer layer, but this represents the remnants of the spore mother cell wall rather than extra-exosporal material derived from a tapetum (Villarreal and Renzaglia 2006).

Three types of spore wall have been recognised in mosses: Bryopsida-type; Andreaeidae-type and Sphagnidae-type (Brown and Lemmon 1990). All three of these types appear to form in the absence of a spore special wall (Brown and Lemmon 1980). Bryopsida-type spore walls are homogeneous except for an inconspicuous foundation layer. This foundation layer forms first via sporopollenin accumulation on WLCL. Subsequently the predominantly homogeneous exospore layer is laid down outside of the foundation layer in a centrifugal manner. This layer is thought to be

mostly extrasporal in origin. Sometimes additional homogeneous material is also deposited inside of the foundation layer. This layer is almost certainly derived from the spore. Following the accumulation of the homogeneous material the spores are coated by an additional extra-exosporal layer, the perine, that is derived from the tapetum. Finally the intine forms.

Spore wall development in the Andreaeidae-type is unique amongst mosses in that they have a spongy exospore which appears to forms in the absence of WLCL (Brown and Lemmon 1984). By studying *Andreaea rothii*, Brown and Lemmon (1984) demonstrated that the exospore is instead initiated as discrete homogeneous globules within the coarsely fibrillar network of the spore mother cell. These globules accumulate and form an irregular layer with numerous interstitial spaces. The sequence of spore wall layer development is essentially the same as that of other mosses and the mature wall consists of an inner intine, a spongy exospore and an outer perine (Brown and Lemmon 1984).

Sphagnidae-type moss spore walls are more complex than those of the other mosses and consist of five layers (Brown *et al*. 1982). Unlike other mosses, the exospore of Sphagnidae-type comprises two layers: an inner lamellate layer (A-layer), and a thick homogenous outer layer (B-layer). In addition to the exospore there is an intine, a unique translucent layer and the outermost perine. The A-layer is the first to form and does so by sporopollenin accumulation on WLCL, and develops evenly around the young spore immediately after meiosis. The homogeneous B-layer is deposited outside the A-layer. Overlying the exospore is a translucent layer which consists of unconsolidated exospore lamellae in a medium of unknown composition. The tapetally-derived perine is deposited on top of this unique layer. The study of spore wall development in *Sphagnum lescurii* by Brown *et al*. (1982) suggests that the ontogeny of the wall layers is not strictly centripetal.

1.2.4 Spore wall development in pteridophytes

Spore walls have been investigated in a number of pteridophyte species representing all of the major pteridophyte groups (reviewed in Lugardon 1990 and Tryon and Lugardon 1991).

Spore wall development is well understood in the homosporous lycopsid *Lycopodium clavatum* (Uehara and Kurita 1991). Shortly after meiosis the plasma membrane of the sporogenous cell folds into a pattern that later becomes the reticulate spore sculpture. Small WLCL form on the plasma membrane and accumulate in a centripetal fashion forming the greater part of the exospore. After the main lamellate part of the exospores is formed an inner granular layer, possibly derived from the spore cytoplasm, is deposited. In some *Lycopodium* there are no extra-exosporal layers (Uehara and Kurita 1991) whereas in others a thin extra-exosporal layer is deposited after the completion of the exospore (Tryon and Lugardon 1991).

Spore structure and development in heterosporous lycopsids differs between microspores and megaspores. In the clubmoss *Selaginella*, microspores possess an exospore consisting of two layers (Fig. 1.2). The thin inner layer is the first to develop and comprises imbricate lamellae which are formed on WLCL in a centripetal direction (Tryon and Lugardon 1991). The outer layer starts to form only once the inner layer is complete. Some *Selaginella* species may also develop a thin perispore or a paraexospore. In the microspores of the heterosporous lycopsid *Isoetes japonica* a large gap is developed between the two exospore layers (Uehara *et al*. 1991). The outer exospore layer is regarded as a paraexospore as it begins to form before the inner exospore, consists of similar sporopollenin, and is completed at the same time as the inner exospore.

Selaginella megaspore walls contain two layers of similar thickness (Morbelli, 1995). The inner and outer layers consist of lamellae and poorly segregated components respectively. The inner layer does not thicken during exospore development and a dense basal layer is formed by the lamellae. In contrast, the outer layer increases significantly in thickness due to self assembly (Hemsley *et al*. 1994, 2000; Gabarayeva 2000). During the final stages of sporogenesis the endospore forms between the plasma membrane and the exospore. In *Isoetes* the megaspore wall is similar to that of *Selaginella* in terms of development and structure, consisting of two layers with the formation of the outer layer commencing prior to the inner layer. Substantial quantities of silica are deposited within and on top of the outer layer before the exospore is completed. Finally, the intine is lain down between the plasma membrane and the exospore.

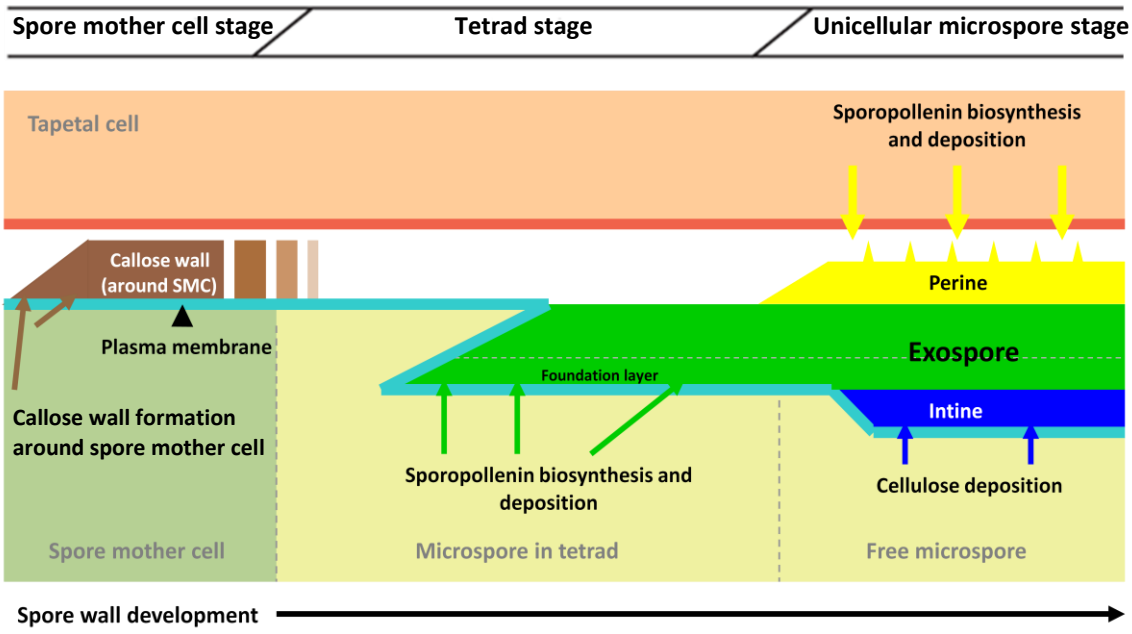

Figure 1.2. Proposed model of spore wall development in *Selaginella* microspores. The thin inner exine layer forms first and comprises lamellae formed centripetally on WLCL. The outer exine starts to form once the inner layer is complete. Note the presence of callose at early developmental stages around the spore mother cell.

The exospore in homosporous ferns develops centrifugally and is once again bilayered. The inner layer acts as a substructure and consists of varying numbers of fused sheets (extensive interconnected laminae) which form by sporopollenin accumulation on WLCL. The homogeneous outer layer is considerably thicker and contains thin radial fissures and small cavities. An extra-exosporal layer (perine) forms once the exospore is complete and is deposited from the decaying tapetum. Spore wall development in heterosporous ferns is similar to that observed in homosporous ferns, and is also similar in both microspores and megaspores.

In Sphenopsids the spore walls appear to be highly derived (Lugardon 1990) and observations of *Equisetum arvense* have shown that four layers are present in the form of an exospore, endospore, middle layer and pseudoelators (Uehara and Kurita 1989). The exospores comprise inner and outer exospores. The broad and homogenous inner exospore forms first by way of plate-like structures accumulating on the plasma membrane. The outer exospore is then formed by the deposition of granular material

on the inner exospore and is similarly wide and homogeneous. Once exospore formation is complete the middle layer forms in the gap between the exospore and the plasma membrane. The pseudoelators are the next structure to form and consist of two layers. The inner of these comprises longitudinal microfibrils during the early stages of development but eventually becomes homogeneous. The outer layer is also homogeneous and is formed by granules which are released from vesicles in the plasmodial cytoplasm. The pseudoelators are connected to the spore, by way of the middle layer, at the aperture. The intine is the final component of the wall to form on the inside of the exospores (Uehara and Kurita 1989; Taylor 1986).

1.2.5 Pollen wall development in gymnosperms

Although differences in pollen wall structure and development are evident in different extant and extinct gymnosperm groups, the main ontogenetic elements appear to be homologous (summarized in Lugardon 1994 and Wellman 2009). The pollen mother cell undergoes meiosis to form four haploid microspores. Subsequent development of the exine consists of a number of stages. Firstly, a callose wall forms around the pollen mother cell and subsequently extends around each of the microspores. Next a matrix develops around each microspore upon which the fibrillar microspore surface coat and later the sexine (the outer pollen exine wall consisting of tectum and infratectum components) pattern is established (Zavada and Gabareyeva 1991). The microspore surface coat is deposited between the surface of the microspore and the surrounding tetrad wall prior to the formation of the wall components. This layer is regarded as being equivalent to the primexine in angiosperms. The sexine then begins to form on and within the microspore surface coat. The nexine (inner pollen exine wall) laminae is then formed below this coat, therefore the sexine is partly developed when the nexine begins to develop. The exine as a whole appears to form in a centripetal direction from the outside inwards (Lugardon 1994). Finally, an intine is deposited on the inside of the pollen exine.

1.2.6 Pollen wall development in angiosperms

Pollen walls in angiosperms typically consist of an outer exine formed of sporopollenin and an inner intine composed of cellulose and pectin (Fig. 1.3) (Paxson-Sowders *et al*., 1997; Morant *et al*. 2007). Models of development have been proposed based on observations on numerous species including *Lilium* and

Arabidopsis thaliana (e.g. Suzuki *et al*. 2008). Similar processes have been described in both of these species.

Once again, prior to meiosis, the pollen mother cell is surrounded by a callose special cell wall (Blackmore *et al*. 2007). Immediately after meiosis four microspores derived from the pollen mother cell form a tetrad. A callose special wall surrounds the microspores (Blackmore *et al*. 2007). A cellulose primexine then forms between the plasma membrane and callose wall of each microspore. Both the callose wall and primexine are deposited at the surface of the microspore through processes mediated by the plasma membrane (Blackmore *et al*. 2007). A section of the primexine is then adapted to form column-like structures called the probaculae upon which sporopollenin, secreted by the microspore, will eventually accumulate and polymerise. Sporopollenin deposition and accumulation extends the probaculae which form the columellae, baculae and tecta (Heslop-Harrison 1963, 1968a). The callose wall then degrades and the developing columellae, baculae and tecta are exposed to the fluid of the locule and receive sporopollenin secreted by the tapetum. Wall formation is complete when the nexine and intine layers are formed and the primexine recedes and disappears (Suzuki *et al*. 2008). The mature pollen grain is then coated by tryphine and pollenkitt which are synthesised by the tapetum (Dickinson and Lewis 1973; Blackmore *et al*. 2007).

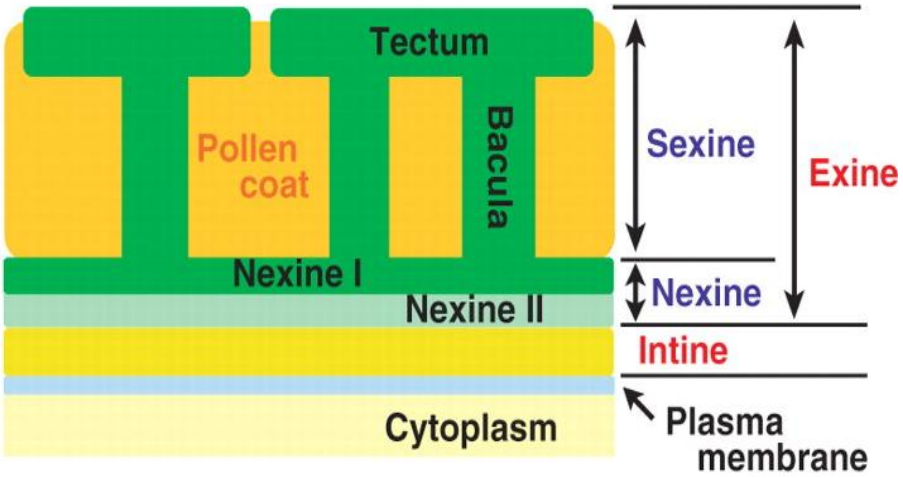

Figure 1.3. Diagram of *A. thaliana* pollen wall structure. The inner intine and the various components of the outer exine are indicated as is the pollen coat (tryphine and pollenkitt) which fills the cavities of the exine sculpture. Taken from Suzuki *et al.* (2008).

1.3 Molecular genetics of pollen wall development

In recent years there has been a surge in papers describing genes involved in pollen wall development. However, our understanding of the molecular genetics of spore/pollen development remains poor due to the complexity of the developmental process and problems in pinpointing the actual function of the genes involved. Furthermore, research has been confined to particular model angiosperms (Table 1.1 and Fig. 1.4), most notably *A. thaliana*, with little or no information on gymnosperm pollen or the spores of 'lower' land plants.

However, this research is now beginning to incorporate model plant species from more primitive groups, such as the bryophytes. This extended research will enable the comparison of the molecular genetics of spore/pollen wall development in angiosperms and more primitive plants. The results from this may allow us to assess how conserved the genes and genetic networks involved in spore/pollen wall development are. The following sections (1.3.1 - 1.3.6) review the current knowledge of the molecular genetics of pollen wall development in *A. thaliana*.

1.3.1 *Arabidopsis thaliana* genes implicated in sporopollenin biosynthesis and exine formation

A number of *A. thaliana* genes associated with the biosynthesis of exine encode proteins with sequence homology to enzymes involved in fatty acid metabolism (Dobritsa *et al*., 2009). Aarts *et al*. (1997) observed expression of the *MALE STERILITY 2* (*MS2*) gene in the tapetum of wildtype plants at, and shortly after, the release of microspores from tetrads and noted that *MS2* mutants produced pollen grains which lacked an exine layer. The exine layer had been replaced by a thin layer of unknown composition. *MS2* encodes a protein with sequence similarity to long chain fatty acyl reductases and expression of the *MS2* protein in bacteria leads to the increased synthesis of fatty alcohols (Doan *et al*., 2009). Taken together, these data suggest that an *MS2*-linked enzymatic pathway is required for the synthesis of sporopollenin (Aarts *et al*. 1997; Ariizumi *et al*. 2008; Dobritsa *et al*. 2009).

Another gene implicated in exine formation is *YORE-YORE* (*YRE*)/*WAX2*/*FACELESS POLLEN1* (*FLP1*). Ariizumi *et al*. (2003) suggested that this gene encodes a transporter or catalytic enzyme that is involved in wax synthesis in stems and siliques,

in the tryphine, and in sporopollenin synthesis. As with *MS2*, the pollen exine in *YRE/FLP1* mutants is poorly constructed and easily damaged, suggestive of defective sporopollenin. Expression analyses in the same study suggest that *FLP1* is expressed in the tapetum, which is supported by the fact that the *FLP1* mutant phenotype is sporophytically controlled (Ariizumi *et al.* 2003). In addition, Rowland *et al*. (2007) demonstrated that the *ECERIFIUM 3* (*CER3*) gene encodes a protein of unknown function identical to *YRE/WAX2/FLP1* and is therefore allelic to *YRE*/*WAX2*/*FLP1*.

Morant *et al.* (2007) showed that the *A. thaliana* cytochrome P450 enzyme *CYP703A2* is also necessary for the synthesis of sporopollenin. The *CYP703* cytochrome P450 family is specific to embryophytes and each plant species contains a single *CYP703* (Morant *et al*. 2007). The exine layer in *CYP703A2* knock-out mutants is significantly underdeveloped. Sporopollenin also appeared to be absent as the fluorescent layer around the pollen associated with the presence of phenylpropanoid units in sporopollenin was absent in *CYP703A2* mutant plants (Morant *et al.* 2007). Morant *et al*. (2007) demonstrated that lauric acid and in-chain hydroxy lauric acids are present in the plant substrate and product for this enzyme. These are important building blocks in the synthesis of sporopollenin and facilitate the formation of ester and ether linkages with phenypropanoid units. Furthermore, the same study showed that *CYP703A2* is expressed in the anthers of developing *A. thaliana* flowers with initial expression detectable at the tetrad stage in the microspores and the tapetum (Morant *et al*., 2007), consistent with a role in exine formation.

Dobritsa *et al.* (2009) described another cytochrome P450, *CYP704B1*, and demonstrated that this gene is essential for exine development. *CYP704B1* mutants produce pollen walls which lack a normal exine layer. The exine layer was replaced with a thin layer of material and irregular distribution of aggregates which may have been sporopollenin. The pollen walls also exhibited a characteristic striped surface, unlike the reticulate pattern displayed by the wildtype, to which Dobritsa *et al.* (2009) designated the name, *zebra* phenotype. It has also been shown that heterologous expression of *CYP704B1* in yeast catalyses ω-hydroxylation of long-chain fatty acids, consistent with a role in sporopollenin synthesis (Dobritsa *et al.* 2009). Dobritsa *et al.* (2009) have suggested that these ω-hydroxylated fatty acids, in concert with the formation of in-chain hydroxylated lauric acids catalysed by *CYP703A2*, may serve as

vital monomeric aliphatic building blocks in the formation of sporopollenin. Analyses of the genetic relationships between *CYP704B1*, *CYP703A2* and *MS2* (which as described above encodes a fatty acyl reductase) along with expression analyses and observation of similar *zebra* phenotypes in all three mutants, indicate that these genes are involved in the same pathway within the sporopollenin synthesis framework and are co-expressed (Dobritsa *et al*. 2009). In addition, an orthologue of *CYP704B1* (*BnCYP704B1)* has recently been identified in *Brassica napus*, and mutants in this gene exhibit defective exine layers (Yi *et al*. 2010).

Table 1.1. *Arabidopsis thaliana* genes implicated in pollen wall development.

Role	Gene	Proposed Expression
Sporopollenin biosynthesis and exine formation	*MS2*	Sporophyte
	YRE/WAX2/FLP1	Sporophyte
	CYP703A2	Sporophyte and microspores
	CYP704B1	Sporophyte
	ACOS5	Sporophyte
	RPG1	Sporophyte and microspores
	NEF1	Sporophyte
	KNS5-10	Sporophyte
	KNS4	Sporophyte
	ABCG26	Sporophyte and microspores
	LAP5/PKSB	Sporophyte
	LAP6/PKSA	Sporophyte
	TKPR1/DRL1	Sporophyte
	TKPR2/CCRL6	Sporophyte
	AtMYB103/MS188 (TF)	Sporophyte
	MS1 (TF)	Sporophyte
	AtbZIP34 (TF)	Sporophyte and gametophyte
Exine formation (probaculae)	*DEX1*	Unknown
	TDE1/DET2	Unknown
	KNS2, 3, 12	Sporophyte
Intine formation	*FLA3*	Sporophyte and microspores
	MS33	Unknown
	RGP1	Sporophyte and microspores
	RGP2	Sporophyte and microspores
Callose wall formation	*CALS5/LAP1*	Sporophyte and gametophyte?
	KNS1, 11	Sporophyte
Tetrad Separation	*QRT1-3*	Sporophyte
	A6	Sporophyte

Note: TF denotes transcription factor.

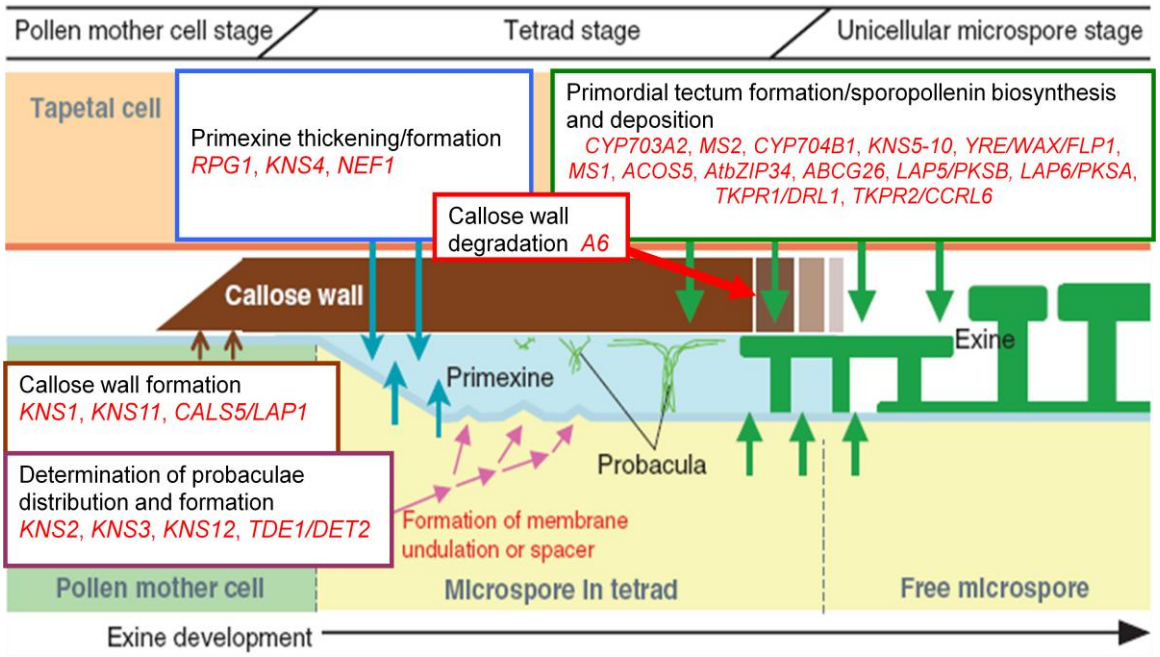

Figure 1.4. Proposed functions of genes implicated in *A. thaliana* pollen wall exine development. Expected time and location of gene expression is indicated. Not all *A. thaliana* genes described in this section are included due to a lack of information regarding the time and locality of their expression. Modified from Suzuki *et al.* (2008).

Another gene reported to participate in exine formation, *ACOS5*, has recently been described (de Azevedo Souza *et al.* 2009). This encodes a fatty acyl-CoA synthetase with broad *in vitro* preference for the medium chain fatty acids required in tapetal cells for sporopollenin monomer synthesis. Mutations in *ACOS5* significantly compromise the development of the pollen wall which appears to lack sporopollenin and exine. The defect in pollen formation in *ACOS5* mutants coincides with the deposition of exine at the unicellular microspore stage (de Azevedo Souza *et al.* 2009). Additionally, after analyses of *ACOS5* expression in developing anthers, de Azevedo *et al*. (2009) proposed that it is also involved in the same biochemical pathway as the *CYP703A2*, *CYP704B1* and *MS2* genes.

The *RUPTURED POLLEN GRAIN1* (*RPG1*) gene encoding a plasma membrane protein and *NO EXINE FORMATION1* (*NEF1*) gene, which encodes a plastid integral

membrane protein, are both required for primexine development (Ariizumi *et al*. 2004; Guan *et al*. 2008). Guan *et al*. (2008) revealed that exine pattern formation in *RPG1* mutants is defective as sporopollenin is randomly distributed over the surface of the pollen grain. Primexine formation of microspores in *RPG1* mutants is abnormal at the tetrad stage, which results in imperfect deposition of sporopollenin on the microspores (Guan *et al*. 2008). *RPG1* plants experience microspore rupture and cytoplasmic leakage suggesting that cell integrity had been impaired in the microspores. The same study demonstrated that *RPG1* is strongly expressed in the tapetum and the microspores during male meiosis (Guan *et al*. 2008). Ariizumi *et al*. (2004) showed that *NEF1* mutants exhibited similarly defective primexine and that although sporopollenin was present it was not deposited onto the plasma membrane of the microspore because of the lack of normal primexine. Ariizumi *et al*. (2004) tentatively suggest that *NEF1* is expressed in the tapetum and is sporophytically controlled. Additionally, it was proposed that *NEF1* is likely to be involved in exine formation at earlier developmental stages than other exine formation genes, such as *MS2* and *FLP1,* since the exine is more poorly developed in *NEF1* plants (Ariizumi *et al*. 2004).

Suzuki *et al*. (2008) also identified a number of genes involved in the construction of exine and pollen development in general. They managed to successfully isolate 12 *KOANASHI* mutants (*KNS1-KNS12*), which were found to be recessive and thus likely to affect pollen development sporophytically. The 12 mutants were categorised into four types. The type 3 (*KNS5-KNS10*) mutants displayed abnormal tectum formation on the pollen surface and these genes therefore appear to be required for either creating primordial tectum (onto which sporopollenin is deposited) in the space between the primexine and the callose wall, or for depositing sporopollenin itself (Suzuki *et al*. 2008). Additionally, the type 2 mutant (*KNS4*) exhibits a thin exine layer mostly due to shortened baculae. It is proposed that baculae extension is closely linked to the thickening of the primexine, therefore, *KNS4* is likely to be a novel gene which regulates the thickening of the primexine layer (Suzuki *et al*. 2008).

Recently, Quilichini *et al*. (2010) proposed that the *ATP-BINDING CASSETTE G26* (*ABCG26*) plays a crucial role in exine formation. *Abcg26-1* mutants lack an exine layer and expression studies showed that *ABCG26* is transiently and locally expressed

in the tapetum post meiosis. Quilichini *et al*. (2010) suggest that *ABCG26* transports sporopollenin precursors across the tapetum plasma membrane to the anther locule for polymerisation on the surface of the developing microspores.

Other genes which have recently been associated with a defective exine include *LESS ADHESIVE POLLEN 5/POLYKETIDE SYNTHASE B* (*LAP5/PKSB*) and *LESS ADHESIVE SYNTHASE 6/POLYKETIDE SYNTHASE A* (*LAP6/PKSA*) which are also specifically and transiently expressed in the tapetum during microspore development (Kim *et al*. 2010). Mutant plants compromised in the expression of *LAP5/PKSB* and *LAP6/PKSA* exhibited significantly defective exine layers and a double *LAP5/PKSB LAP6/PKSA* mutant appeared to completely lack an exine layer. These two genes are co-expressed with *ACOS5,* and recombinant *LAP5/PKSB* and *LAP6/PKSA* proteins were able to generate tri- and tetraketide alpha-pyrone compounds *in vitro* from a wide range of potential *ACOS5*-generated fatty acyl-CoA starter substrates via condensation with malonyl-CoA. These compounds would therefore appear to be required for sporopollenin biosynthesis (Kim *et al*. 2010). Additionally, two closely related genes, *TETRAKETIDE alpha-PYRONE REDUCTASE1* (*TKPR1/DRL1*) and *2* (*TKPR2/CCRL6*), encode oxidoreductases which have been found to be active on the tetraketide products produced by *LAP5/PKSB* and *LAP6/PKSA*. TKPR activity reduces the carbonyl function of the tetraketide alpha-pyrone compounds synthesized by *LAP5/PKSB* and *LAP6/PKSA*, and together with the activities associated with *LAP5/PKSB*, *LAP6/PKSA* and *ACOS5*, form a biosynthetic pathway which ultimately produces hydroxylated alpha-pyrone compounds, potential precursors for sporopollenin (Grienenberger *et al*. 2010).

1.3.2 *Arabidopsis thaliana* transcription factors involved in sporopollenin and exine formation

A number of transcription factors participating in the development of exine have been described. *AtMYB103*/*MS188* is a MYB transcription factor that is specifically expressed in the anthers and trichomes of *A. thaliana* (Li *et al*. 1999; Higginson *et al*. 2003). Zhang *et al*. (2007) have shown that *AtMYB103/MS188* directly regulates the expression of the previously described exine formation gene *MS2* and the callase-related *A6* gene. Knock-out mutants of *AtMYB103*/*MS188* resulted in early tapetal degeneration and abnormal microspores. Additionally, expression of the *MS2* gene

was not detected in the anthers of the *AtMYB103*/*MS188* mutants (Zhang *et al*. 2007). The *MALE STERILITY1* (*MS1*)/*HACKLY MICROSPORE* (*HKM*) gene, encoding a leucine zipper-like, PHD-finger motif transcription factor, is also involved in tapetum function (Ariizumi *et al*. 2005; Vizcay-Barrena and Wilson 2006; Ito *et al*. 2007; Yang *et al*. 2007). Phenotypic analysis of *MS1* mutants by Ito *et al*. (2007) indicated that *MS1* is required for transcriptional regulation of genes involved in primexine formation, sporopollenin synthesis and tapetum development. Lack of *MS1* expression results in changes in tapetal secretion and exine structure with the appearance of autophagic vacuoles and mitochondrial swelling, suggesting that the tapetum is broken down by necrosis rather than by apoptosis as observed in the wildtype (Vizcay-Barrena and Wilson 2006; Yang *et al*. 2007). Yang *et al*. (2007) further demonstrated that *MS1* is expressed in the tapetal cells in a developmentally regulated manner between the late tetrad stage and microspore release.

Another transcription factor involved in exine formation has been identified by Gibalova *et al*. (2009) who demonstrated that *AtbZIP34* mutants exhibit defects in exine structure. The exine layer is wrinkled and the baculae and tecta are deformed. Additionally, 50% of mutant pollen exhibited a wrinkled intine layer. Despite these abnormalities, high levels of pollen abortion or male sterility were not observed (Gibalova *et al*. 2009). Transcriptomic analyses revealed that expression of the proposed primexine development gene, *RPG1*, is significantly down-regulated in *AtbZIP34* mutant pollen. Given the expression profiles of both genes, it is possible that *RPG1* expression is regulated by *AtbZIP34* (Gibalova *et al*. 2009). Analyses also suggested sporophytic and gametophytic roles for *AtbZIP34* in exine and intine formation.

The observation that many of the genes described in the previous sections are predominately expressed sporophytically is a little at odds with the fact that exine development mostly occurs at the surface of individual microspores after meiosis. Suzuki *et al*. (2008) propose that this apparent contradiction may possibly be partly explained by many of these genes being expressed in pollen mother cells so that the relevant mRNA or proteins are inherited by the derived microspores. Furthermore it would appear that the interaction of gametophytic and sporophytic genes is important for the development of viable pollen (Wilson and Zhang 2009). A recent study

focusing on a rice fasciclin glycoprotein, *MICROSPORE AND TAPETUM REGULATOR1* (*MTR1*), demonstrates the cooperation between microspores and the tapetum. *MTR1* is specifically expressed in microspores yet its mutant has defects in the development of the tapetum as well as microspores (Tan *et al*. 2012). Tan *et al*. (2012) propose that *MTR1* is a vital signalling molecule that coordinates microspore and tapetum development.

1.3.3 *Arabidopsis thaliana* genes associated with probaculae formation

At present five *A. thaliana* genes have been specifically associated with the formation of probaculae, which is an important component in the exine development process. The *DEFECTIVE IN EXINE1* (*DEX1*) gene encodes a novel membrane protein which is required for anchoring sporopollenin to the surface of the microspores and is implicated in probacula formation (Paxson-Sowders *et al*. 1997; Paxson-Sowders *et al*. 2001). Sporopollenin synthesis still takes place in *DEX1* mutants but primexine development is delayed and ultimately reduced, which alters membrane formation and therefore the deposition of sporopollenin. Spacers do not form in the primexine which results in sporopollenin being randomly deposited on the plasma membrane (Paxson-Sowders *et al*. 2001). Additionally, sporopollenin does not appear to be anchored to the microspore and forms bulky aggregates on the developing microspore and locule walls, and the pollen wall does not form, which results in pollen degradation (Paxson-Sowders *et al*. 2001).

Ariizumi *et al*. (2008) suggested that the *TRANSIENT DEFECTIVE EXINE1* (*TDE1*)/*DE-ETIOLATED2* (*DET2*) gene is also involved in probacula development. Specifically, they proposed that *TDE1*/*DET2* is involved in brassinosteroid synthesis, a hormone purported to control the rate or efficiency of the initial process of exine formation. Primexine synthesis is defective in *TDE1*/*DET2* mutant plants which ultimately fail to produce probacula at the tetrad stage (Ariizumi *et al*. 2008). Additionally, globular sporopollenin is haphazardly deposited onto the microspore at the early uninucleate microspore stage (Ariizumi *et al*. 2008). As with *DEX1* mutants, sporopollenin apparently failed to anchor to the plasma membrane of the microspore and instead aggregated on the locule wall and in the locule at the uninucleate microspore stage (Paxson-Sowders *et al*. 2001; Ariizumi *et al*. 2008). However, despite these defects reticulate exine was clearly formed at the later stage in

TDE1/*DET2* mutants which is in contrast to other mutants displaying primexine defects, such as *DEX1*, which always fail to produce normal exine at the later stages. This suggests that mutations in *TDE1*/*DET2* do not result in defects at critical stages of exine development (Ariizumi *et al*. 2008). Expression analysis also demonstrated that brassinosteroids may be synthesised in developing microspores. The same analysis also showed that *TDE1*/*DET2* mutations did not affect the expression of genes implicated in exine development. This suggests that brassinosteroids support exine development in a distinct pathway (Ariizumi *et al*. 2008).

The *KNS2*, *3* and *12* genes, designated type 4 genes by Suzuki *et al*. (2008), have also been associated with probacula formation. Type 4 mutants were shown to exhibit abnormal positioning of baculae which were densely distributed. This suggests that the type 4 genes govern the position of probacula formation by either forming undulations on the microspore plasma membrane at the tetrad stage, or by forming spacers (Suzuki *et al*. 2008). Additionally, Suzuki *et al*. (2008), using map-based cloning, were able to reveal that one of the type 4 genes, *KNS2*, encodes sucrose phosphate synthase which is proposed to be potentially involved in primexine synthesis or callose wall formation, which are known to be important for the positioning of probaculae. Further studies are required to specifically determine the time and location of expression of *KNS* type 4 genes.

1.3.4 *Arabidopsis thaliana* genes connected to intine formation

Recently, Li *et al*. (2010) have proposed that the fasciclin-like arabinogalactan protein gene *FLA3* is involved in the development of the intine layer by playing a role in the deposition of cellulose. The down-regulation of *FLA3* via RNAi results in the appearance of a thinning intine layer and the production of approximately 50% non-viable pollen grains, many of which display a wrinkled or shrunken phenotype. Expression studies showed that *FLA3* is specifically expressed in pollen tubes and pollen grains, and is localised to the cell membrane (Li *et al*., 2010). Other *A. thaliana* genes have also been implicated in intine formation, including the reversibly glycosylated peptide genes, *RGP1* and *RGP2*. Pollen in double knockout plants of *RGP1* and *RGP2* exhibit unusually enlarged vacuoles and a poorly defined intine layer (Drakakaki *et al*. 2006). Additionally, in *MALE STERILITY33 (MS33)* mutants the

intine forms prematurely and exhibits a thinner exintine and a much thicker endintine than in wildtype pollen (Fei *et al*. 2004).

1.3.5 *Arabidopsis thaliana* genes implicated in callose wall formation

To date, three *A. thaliana* genes have been associated with callose wall formation. Dong *et al*. (2005) and Nishikawa *et al*. (2005) have demonstrated that the *CALLOSE SYNTHASES (CALS5)/LESS ADHERENT POLLEN (LAP1)* gene encodes a callose synthase essential for callose wall formation. *CALS5/LAP1* mutants lack callose on the cell wall of pollen mother cells, tetrads and microspores which ultimately results in the development of sterile pollen due to the degeneration of microspores (Dong *et al*. 2005). Additionally, exine structure in the mutant plants was severely deformed, affecting the baculae and tecta structure, and tryphine was haphazardly deposited as globular structures (Dong *et al*. 2005). This implies that the callose wall is vitally important for the formation of a properly sculpted exine (Dong *et al*. 2005). Expression analyses have produced varied results with regards to *CALS5/LAP1* and suggest the gene is expressed in either pollen mother cells or pollen tetrads, or possibly both cell types (Nishikawa *et al*. 2005). Abercrombie *et al*. (2011) propose that sporophytic expression of *CALS5*/*LAP1* accounts for its role in the formation of the callose wall in pollen mother cells and pollen tetrads, and secondary expression in the gametophyte is linked to pollen germination.

The *KNS1* and *KNS11* genes constitute the type 1 genes as described and classified by Suzuki *et al*. (2008). Type 1 mutant plants exhibit pollen grains which display a highly collapsed exine structure in which the tecta disappear and the baculae deform into globular protrusions. Additionally, mature pollen grains of both genes were reduced in size and in number, and were distorted in shape (Suzuki *et al*. 2008). This phenotype closely resembled the pollen phenotype of *CALS5/LAP1* mutants described above (Dong *et al*. 2005; Nishikawa *et al*. 2005; Suzuki *et al*. 2008). This resemblance, along with the recessive nature of the type 1 genes, suggests that *KNS1* and *KNS11* are expressed in pollen mother cells and are important in synthesising or secreting callose (Suzuki *et al*. 2008).

1.3.6 *Arabidopsis thaliana* genes involved in tetrad separation

The *QUARTET* (*QRT*) genes have been identified as being required for pollen separation during normal pollen development (Preuss *et al*. 1994; Rhee and Somerville 1998; Francis *et al*. 2006). In wildtype *A. thaliana* pollen, degradation of the pollen mother cell walls takes place which releases the individual microspores as single pollen grains (Francis *et al*. 2006). Mutations in any of the *QRT1, QRT2* or *QRT3* genes cause the outer walls of the microspores to become fused following meiosis, resulting in pollen grains being released as tetrads (Preuss *et al*. 1994; Rhee and Somerville 1998; Francis *et al*. 2006). Rhee and Somerville (1998) have demonstrated that the enzymatic removal of callose at the tetrad stage is not sufficient to release the microspores. In *QRT1* and *QRT2* mutants pectic components were detectable at the time of tetrad separation which was not the case in the wildtype. This suggests that the persistence of pectin in the pollen mother cell wall is associated with tetrad separation failure (Rhee and Somerville 1998).

Pollen mother cell primary cell walls have been proposed to play a significant part in cell-cell adhesion mechanisms (Rhee and Somerville 1998). The pectins of the primary cell wall have been shown to consist mostly of homogalacturan, a polymer of b-1, 4-galacturonic acid (GalUA), rhamnogalacturonan I and rhamnogalacturonan II (branching polymers of GalUA, Ara and Rha) (Brett and Waldron 1996; Tucker and Seymour 2002). As pectin is synthesised the backbone of GalUA is in a methylesterified state which can then be demethylesterified by pectin methylesterases and cleaved by endo-polygalacturonases, which results in loosening of the cell wall (Schols and Voragen 2002; Francis *et al*. 2006). *QRT1* has been proposed to encode a pectin methylesterase (Francis *et al*. 2006), whereas the gene product of *QRT2* has not yet been determined. Expression analysis has shown that *QRT1* is expressed shortly after meiosis is complete (Francis *et al*. 2006). Additionally, Rhee *et al*. (2003) have identified *QRT3* as being an endopolygalacturonase which degrades the pectic polysaccharides of the pollen mother cells. It has been demonstrated that the *QRT3* gene is specifically and transiently expressed in tapetal cells during microspore release from the tetrad (Rhee *et al*. 2003). Immunohistochemical localisation of *QRT3* suggests that the protein it encodes is secreted from the tapetum during the early stages of microspore development (Rhee *et al*. 2003).

Genes associated with callose wall degradation have, to date, not been definitively identified. Frankel *et al*. (1969) and Stieglitz and Stern (1973) demonstrated that the tetrad callose wall is degraded by β-1,3-glucanases activity secreted from the tapetal cells. Whilst a number of candidate β-1,3-glucanase encoding genes have been identified, none have been confirmed as a callase (Hird *et al*. 1993). However, Hird *et al*. (1993) have proposed that the *A6* gene may encode a component of the callase enzyme complex due to the fact that it is tapetum-specific, has a strong sequence similarity to other β-1,3-glucanases, and is temporally expressed at peak levels when the plant normally expresses callase. Future identification of *A6* mutant plants is needed to confirm the gene as a callase. Additionally, real-time RT-PCR analysis conducted by Zhang *et al*. (2007) has suggested that *A6* is regulated by the *AtMYB103/MS188* gene.

1.4 The utility of *Physcomitrella patens*

The bryopsid moss *P. patens* is now a commonly used model species primarily because of the high levels of gene targeting associated with it, and is proving to be a powerful tool for the comparative analyses of embryophyte genomes (Quatrano *et al*. 2007). For example, transcriptomic analyses can demonstrate shared characteristics among plant divisions in gene structure, content, and regulation. Two large scale transcriptome analyses of approximately 100,000 expressed sequence tags have shown that there is a significant amount of sequence similarity (*circa* 65%) between *P. patens* and angiosperms. Additionally, around 66% of genes identified from expressed sequence tag analyses of gene expression in *P. patens* gametophytes have homologues in the *A. thaliana* genome which supports the hypothesis that genes expressed in angiosperm diploid plant bodies were expressed in the gametophyte bodies of early embryophytes and were recruited for sporogenesis in later plants (Nishiyama *et al*. 2003). Splice sites and codon usage are also conserved among similar genes found in *P. patens* and *A. thaliana*.

Gene targeting involves the generation of specific mutations in a genome through the integration of foreign DNA at targeted locations by homologous recombination (Schaefer, 2002). Transformation constructs which contain genomic sequence are targeted at high frequency to the equivalent genomic locus allowing the inactivation of

genes by targeted gene replacement (TGR). With TGR a selection cassette is inserted into a cloned gene, ideally replacing the coding sequence. Gene transformation is conducted using linear DNA which consists of the selection cassette flanked by two stretches of genomic sequence (Quatrano *et al*. 2007). When homologous recombination takes place in both of the flanking sequences, targeting facilitates the substitution of the genomic locus with the targeting construct (Quatrano *et al*. 2007).

Physcomitrella patens has the highest ratio of homologous recombination to nonhomologous recombination of all land plants (Nishiyama *et al*. 2003; Quatrano *et al*. 2007), and transformational experiments conducted by Schaefer and Zryd (1997) have indicated that its level of gene targeting efficiency is above 90% which is comparable to that of yeast, i.e. five orders of magnitude greater than in any other plant species (Reski and Cove 2004). This efficiency enables reverse genetics approaches in *P. patens* to be carried out at high throughput levels as several independent knock-out plants can be produced for one single construct, facilitating rapid and reliable gene function annotations (Kamisugi *et al*. 2005; Reski and Frank 2005). *Physcomitrella patens* is also straightforward to propagate vegetatively allowing mutant strains to be maintained indefinitely and the haploidy of the dominant gametophyte generation in mosses allows mutant phenotypes to be immediately identified as a loss-of-function mutation cannot be counteracted by a functional allele in a homologous chromosome (Cove 2000; Reski and Cove 2004; Prigge and Bezanilla 2010).

1.5 Research outline

Whilst a substantial amount of research has been conducted with regards to pollen wall development in angiosperms, particularly *A. thaliana*, research into spore wall development in basal plants has thus far been extremely limited particularly in terms of the molecular genetics of sporogenesis. Schuette *et al*. (2009), using immuno-light and immuno-electron microscopy, have identified the presence of callose in the spores of *P. patens* where it was deposited in the inner exospore layer near the expanded aperture region (local expansion of the intine layer) at the proximal pole, suggesting that callose is involved in aperture expansion during wall development. It is proposed that a *CALS5* homologue is present in the *P. patens* genome and is involved

in spore wall development (Schuette *et al*. 2009). Additionally, Aya *et al*. (2011) generated knockouts of *GAMYB* homologues in *P. patens* which produced abnormal spores with defective perine and outer exine layers. In rice, the *GAMYB* gene has been identified as a transcription factor, controlled by the hormone gibberellin, which positively regulates *CYP703A3* which encodes an enzyme essential in sporopollenin biosynthesis (Aya *et al*, 2009). Further research has not yet been forthcoming in this area therefore this thesis will contribute to filling this void. By comparing *P. patens* genes which are upregulated during sporogenesis with those known to be involved in pollen wall development in *A. thaliana* it will be possible to identify candidate genes likely to be involved in the development of the spore wall and consequently the ability of the moss to survive in the terrestrial environment. Additionally, by conducting gene knock-out and gene swap experiments between *P. patens* and *A. thaliana* it will be possible to test hypotheses regarding the conservation of gene function in the spore wall, as has already been achieved in the area of leaf, root and stomata EvoDevo studies (Harrison *et al*. 2005; Menand *et al*. 2007; Chater *et al*. 2011; Ruszala *et al*. 2011).

1.5.1 Aims

1. To utilise the genomic resources and tools afforded by *A. thaliana* and *P. patens* to test the overarching hypothesis that the biochemical and developmental pathway required for pollen wall development in higher plants is ancient and highly conserved.

1.5.2 Objectives

1. Characterise the structure and ultrastructure of the spore wall in *P. patens* at various developmental stages of sporogenesis using electron microscopy.
2. To use a bioinformatic approach in conjunction with literature/data mining to determine genes which are involved in pollen wall development in *A. thaliana*.
3. To use the gene list generated in (2) to interrogate a fully replicated unpublished microarray database derived from early and mid stages of sporophyte development in *P. patens* to identify candidate genes likely to be involved in *P. patens* spore wall development.

4. To generate knock-out mutants and perform complementation experiments in *P. patens* and *A. thaliana* respectively, to test the function of selected candidate gene(s).
5. To apply and develop appropriate morphological and physiological techniques for phenotyping mutated spore and pollen walls.

1.5.3 Hypotheses

1. The biochemical and developmental pathway required for pollen wall development in higher plants is ancient and highly conserved.
2. Spore wall development is controlled by both the diploid sporophyte and the haploid spore.

1.6 Thesis outline

This chapter has introduced and summarised the research carried out to date with regards to spore and pollen wall development and the associated molecular genetics, and outlines the motivation for the work reported in the following chapters.

In Chapter 2 the materials and methods used for this study are described. The work in Chapter 3 characterises spore wall development, using electron microscopy, to analyse wall structure and ultrastructure at various developmental stages of sporogenesis in *P. patens*. Chapter 4 describes the process of identifying genes in *P. patens*, likely to be involved in spore wall development using expression analyses and bioinformatics. Justification for the selection of a lead gene for the work outlined in later chapters is also provided. In Chapter 5 the results from gene swap experiments, involving the transformation of a *P. patens* spore wall candidate gene (selected in Chapter 4) into an appropriate *A. thaliana* loss-of-function mutant, are reported along with a description of the morphological and physiological phenotyping of *P. patens* lead gene knockout mutants generated by homologous recombination. Chapter 6 gives a summation of the overall findings presented in this thesis and discusses how they progress our knowledge with regard to the evolutionary development of the spore and pollen wall. Future research directions are also discussed.

CHAPTER 2. **Materials and methods**

2.1 Materials

2.1.1 General laboratory materials

General laboratory chemicals of analytical grade, or comparable grade, were purchased from Melford, Duchefa Biochemie, Sigma-Aldrich UK, BDH or Fisher Scientific.

Modification enzymes were obtained from a variety of sources. BIOTAQ™ DNA Polymerase was purchased from Bioline (www.bioline.com), M-MLV Reverse Transcriptase was ordered from either Promega (www.promega.com) or Fisher Scientific (www.fisher.co.uk) and KOD Hot Start DNA Polymerase was purchased from Toyobo (www.toyobo.co.jp), via Merck Millipore (www.merckmillipore.com). T4 DNA Ligase, T4 Polynucleotide Kinase and Calf Intestinal Alkaline Phosphatase (CIAP) were obtained from Promega. DNA Polymerase I (Klenow) was purchased from New England Biolabs (UK) (www.neb.uk.com).

The pENTR™/D-TOPO® Cloning Kit and Gateway® LR Clonase™ II Enzyme mix were acquired from Invitrogen (www.invitrogen.com). Restriction Enzymes were obtained from New England Biolabs (UK) and Promega. Hyperladder I was purchased from Bioline.

The Qiagen (www.qiagen.com) DNeasy® Plant Mini Kit was used for extracting total plant genomic DNA, and the Qiagen QIAquick Gel Extraction Kit was used for the extraction and purification of DNA fragments from agarose gels. The Qiagen QIAprep Spin Miniprep Kit facilitated plasmid DNA isolation and purification. Total plant RNA was extracted using the Spectrum™ Plant Total RNA Kit from Sigma-Aldrich (www.sigmaaldrich.com) or TRIzol® Reagent supplied by Invitrogen. The Extract-N-Amp Plant PCR Kit (Sigma-Aldrich) was used for quick low quality DNA extractions for the purposes of genotyping numerous putative arabidopsis transformants at once.

The DNA-free™ kit was used to clean RNA and was purchased from Ambion. Custom oligonucleotides/primers were synthesised by Sigma-Aldrich UK. Automated DNA sequencing was conducted by the Core Genomic Facility at the University of Sheffield (www.shef.ac.uk/medicine/research/corefacilities).

The DIG Probe Synthesis Kit purchased from Roche (www.roche-applied-science.com), and Hybond N nylon membranes purchased from GE Healthcare (www.gehealthcare.com), were used for Southern blot experiments.

Water for media, buffers, solutions and plant irrigation was purified by either reverse osmosis (RO) or by the ELGA ion exchange system (ELGA, Purelab). Ambion nuclease-free water was used for nucleic acid techniques.

2.1.2 Plasmids

The destination vector p$POHA was generously provided by Dr Sébastien Thomine (CNRS, France). The pMBL8a and pGUSGW, ESfill C1 vectors were kindly supplied by Dr Yasuko Kamisugi and Dr Andrew Cuming (University of Leeds).

2.1.3 Bacterial strains

One-Shot® TOP10 and Mach1™-T1^{R} chemically competent *E. coli* cells were acquired from Invitrogen. Their genotypes are F^{-} *mcr*A Δ(*mrr-hsd*RMS-*mcr*BC) φ80*lacZ*ΔM15 Δ*lac*X74 *rec*A1 *ara*D139 Δ(*ara-leu*) 7697 *gal*U *gal*K *rps*L (Str^{R}) *end*A1 *nup*G λ- (TOP10) and F^{-} φ80(*lacZ*)ΔM15 Δ*lac*X74 *hsd*R($r_K^- m_K^+$) Δ*rec*A1398 *end*A1 *ton*A (Mach1™-T1^{R}).

Chemically competent α-select (silver and bronze efficiency) *E. coli* cells for bacterial transformation were obtained from Bioline. Their genotype is F^{-} *deo*R *end*A1 *rec*A1 *rel*A1 *gyr*A96 *hsd*R17 ($r_K^- m_K^+$) *sup*E44 *thi*-1 *pho*A Δ(*lac*ZYA *arg*F)U169 Φ80*lac*ZΔM15 λ^{-}.

Electrocompetent *Agrobacterium tumefaciens* cells of strain GV101::pMP90RK were used for the transformation of *A. thaliana*.

2.1.4 Plant Materials

Five ecotypes and mutants of *A. thaliana* were used during this study. Seeds of Columbia 3 (Col-3) wildtype were purchased from the European Arabidopsis Stock Centre (http://arabidopsis.org.uk) as were two mutant lines with T-DNA insertions in the *MS2* gene (SAIL_75_E01 and SAIL_92_C07) and two mutant lines with T-DNA insertions in the *RPG1* gene (SALK_142803 and SALK_092239). All four of these T-DNA insertion lines were advertised as being homozygous for their insertions and this was verifed by PCR genotyping and by checking their phenotypes.

Physcomitrella patens subspecies *patens* (Hedwig) wildtype strains 'Villersexel', 'Gransden 2004' and 'GrD12' were kindly supplied by Dr Andrew Cuming (University of Leeds).

2.2 Plant growth conditions and tissue culture

2.2.1 *Arabidopsis thaliana*

Seeds were stratified in the dark at 4°C for 4-5 days in 300 µl sterile water and were then sown onto M3 compost (Levingtons), containing 5 % perlite, in 4 cm pots. The seeds were germinated, and subsequent developing plants propagated, in growth chambers with a 16-hour photoperiod (irradiance of 100 µmol m^{-2} s^{-1}) at 20°C. The plants were irrigated every 2-3 days with RO water.

2.2.2 *Physcomitrella patens*

Physcomitrella patens was grown axenically in Sanyo MLR incubators under continuous light (irradiance of 140 µmol m^{-2} s^{-1}) at 25°C. Wildtype and mutant lines were grown on BCDA routine basal medium (Cove 2000) supplemented with sterile 1 mM calcium chloride and overlaid with sterile cellophane discs (AA Packaging, UK), in sterile 9 cm Petri dishes sealed with micropore tape (3M).

2.2.3 Protonemal culture and maintenance

Wildtype and mutant *P. patens* lines were maintained indefinitely by sub-culturing bi-weekly in a sterile laminar flow hood. Protonemal tissue was disrupted and blended in sterile autoclaved water using a Polytron® homogeniser (Kinematica, Switzerland).

The homogenate was then plated onto BCDA medium or into 7.7 cm Magenta™ tissue culture vessels (Sigma-Aldrich) filled with BCDA medium. For sub-cultures carried out for the purpose of eventually harvesting protonemal tissue the homegenate was plated onto BCDA medium overlaid with sterile cellophane discs. Gametophore development was initiated by allowing the protonemal homogenate to grow for longer than 14 days.

2.2.4 Gametangia and sporophyte induction

For *P. patens* lines designated for sporophyte induction sterile ~30 mm diameter peat pellets (Jiffy-7; Jiffy Products International) were inoculated with ~2-3 ml of protonemal and/or gametophore homogenate. The inoculated pellets were cultured at 25°C under continuous light in a growth chamber. After 4-6 weeks, when dense gametophore tissue can be observed, the cultures were transferred to a 15°C growth cabinet with an 8 hour photoperiod to initiate gametogenesis. Shortly after transference to these conditions the cultures were flooded for ~4-5 hours with sterile RO water to promote the fertilisation of archegonia. Three weeks after flooding the cultures were transferred to room temperature (variable photoperiod) at which point early stage sporophytes could be observed. The sporophytes took a further 2-3 weeks to reach maturity. Sporophytes at various developmental stages could then be harvested for either DNA/RNA extraction (in liquid nitrogen and stored at -80°C), or for microscope observation or spore germination (dried and then stored in 1.5 ml Eppendorf tubes at room temperature in the dark).

2.2.5 Spore germination

New *P. patens* lines were generated by germinating spores. Sporangia were surface-sterilised with 4 % bleach solution for five minutes and washed four times (five minutes each time) with sterile RO water. The sporangia were then crushed with a sterile pipette tip in 1ml of sterile RO water to create a spore solution which was then plated onto BCDA routine basal medium supplemented with sterile 10 mM calcium chloride. Spores germinated after two days.

2.3 Bioinformatics

2.3.1 Genome searches

Arabidopsis thaliana genes implicated in the development of the pollen wall were identified from literature searches. The majority of these genes have been annotated and their sequences were retrieved from The Arabidopsis Information Resource (TAIR) website (www.arabidopsis.org). The protein sequences were used to search for homologous genes in the *P. patens* genome (www.cosmoss.org) and the *Selaginella moellendorffii* genome (selaginella.genomics.purdue.edu/ and www.ncbi.nlm.nih.gov) using TBLASTN with default parameters employed (E-value cut-off of 1E-4).

2.3.2 Transcriptomic microarray preparation, design and analysis

The triplicated *P. patens* two colour microarray was designed and prepared by C. Chater (University of Sheffield, UK) to maximise genome coverage and compare gametophyte gene expression with that of early and mid stage sporophytes. Gametophyte and sporophyte RNA samples were isolated and purified using extraction protocols described in section 2.4.2. Gametophyte RNA was isolated from seven day old protonemal tissue grown on BCDA medium. RNA was also isolated from early stage sporophytes (pre-expanded columnar capsules with calyptras removed) and mid stage stage sporophytes (ovoid to near spherical translucent lime green capsules with calyptras removed). In order to minimise the condensation of water into samples, ~50 sporophytes from both developmental stages were harvested in a single sitting with fine-tip forceps into Eppendorf tubes sitting in liquid nitrogen. To satisfy the quality requirements for the microarray experiment a minimum of 400 sporophytes were used for each isolation. Three or four RNA extracts were then consolidated for further precipitation to increase sample concentration and purity. Tissue harvested from the Villersexel K3 ecotype was used for the microarray analysis, and subsequent validation, due to its propensity to sporulate abundantly, unlike Gransden 2004, the strain used to construct the microarray probes. However, there is very little polymorphic difference between the two ecotypes with 829 base pairs/SNP and therefore there is minimal effect on hybridisation to the microarray (Kasahara 2011).

One of three independent replicate RNA samples of each sporophyte stage was co-hybridised with one of six independent gametophyte sample replicates. The samples were co-hybridised as total RNA with Cyanine (Cy-3 (green)/Cy-5 (red)) fluorescent Universal Linkage System labels onto an Agilent custom array with antisense probes (synthesised as 60 mer length oligonucleotide probes on glass slides using Agilent Technologies' 'SurePrint' inkjet technology (Reski and Frank 2005) in collaboration with MOgene LC, an Agilent certified facility based in St Louis, MO, USA (www.mogene.com)).

35, 939 filtered transcripts (derived from combining predicted models and EST evidence) were identified from the genome assembly. The transcripts from the Joint Genome Institute (JGI) assembly version 1.1 were used as input (http://genome.jgi-psf.org/physcomitrella/physcomitrella.download.ftp.html). Only 31,000 of the 35,939 transcripts were designed. The remaining five thousand transcripts are either redundant (>99 % identical) or consist of low-complexity sequences unsuitable for high quality probe design. The format of the array was 4 x 44,000, and the number of user defined probes was 41,384. The additional probes were used for quality control purposes by MOgene. A number of the 31,000 designed transcripts were randomly selected and duplicated to fill out the 41,384 probe real estate and therefore could be utilised as spot replicates.

Basic quality control and data and image analysis of the microarray was conducted by MOgene. Normalisation was performed using the R (http://www.r-project.org) package LimmaGUI (Linear Modelling of Microarrays Graphical User Interface (bioinf.wehi.edu.au/limmaGUI/)) (Smyth 2004; Smyth 2005). The data was normalized within arrays using Global LOESS (LOcally wEighted polynomial regreSSion) and between arrays using Aquantile (Fig. 2.1). Normalisation was required to eliminate systematic biases in the microarray data. Background correction of 'half' was selected.

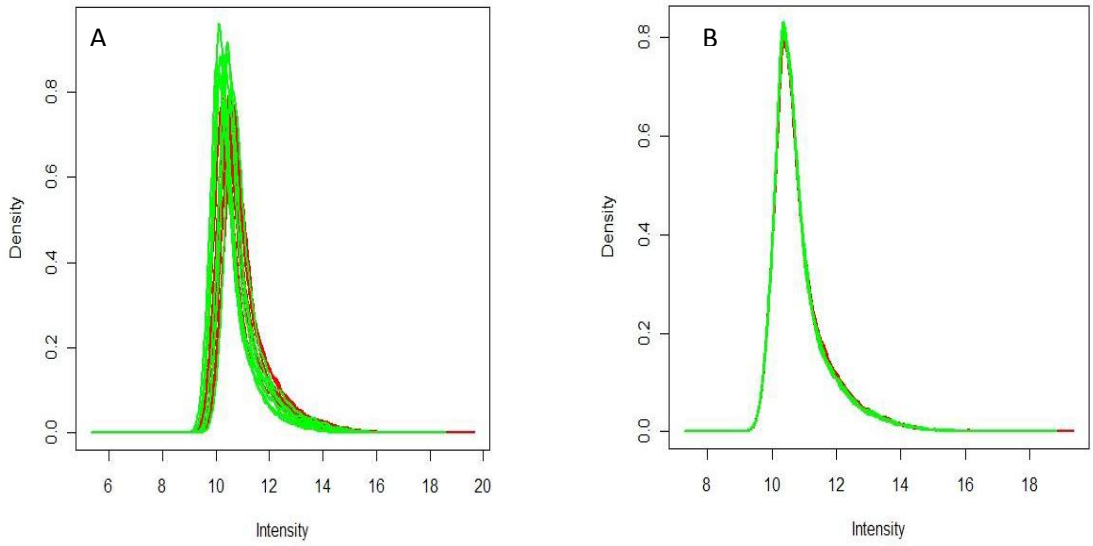

Figure 2.1. Density plots showing green (Cy-3) and red (Cy-5) signals distributions across the microarray chip. A, Pre-normalisation. B, Post-normalisation (within and between arrays).

2.3.3 Sequence alignment and phylogenetic analyses

Multiple alignments of putative protein sequences were conducted using Multiple Sequence Comparison by Log-Expectation (MUSCLE) (Edgar 2004) with a gap opening penalty of -2.9. Alignment of protein sequences of *A. thaliana*, *S. moellendorffii* and *P. patens MS2* homologues for domain analysis was conducted using ClustalW2 (www.ebi.ac.uk/Tools/clustalw). Phylogenetic trees were generated by both maximum parsimony and maximum likelihood methods using MEGA5.1 (Tamura *et al*. 2011). Maximum parsimony trees were obtained using the Tree Bisection and Reconnection algorithm (Nei and Kumar 2000) with search level 1 in which the initial trees were obtained by the random addition of sequences (10 replicates). Gaps were treated as missing data. Phylogenetic support for each clade was determined by bootstrap analysis (1000 replicates) (Felsenstein 1985). The consistency index, retention index and the composite index were calculated using MEGA5.1. Maximum likelihood trees were obtained using the Whelan and Goldman model (Whelan and Goldman 2001). Initial tree(s) for the heuristic search were obtained automatically by applying Neighbour-Join (NJ) and BioNJ algorithms to a matrix of pairwise distances estimated using a JTT model (Jones *et al*. 1992), and then

selecting the topology with superior log likelihood. Phylogenetic support for each clade was once again assessed by bootstrap analysis of 1000 replicates.

2.4 Nucleic acid techniques

2.4.1 Plant genomic DNA extraction

For small-scale DNA extractions (for PCR) in all plant tissues the Qiagen DNeasy® Plant Mini Kit was used. Plant tissue (~100 mg wet weight) was ground in liquid nitrogen to a fine powder using a mortar and pestle. For extractions involving *P. patens* protonema the plant tissue was pressed between two sheets of filter paper (Whatman) to remove as much extraneous liquid as possible prior to flash freezing in liquid nitrogen and eventual DNA extraction. Additionally, in order to reduce the co-extraction of enzyme-inhibiting compounds only six to seven day old protonemal tissue was used. The liquid nitrogen was allowed to evaporate and before the sample could thaw 400 µl of Lysis Buffer AP1 (kit reagent) and 4 µl of RNase A were added. The sample was then mixed vigorously, in a 1.5 ml Eppendorf tube, using a vortex, and incubated for ten minutes at 65°C with occasional mixing. This step lyses the cells. 130 µl of Precipitation Buffer AP2 (kit reagent) was then added to the lysate which was mixed by tube inversion and then incubated on ice for five minutes. This step precipitates detergent, proteins and polysaccharides. The lysate was then centrifuged for five minutes at 13,200 rpm (maximum speed) to pellet precipitates and the resultant supernatant was added to a QIAshredder™ spin column sitting in a 2 ml collection tube and centrifuged for two minutes at maximum speed. The flow-through fraction was transferred to a new tube to which 1.5 volumes of Precipitation Buffer AP3/E (kit reagent) was added, and mixed by pipetting, to the cleared lysate. The sample mixture was then added to a DNeasy mini spin column, sitting in a 2 ml collection tube, and centrifuged for one minute at 8,000 rpm. The flow-through was discarded and the centrifugation step repeated after which the column was transferred to a clean 2 ml collection tube. 500 µl of Wash Buffer AW (kit reagent) was added to the column which was then centrifuged for 1 minute at 8,000 rpm. The flow through was one again discarded and a further 500 µl of buffer AW was added to the column which was then centrifuged for two minutes at maximum speed in order to dry the column membrane. The column was finally transferred to a 1.5 ml Eppendorf tube.

30-50 µl of Elution Buffer AE (kit reagent) was then added directly onto the column membrane which was then incubated at room temperature for 5-10 minutes. The column was then centrifuged at 8,000 rpm for one minute and the DNA was in the resultant eluate which was stored at -20°C.

A modified version of the CTAB extraction protocol described by Knight *et al*. (2002) was used for large-scale extractions (for Southern blotting experiments involving *P. patens*). Immediately prior to use, 7 µl of 2-mercaptoethanol and 10 mg ascorbic acid were added to 10 ml stock of extraction buffer (0.1 M Tris-Cl, pH 8.0, 1.42 M NaCl, 2.0 % CTAB, 20 mM Na_2EDTA, 2 % PVP-40 autoclaved) which was then warmed to 65°C. Once again protonemal tissue (200-300 mg wet weight) was ground in liquid nitrogen using a mortar and pestle. 1 ml of extraction buffer was then added to the sample and was gently mixed to form a smooth paste. A further 1 ml extraction buffer was then added and stirred to obtain a uniform homogenate. The homogenate was then transferred to a 50 ml Falcon tube and 30 µl of 10 mg/ml pre-boiled RNase A was added. This mix was then incubated at 65°C for 5 minutes. After incubation 3 ml of chloroform/*iso*-amyl alcohol (24:1) was added and the sample was mixed further using a vortex to emulsify. Phases were then separated by centrifuging at 10,000 rpm for 10 minutes. The upper aqueous phase was transferred to a fresh tube and DNA was precipitated by adding and mixing in 2.1 ml of *iso*-propanol followed by centrifugation at 10,000 rpm for 5 minutes. The resultant supernatant was discarded and the pellet was washed with 70 % ethanol and then air dried. The pellet was then dissolved in 200 µl of TE buffer (10m M Tris-Cl, pH8, 1 mM Na_2 EDTA) and the solution was transferred to a 1.5 ml Eppendorf tube. The solution was then centrifuged at maximum speed for two minutes in a microcentrifuge and the supernatant was recovered and transferred to a clean tube for storage at -20°C.

For initial genotyping of putative *A. thaliana* transformants DNA was extracted using The Extract-N-Amp Plant PCR Kit. The DNA was extracted from a small volume of plant tissue (~25 mg wet weight) by incubation in 100 µl Extraction Solution (kit reagent) at 95°C for ten minutes. 100 µl of Dilution Solution (kit reagent) was then added and mixed to neutralise inhibitory substances. The resultant extract was then ready for polymerase chain reaction (PCR) as described in section 2.4.5.

2.4.2 Plant total RNA extraction

For *P. patens* sporophyte and protonemal tissue, and *A. thaliana* leaf tissue, total RNA was extracted using the Spectrum™ Plant Total RNA Kit (Sigma-Aldrich). Approximately 100 mg of tissue was ground to a fine powder in liquid nitrogen with a mortar and pestle. 500 µl of Lysis Solution (kit reagent) supplemented with 5 µl 2-mercaptoethanol was added to each sample. This mixture was then transferred to a 1.5 ml Eppendorf tube, vortexed and incubated at 56°C for 3-5 minutes. The sample mixture was then centrifuged for three minutes at maximum speed to pellet cellular debris. The resultant lysate supernatant was added to a filtration column sitting in 2 ml collection tube and centrifuged at maximum speed for one minute. 750 µl of Binding Solution (kit reagent) was thoroughly mixed with the clarified lysate. This mixture was then applied (maximum of 700 µl at a time) to a binding column sitting in a 2 ml collection tube and centrifuged at maximum speed for one minute. The flow-through liquid was discarded and 500 µl of Wash Solution 1 (kit reagent) was added to the column followed by centrifugation at maximum speed for one minute. The flow-through liquid was decanted and 500 µl of Wash Solution 2 (kit reagent) was added to the column which was then centrifuged at maximum speed for 30 seconds. The flow through-liquid was decanted and this step was then repeated. The empty column was then centrifuged at maximum speed for one minute in order to dry the column. Any further residual flow-through liquid was then discarded. The column was then transferred to a clean 1.5 ml Eppendorf tube. 30-50 µl of Elution Solution (kit reagent) was then pipetted directly onto the centre of the binding matrix in the column and incubated at room temperature for one minute followed by centrifugation at maximum speed for one minute to elute. The purified RNA was in the resultant flow-through eluate which was stored at -80°C.

For mature *A. thaliana* anthers, thought to be high in enzyme-inhibiting compounds such as carbohydrates and phenolics, RNA was extracted using TRIzol® Reagent with an appropriate protocol. Once again approximately 100 mg of tissue (*A. thaliana* flowers) was ground in liquid nitrogen using a mortar and pestle. 1 ml of TRIzol® was added to the sample during grinding. After grinding, the sample was incubated at 37°C for two minutes and then left at room temperature for a further 5 minutes after which it was centrifuged at 12,000 rpm for 10 minutes at 4°C. The resultant supernatant was then collected into 1.5 ml Eppendorf tubes and placed on ice. 100 µl

of chloroform was mixed with the sample which was then incubated for three minutes at room temperature and centrifuged at 12,000 rpm for 20 minutes at 4°C. The supernatant was collected into fresh tubes, mixed with 300 µl of isopropanol, and incubated for 10 minutes at room temperature and a further 60 minutes at -20°C. The sample was then centrifuged at 12,000 rpm for 15 minutes after which the isopropanol was discarded and the resultant pellet washed with 70 % ethanol. The sample was then centrifuged at 7,500 rpm for five minutes. The ethanol was decanted and the pellet was air dried for approximately 20 minutes. Once dry, the pellet was dissolved in 40 µl of nuclease-free water.

2.4.3 DNA and RNA quantification

Quality analysis and quantification of DNA and RNA was conducted with 1.5 µl of sample using a NanoDrop ND-8000 UV-Vis spectrophotometer (ThermoScientific). Plasmid DNA quality and quantity was obtained using the same method. RNA integrity was also initially analysed with agarose gel electrophoresis. Samples exhibiting significantly degraded ribosomal RNA smears were discarded.

2.4.4 Reverse transcription/cDNA synthesis

0.1-10 µg of total RNA (in 12.5 µl nuclease-free water) was cleaned using a DNA-free™ kit in a 0.2 ml tube. 1.5 µl 10x DNase buffer and 1 µl of the enzyme rDNase I were added to the RNA solution which was then incubated for 30 minutes at 37°C in a Techne Touch Gene Gradient PCR Thermal Cycler (Krackeler Scientific). 1 µl of inactivation buffer was then mixed with the RNA solution and incubated at room temperature for two minutes to inactivate the enzyme. The mixture was then centrifuged at 13,200 rpm for 90 seconds in a microcentrifuge. The resultant supernatant was collected into new tubes. 10 µl of DNase-free RNA solution was then used as a template for synthesising the first strand of complementary DNA (cDNA). 2 µl of oligodT(18) (0.5 µg/µl) and 3 µl of nuclease-free water were added to the RNA solution which was then incubated at 70°C for five minutes. 5 µl of 5x RT Buffer and 5 µl of dNTP mix (10 mM) were then added to the solution which was incubated at 42°C for two minutes. 1 µl (200 units) of M-MLV Reverse Transcriptase was then added to the solution which was then incubated for a further 60 minutes at 42°C in a thermocycler.

2.4.5 Polymerase chain reaction (PCR)

BIOTAQ™ DNA polymerase was used for PCR amplifications carried out for the purposes of expression studies and general genotyping. For the production of high fidelity DNA amplicons for use in cloning, and for genotyping involving the amplification of fragments in excess of 5,000 base pairs, the proofreading DNA polymerase, KOD was used. Oligonucleotides were designed using Primer3 (frodo.wi.mit.edu).

PCR amplifications using BIOTAQ™ DNA polymerase were generally conducted using the following reaction conditions:

Template DNA/cDNA (50-1000 ng)	X µl
10 µM forward primer	2.5 µl
10 µM reverse primer	2.5 µl
10 mM dNTP mix	0.5 µl
10 x NH_4 buffer	2.5 µl
50 mM $MgCl_2$	1 µl
BIOTAQ™ DNA polymerase	0.2 µl
Sterile H_2O	up to 25 µl

Once mixed the reagents were cycled using a Techne Touch Gene Gradient PCR Thermal Cycler with the following protocol:

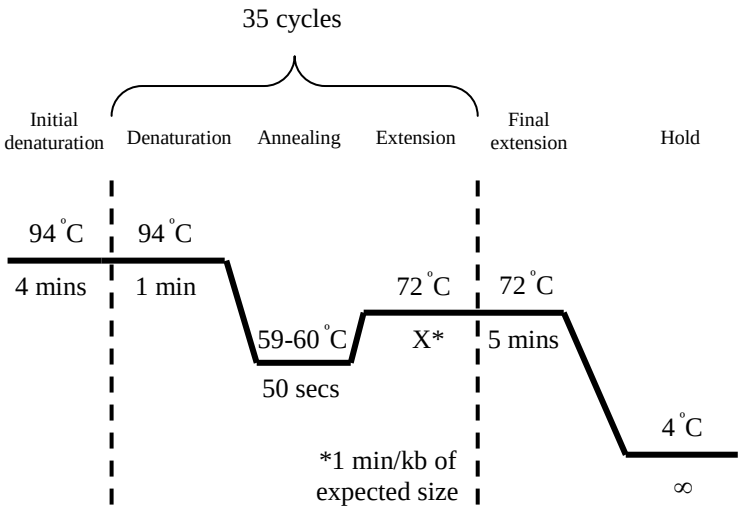

Amplifications using KOD Hot Start DNA Polymerase were generally carried out using the following reaction conditions:

Template DNA/cDNA (50-1000 ng)	X µl
10 µM forward primer	1.5 µl
10 µM reverse primer	1.5 µl
8 mM dNTP mix	3 µl
10 x PCR buffer	5 µl
25 mM $MgSO_4$	4 µl
KOD Hot Start DNA Polymerase	1 µl
Sterile H_2O	up to 50 µl

Once mixed the reagents were once again cycled using a Techne Touch Gene Gradient PCR Thermal Cycler with the following protocol:

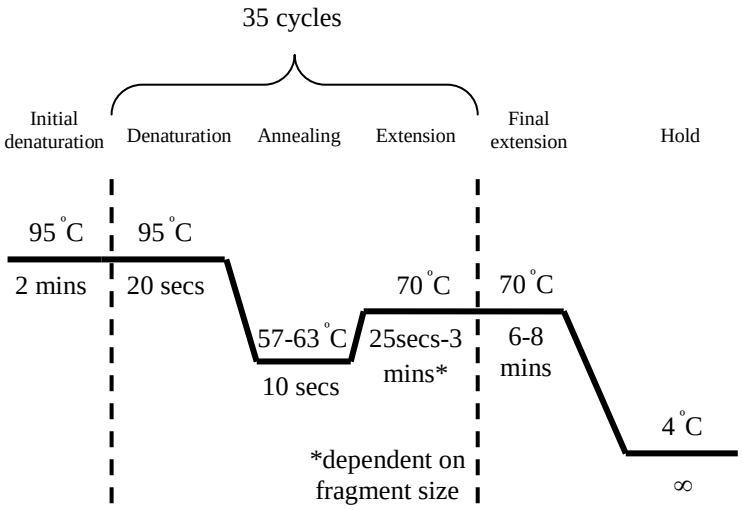

Table 2.1. Sequences of oligonucleotide pairs used in sq-RT-PCR *P. patens* microarray validation.

Oligo/Primer ID	**Forward Primer** (Sequence 5'→3')	**Reverse Primer** (Sequence 5'→3')
11916	TGGACATGCGACCTACTCTGG	CGCCAAACCCGTAGCAAATA
120173	GCTATGGGTGAAATGCTGGT	CCAAAAGGGCATTGACAACT
146196	TGCTCAATTGCCTACTGTGG	AACCGTCACCGCAATAAAAG
149962	CACTGCCATCTGCCTGTTTA	CGCTGCATTGATGGAGATTA
163268	ATGGGTCACGTCGACTTCAAA	CATGACTGTGAGGGGAGAAACA
100530	ACTGACCTCCAGGCAGTTGT	TACACAAATCCCCAATGCAC
184189	AGCTGTTCAGCTGGGAGAAA	TGCATTTCAGCCTTCACTTG
PpActin2*	GCGAAGAGCGAGTATGACGAG	AGCCACGAATCTAACTTGTGATG
Rubisco*	TTGTGGCTCCTGTCTCTGTG	CGAGAAGGTCTCGAACTTGG

* Housekeeping genes.

2.4.6 Semi-quantitative reverse transcription PCR (sq-RT-PCR)

Sq-RT-PCR, using cDNA obtained with the protocol described in section 2.4.4, was used for microarray validation. PCR reactions were set up in the same way as described in section 2.4.5. However, the reaction was paused at the beginning of the annealing stage (59-60°C) of cycles 20, 24, 28 and 32. At these intervals individual aliquots of 4 µl were taken and immediately placed on ice to stop the reaction. On completion of the program the aliquots were loaded in order into wells on an agarose gel (for protocol see section 2.4.7) followed by electrophoresis. The difference in rates of amplicon synthesis and associated band intensities provided a semi-quantitative approach for ascertaining relative gene expression levels. Oligonucleotides used for the sq-RT-PCR microarray validation are outlined in Table 2.1.

2.4.7 Agarose gel electrophoresis

DNA and RNA samples were separated on 1 % w/v agarose gels. Electrophoresis grade agarose was dissolved in 1x TAE buffer (0.04 M tris-acetate, 0.001M EDTA; 50x stock/litre, 2 M tris base, 57.1 ml glacial acetic acid, 0.05 M EDTA pH 8.0) by heating in a microwave. In a fume hood ethidium bromide was added to, and mixed with, the agarose solution (to a final concentration of approximately 0.5 µg/ml). The agarose solution was then poured into a gel rig with an appropriate tooth comb and

allowed to set. The comb was then removed and 1x TAE buffer was added to the gel rig so that the gel was submerged. Each DNA/RNA sample was mixed with 6x loading buffer (0.2 % w/v bromophenol blue, 50 % v/v glycerol) and loaded into separate wells. 5 µl of a size standard, Hyperladder I, which enabled the size and concentration of DNA/RNA fragments to be determined, was also loaded into a gel well. The gel was then electrophoresed at 90 V for 45-60 minutes. On completion of electrophoresis the DNA/RNA was either gel purified (section 2.4.8) or visualised with a BXT-20.M UV-transilluminator (Progen Scientific) and an UVItech Digital camera.

2.4.8 DNA gel extraction

DNA fragments were recovered from agarose gels using the QIAquick Gel Extraction Kit following a modified version of the manufacturer's protocol.

After electrophoresis, the DNA fragment was visualised with a UV-transilluminator and quickly excised from the gel using a clean scalpel blade and transferred to a pre-weighed 1.5 ml Eppendorf tube. The weight of the gel slice was then determined and three volumes of Buffer QG (kit reagent) were added. The sample was then incubated for 20-25 minutes at 50°C with regular mixing with a vortex to dissolve the gel slice. One gel volume of isopropanol was then mixed with the sample. The dissolved sample was then transferred to a QIAquick spin column seated in a 2 ml collection tube and centrifuged at 13,000 rpm for one minute to bind the DNA to the column membrane. The resultant flow-through was then decanted and 500 µl of Buffer QG was added followed by centrifugation at 13,000 rpm for one minute. This step removes all remaining traces of agarose. The flow-through was discarded and the column membrane was then washed with 750 µl of Buffer PE (kit reagent) for 20-25 minutes followed by centrifugation at 13,000 rpm for one minute. The flow-through was decanted and the column was centrifuged at 13,000 rpm for a further minute to dry the column. The column was then transferred to a clean 1.5 ml Eppendorf tube and 30 µl of nuclease-free water was added followed by incubation at room temperature for 20-25 minutes. The column was then centrifuged for one minute at maximum speed to elute the DNA which was in the resultant flow-through liquid and stored at -20°C.

2.4.9 Ethanol precipitation of DNA

Ethanol precipitation of DNA samples extracted using the CTAB protocol described in section 2.4.1 was undertaken to purify the samples prior to Southern blot experiments involving *P. patens*. 1/10 volume of 3 M sodium acetate (pH 5.2) and three volumes of 100 % ethanol were thoroughly mixed with each sample. Samples were then placed at -80°C for one hour. The DNA was then pelleted by centrifugation at maximum speed for 30 minutes at 4°C. The resultant supernatant was then decanted and the pellet was washed with 300 µl of 70 % ethanol and centrifuged at maximum speed for five minutes at 4°C. The supernatant was discarded and the pellet air dried for 15-20 minutes at room temperature. The DNA was then dissolved in 200 µl of TE buffer.

2.4.10 Southern blot

In order to determine whether *P. patens* knockout lines were single-copy replacement transformants a DNA probe was hybridised to a Southern Blot. The PCR DIG Probe Synthesis Kit was used to make and label the DNA probe using the following PCR reaction mix:

Template DNA (1-50 ng)	X µl
10 µM forward primer	2.5 µl
10 µM reverse primer	2.5 µl
PCR DIG Probe Synthesis Mix	2.5 µl
10 x PCR buffer with $MgCl_2$	2.5 µl
Enzyme mix	0.38 ul
Sterile H_2O	up to 25 ul

The labelled DNA probe consisted of a fragment (783 base pairs in size – FP, 5'-CGCACAATCCCACTATCCTT-3'; RP, 5'-AATATCACGGGTAGCCAACG-3') amplified from the CaMV35S-*npt*II-CaMV terminator selection cassette which had been excised from the pMBL8a vector. Once mixed the reagents were cycled using a Techne Touch Gene Gradient PCR Thermal Cycler with the following protocol:

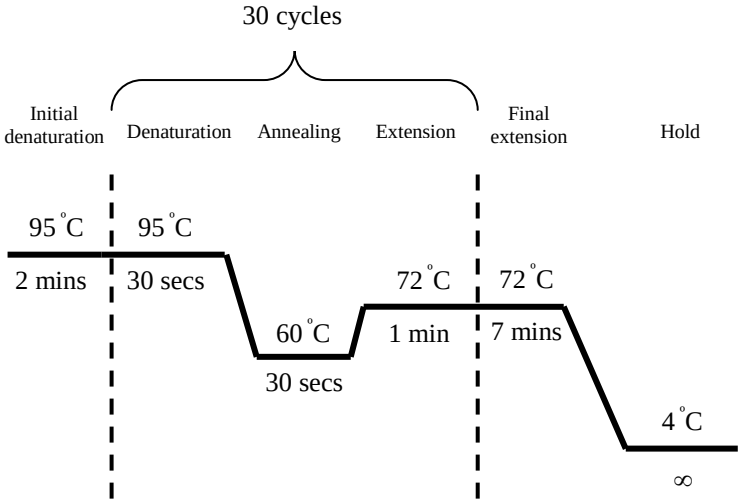

Genomic DNA from five putative *P. patens* knock-out lines were then cut by restriction digest with *Hin*dIII using the following reaction mix:

DNA (~10 ug)	X µl
10x restriction digest buffer 2	15 µl
10x Bovine Serum Albumin (BSA)	1.5 µl
*Hin*dIII restriction enzyme (1 U/µl)	14 µl
Sterile H_2O	up to 150 µl

The reaction mix was incubated overnight at 37°C and 'spiked' with 2 µl of additional *Hin*dIII followed by incubation for two further hours at 37°C. The digested DNA was ethanol precipitated and the pellet was resuspended in 30 µl of TE buffer and loaded onto an agarose gel (ethidium bromide replaced with SYBR® safe) and electrophoresed at 15-20 V overnight to separate the DNA fragments. A UV image of the gel was then taken with a ruler beside it for subsequent measurement. The gel containing the separated DNA was then depurinated by submerging and gently shaking the gel in 250 mM of hydrochloric acid for 10-20 minutes. The gel was then

rinsed with sterile water. The DNA was then denatured by submerging and gently shaking the gel in denaturation solution (0.5 M NaOH, 1.5 M NaCl) for 2 x 15 minutes followed by rinsing. The gel was then submerged in neutralisation solution (0.5 M Tris-HCl, pH 7.5; 1.5 M NaCl) for 2 x 15 minutes followed by equilibration for 10-20 minutes in 20x SSC. In order to transfer the DNA to a nylon membrane by capillary action a blot was set up (Fig. 2.2). A piece of Whatman 3MM paper, soaked

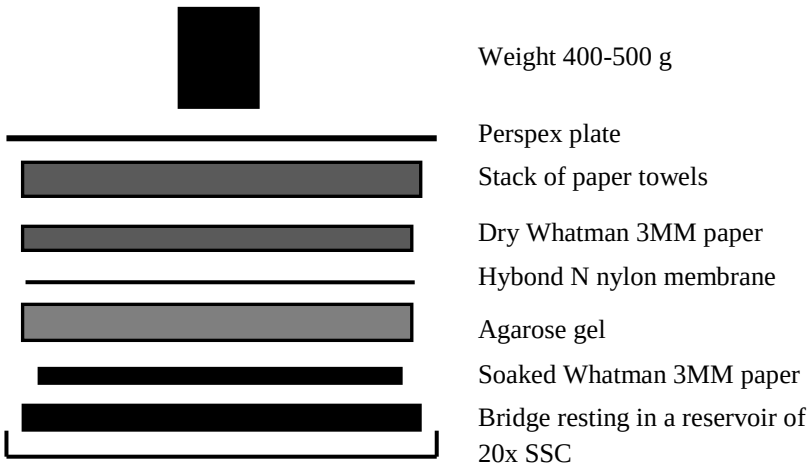

Figure 2.2. Southern blot assembly for capillary transfer of DNA from an agarose gel to a nylon membrane as recommended by Roche.

with 20x SSC, was placed atop a 'bridge' which rested in a shallow reservoir of 20x SSC. The gel was then placed atop the soaked sheet of Whatman 3MM paper (avoiding air bubbles). The positively charged nylon membrane, cut to the size of the gel, was then placed on top of the gel (any air bubbles were eliminated with a pipette tip). The blot assembly was completed by adding a dry sheet of Whatman 3MM paper, a stack of paper towels (~10 cm thick), a Perspex plate and a 400-500 g weight. The blot was allowed to transfer overnight in 20x SSC.

The following morning, while the blot was still damp, the DNA was covalently bound to the nylon membrane by UV crosslinking with a UV Stratalinker (at 120 mJ). The membrane was then allowed to dry and then placed into a clean hybridisation bag

which was heat sealed closely around the membrane. 15 ml of prewarmed (~46°C) DIG Easy Hyb was added to the bag which was then securely laid flat on the bottom of a rotating water bath and incubated at approximately 46°C for 30 minutes to prehybridise the membrane with the DIG Easy Hyb. 2 µl of the DIG labelled DNA probe was then mixed with 50 µl of nuclease-free water in a 1.5 ml Eppendorf tube and placed in a boiling water bath for five minutes to denature the probe. The probe was then quickly chilled in an ice bath. The denatured probe was then immediately added to a tube containing 5.25 ml of prewarmed DIG Easy Hyb and mixed by inversion to form the hybridisation solution. The hybridisation bag was cut open and the 15 ml of DIG Easy Hyb was removed by pouring. The hybridisation solution was quickly added to the bag which was then resealed (whilst minimising air bubbles) and securely placed back in the rotating water bath and incubated at approximately 46°C for 16 hours. At the end of the incubation the bag was opened and the hybridisation solution was poured off the membrane. The membrane was then quickly placed in a plastic tray containing 200 ml of low stringency buffer (2x SSC containing 0.1 % SDS) and incubated for five minutes at room temperature with gentle shaking. The used buffer was then poured off and 200 ml of fresh buffer was added to the membrane followed by incubation for a further five minutes. The low stringency buffer was poured off once more and 200 ml of high stringency buffer (0.1x SSC containing 0.1 % SDS), prewarmed to 68°C, was immediately added to the tray containing the membrane followed by incubation for 2 x 15 minutes with gentle shaking. The membrane was then rinsed in 200 ml of washing buffer (0.1 M maleic acid, 0.15 M NaCl; pH 7.5; 0.3 % (v/v) tween 20) for five minutes. The membrane was then incubated for 30 minutes in 100 ml of blocking solution (10 % (w/v) in maleic acid buffer) at room temperature followed by incubation in 20 ml of antibody solution for 30 minutes. Prior to incubation the antibody solution was centrifuged for five minutes at 10,000 rpm and the appropriate amount was carefully pipetted from the surface. Unbound antibody was then removed by way of incubation for 2 x 15 minutes in washing buffer (0.1 M maleic acid, 0.15 M NaCl; pH 7.5; 0.3 % (v/v) tween 20). After washing the membrane was equilibrated in 20 ml of detection buffer (0.1 M tris-HCl, 0.1 M NaCl, pH 9.5) for five minutes. The membrane was then placed in a clean hybridisation bag and 1 ml of CSPD (chemiluminescent substrate for alkaline phosphatase) was applied evenly over the membrane which was then incubated for five minutes at room temperature. Excess liquid was then squeezed out

of the bag and the damp membrane was incubated for 10 minutes at 37°C to enhance the luminescent reaction. The membrane, whilst in the sealed bag, was then exposed to X-ray film inside a cassette for 1-10 minutes. The film was then developed, visualised and imaged.

2.5 Cloning techniques

Oligonucleotides used in the techniques described in the following section are outlined in Table 2.2.

2.5.1 Generation of *ATMS2pro::PPMS2-1* and *ATUBQ14pro::PPMS2-1* constructs

For the attempted complementation of *A. thaliana ms2* mutants with the homologous *P. patens* gene, the Coding DNA Sequence (CDS) of the *PPMS2-1* gene (2202 base pairs) was amplified by PCR from *P. patens* sporophyte cDNA using the PpMS2-1 CDSF and PpMS2-1 CDSR primers. The destination vector p$POHA (Fig. 2.3) was then digested with *Eco*RV to excise the 'suicide cassette' and *PPMS2-1* CDS was then blunt-end ligated (section 2.5.4) into the vector. The resultant p$POHA::*PPMS2-1* vector was then digested with *Pme*I and *Spe*I to remove the *ATOST1* promoter. The *A. thaliana Hin*dIII *MS2* promoter fragment (1,077 base pairs), identified by Aarts *et al*. (1997), was then amplified by PCR (AtMS2proF and AtMS2proR primers) with a 3' *Spe*I overhang (sticky-end created by restriction digest with *Spe*I with the reaction mix outlined in section 2.5.4) and ligated into the cut p$POHA::*PPMS2-1* vector to create *ATMS2pro::PPMS2-1*. Sequencing showed that a histidine-tag located in the backbone in the linker region at the 5' end of *PPMS2-1* was not in reading frame with the moss gene and was therefore removed by digestion with *Aat*II and *Spe*I followed by self-ligation of the vector.

During PCR amplification of the CDS of *PPMS2-1* a splice variant of the gene (2,951 base pairs - CDS with introns 3,4 and 6) was also amplified and this was cloned into p$POHA using Gateway® cloning (sections 2.5.5 and 2.5.6) and then put under the control of the *ATMS2* promoter using the previously described method.

The *ATMS2pro::PPMS2-1* vector was also used to create a construct where *PPMS2-1* was placed under the control of the constitutive *A. thaliana UBIQUITIN* (*UB14*) promoter. *ATMS2pro::PPMS2-1* was digested with *Hin*dIII and *Xba*I in order to remove the *ATMS2* promoter. The *UB14* promoter (1,061 base pair fragment 12 base pairs upstream from the start codon) was amplified by PCR from *A. thaliana* genomic DNA (UBQ14F and UBQ14R primers) and blunt-end ligated into the cut vector to create *ATUBQ14pro::PPMS2-1*.

2.5.2 Generation of *Physcomitrella patens MS2-1* knock-out construct

To create the *PPMS2-1* construct, used to generate *P. patens* knock-out lines, the 5' and 3' flanking sequences (933 and 974 base pairs respectively) of the *PPMS2-1* CDS were amplified by PCR from genomic DNA (MS2upstF, MS2upstR, MS2downF and MS2downR primers). The 5' fragment was then blunt-end ligated into a *Hin*dIII site in a linker region of the pMBL8a (Fig. 2.4) vector immediately upstream of a CaMV35S-*npt*II-CaMV terminator selection cassette. The 3' fragment was introduced, again by blunt-end ligation into a *Sac*I site in the linker region on pMBL8a immediately downstream of the CaMV35S-*npt*II-CaMV terminator selection cassette. The knock-out construct was then linearised by PCR (3,711 base pair fragment amplified with MS2-1intF and MS2-1intR primers) in preparation for PEG-mediated protoplast transformation of *P. patens* (Fig. 2.5).

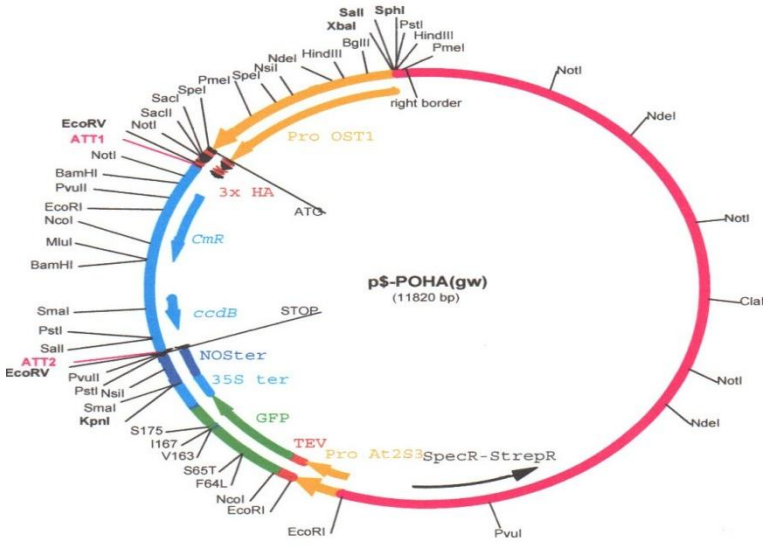

Figure 2.3. Map of the p$POHA vector used for complementation experiments involving homologous genes in *P. patens* (Belin 2006).

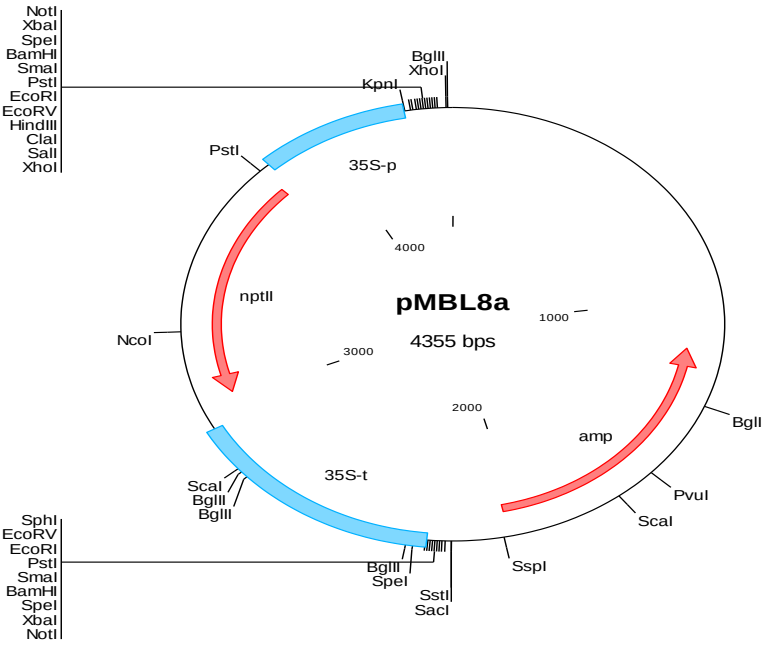

Figure 2.4. Map of the pMBL8a vector used for generating *P. patens* knock-out constructs.

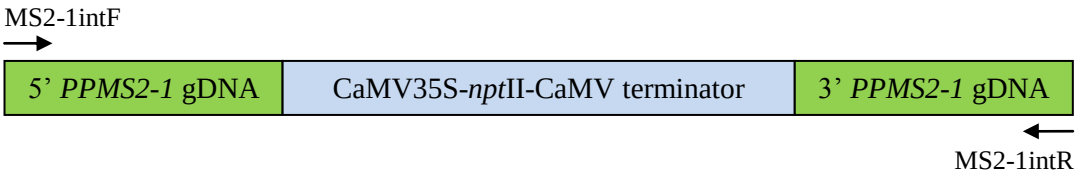

Figure 2.5. Schematic of the linearised *PPMS2-1* knock-out construct used for PEG-mediated transformation of *P. patens*.

2.5.3 Generation of *PPMS2-1pro::GUS* construct

To produce the *PPMS2-1pro::GUS* construct, used to examine the timing and locality of *PPMS2-1* expression, a 1,791 base pair fragment, 9 base pairs upstream of the *PPMS2-1* start codon, was amplified by PCR (PpMS2-1proF and PpMS2-1proR primers). The fragment was then cloned into the pGUSGW, ESfill C1 vector (Fig. 2.6), using Gateway® cloning, to generate vector *PPMS2-1pro::GUS* where the beta-

glucuronidase reporter gene was under the control of a putative *PPMS2-1* promoter fragment.

Table 2.2. Sequences of oligonucleotide pairs used in cloning experiments involving *A. thaliana* and *P. patens*.

Oligo/Primer name	Sequence (5'→3')
PpMS2-1 CDSF	CACCATGGAGGCAGTGTACAAGAC
PpMS2-1 CDSR	TCAAATTATGTGTGGAAAAGAACG
AtMS2proF	GCATTCTAGAGATCTAAGACAAAAACGTGGCCATT
AtMS2proR	CGCGACTAGTAAGCTTGTTGGTTAAGAAATTGG
UBQ14F	ATCCGAACAGAGTTAAACCGG
UBQ14R	AAAAACTGAGATTAATCGCTTGG
MS2upstF	CAAGGCGATTTGGTGAGTTA
MS2upstR	TCAGAGGAAGCTGCTTAGTTTCT
MS2downF	CTGACGGGGTAAGCGTTTTA
MS2downR	TTGGTTTCATAGCAGCAAGC
MS2-1intF	GCTGCATGTGTGAGGAGAGA
MS2-1intR	CAACGCTCAACCAATTAGCA
PpMS2-1proF	CGGTTCTCAATCTTGATACGA
PpMS2-1proR	AGAACCGCTTCTTCACTAGATA

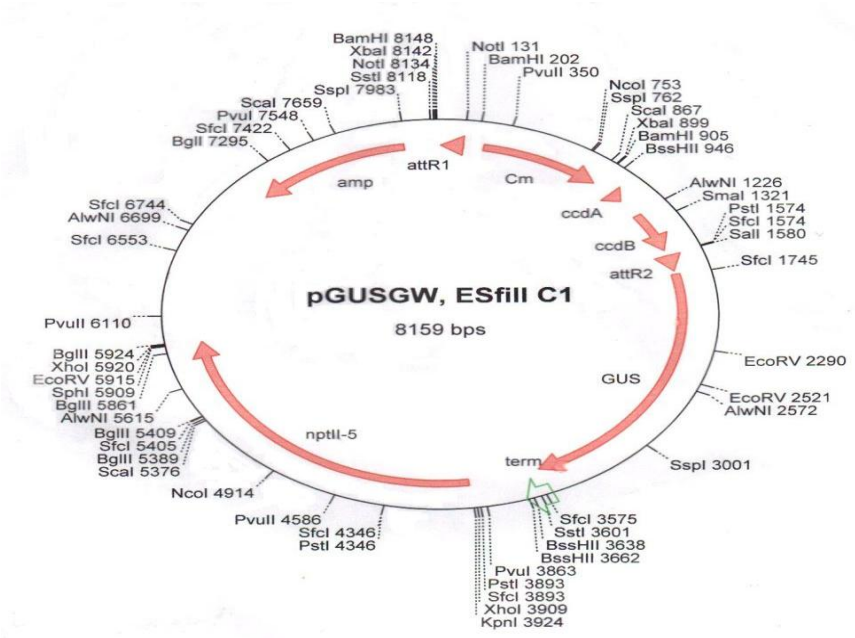

Figure 2.6. Map of the pGUSGW, ESfill C1 vector used for generating the *PPMS2-1*::GUS construct and subsequently examining the timing and locality of *PPMS2-1* expression.

2.5.4 DNA ligation

For blunt-end cloning the plasmid vector was digested with the appropriate enzyme(s). Typical reaction conditions were as follows:

Plasmid DNA (~2 ug)	X µl
10x restriction digest buffer	2 µl
10x BSA	2 µl
restriction enzyme(s) (1 U/µl)	1 µl (for each enzyme)
Sterile H_2O	up to 20 µl

The above mix was incubated for 2-3 hours at the appropriate restriction enzyme temperature (typically 37°C). The restriction enzyme(s) was heat inactivated at 65-80°C (depending on enzyme). 1 µl of DNA Polymerase I (Klenow) and 0.75 µl of dNTP mix (10 mM) were then added to the mix which was then incubated for 25 minutes at 37°C to fill-in 5'-sticky ends and/or trim 3'-sticky ends in order to create blunt-ends. DNA Polymerase I (Klenow) was then inactivated by incubating the mix at 75°C for 20 minutes. The blunt-ends of the plasmid were then dephosphorylated by the addition of 1 µl CIAP followed by incubation at 37°C for 60 minutes. The mix was then run on an agarose gel so that the digested blunt-ended DNA could be gel purified and quantified ready for ligation with an insert. If a restriction enzyme(s) which creates a 'natural' blunt-end was used then the fill-in/trimming step was not necessary.

Prior to ligation the insert was phosphorylated using T4 Polynucleotide Kinase in a reaction mix set up as follows:

Insert DNA	19 µl
5x DNA ligase buffer	5 µl
T4 Polynucleotide Kinase	1 µl

The mix was then incubated for one hour at 37°C and then for 15 minutes at 65°C to inactive the T4 Polynucleotide Kinase. The following 20 µl ligation mix could then be assembled:

Phosphorylated insert DNA	X µl	A molar ratio (insert:vector) of 3:1 was used
Digested plasmid vector	X µl	
10 mM ATP	1 µl	
5x DNA ligase buffer	4 µl	
Sterile H_2O	up to 10 µl	
T4 DNA Ligase	1 µl	

This mix was incubated overnight at 16°C in a thermocycler. The following morning the ligation mix was either stored at -20°C or immediately transformed into competent α-select (silver and bronze efficiency) *E. coli* cells (section 2.5.7). Putative transformed colonies were then cultured overnight in Luria-Bertani (LB) broth and the resultant plasmids were isolated (section 2.5.8), quantified and definitively verified.

For sticky-end ligation the fill-in/trimming, dephosphorylation and phosphorylation steps were not required and the molar ratio of insert:vector was less critical than with blunt-end ligation so a ratio of 1:1 to 3:1 was applied.

2.5.5 pENTR™/D-TOPO® topoisomerase reaction

Gel purified blunt-end inserts, generated by PCR with pENTR™/D-TOPO® compatible olignucleotides (CACC motif on 5' end of the forward primer), were initially cloned into the pENTR™/D-TOPO® entry vector and then recombined, using LR Clonase™ II, into an appropriate Gateway®-compatible destination vector. The TOPO® cloning reaction was assembled according to the manufacturer's protocol as follows:

Fresh PCR product	0.5 to 4 µl*
Salt solution	1 µl
Sterile H_2O	up to a final volume of 5 µl
TOPO® vector	1 µl
	6 µl

*0.5:1 to 2:1 molar ratio of PCR product: TOPO® vector.

The reaction mix was gently stirred and incubated for 5-30 minutes at room temperature. The mix was then placed on ice and 2µl of the reaction was used to transform either One-Shot® TOP10 or Mach1™-T1^R chemically competent *E. coli* cells. Putative transformed colonies were cultured overnight in LB broth and the resultant plasmids were isolated, purified, and quantified followed by definitive verification.

2.5.6 LR clonase reaction

Inserts from pENTR™/D-TOPO® were cloned into Gateway®-compatible destination vectors using LR Clonase™ II with an entry vector and destination vector reaction ratio of 1:1 in a reaction mix assembled in the following way:

Entry clone (50-150 ng)	1-7 µl
Destination vector (150 ng/µl)	1 µl
TE buffer, pH 8.0	up to 8 µl

The LR Clonase™ II enzyme mix was thawed on ice for two minutes and briefly mixed with a vortex. 2 µl of the enzyme mix was then added to the reaction which was then mixed briefly with a vortex and centrifuged for 5-6 seconds. The mix was incubated for 60 seconds at 25°C after which the reaction was terminated by the addition of 1 µl of Proteinase K solution, brief mixing by vortex and incubation for ten minutes at 37°C. 1 µl of the reaction mix was then transformed into either One-Shot® TOP10 or Mach1™-T1^R chemically competent *E. coli* cells. Putative transformed colonies were then cultured overnight in LB broth and the resultant plasmids were isolated, quantified and definitively verified.

2.5.7 Transformation of competent *Escherichia coli*

A 50-100 µl aliquot of competent *E. coli* cells was thawed on ice. 1-2 µl of a DNA ligation reaction mix or LR Clonase reaction mix was added and gently mixed with a pipette tip. The DNA and cell mix was then incubated on ice for 5-30 minutes. The mix was then heat-shocked for 30 seconds at 42°C and immediately transferred to ice. 250 µl of room temperature SOC medium (Super Optimal broth with Catabolite repression – 2 % w/v tryptone, 0.5 % w/v yeast extract, 0.4 % w/v glucose, 10 mM NaCl, 2.5 mM KCl, 10 mM $MgCl_2$, 10 mM $MgSO_4$) was then added to the mix which

was then shaken at 200 rpm for 60 minutes at 37°C. 50-200 µl of the transformation mix was then plated on LB plates (1 % w/v tryptone, 0.5 % w/v yeast extract, 1 % w/v NaCl, 0.5 % w/v agar, adjusted to pH 7.5) supplemented with the appropriate antibiotic (pENTR™/D-TOPO®: 50 µg/ml kanamycin, p$POHA derived vectors: 100 µg/ml spectinomycin, pMBL8a and pGUSGW, ESfill C1 derived vectors: 100 µg/ml ampicillin) for selection. Plates were then incubated overnight at 37°C. Verification of successful insertions was initially conducted with colony PCR (as per section 2.4.5 with a small amount of appropriate bacterial colony, transferred from an LB plate, as the DNA template). Putative positive colonies were then transferred and bulked up in LB broth (1 % w/v tryptone, 0.5 % w/v yeast extract, 1 % w/v NaCl, adjusted to pH 7.5) supplemented with the appropriate antibiotic and incubated for 16 hours at 37°C with shaking at 200 rpm.

2.5.8 Plasmid DNA preparation

Plasmid DNA preparation was conducted at room temperature using the QIAprep Spin Miniprep Kit following the manufacturer's protocol with minor modifications. 2 ml of an antibiotic supplemented LB broth culture was pelleted in a 2 ml microcentrifuge tube by centrifugation at 13,000 rpm for three minutes. The supernatant broth was then discarded. This step was repeated two more times using the same tube. The pelleted bacterial cells were resuspended in 250 µl of resuspension buffer P1 (kit reagent) using a vortex. 250 µl of lysis buffer P2 (kit reagent) was then added and mixed by gently inverting the tube 4-6 times. 350 µl of neutralisation buffer N3 (kit reagent) was then quickly added and the tube was gently inverted 4-6 times until the solution became cloudy. The solution was then centrifuged at 13,000 rpm for 10 minutes. The resultant supernatant was then applied to a QIAprep Spin Column seated in a 2 ml microcentrifuge tube and centrifuged at 13,000 rpm for one minute. The flow-through was discarded and the column was initially washed by adding 500 µl of buffer PB (kit reagent) and centrifuging the column for one minute at 13,000 rpm. The flow-through was decanted and further washing was carried out by adding 750 µl of wash buffer PE (kit reagent) to the column followed by incubation at room temperature for 5-10 minutes and centrifugation for one minute at 13,000 rpm. The flow-through was once again discarded and the column was centrifuged for a further minute at 13,000 rpm to remove residual wash buffer. The column was then placed in a clean 1.5 ml Eppendorf tube. 40-50 µl of nuclease-free water was then

applied to the centre of the column which was the left to stand for 10-15 minutes. The column was then centrifuged for one minute at 13,000 rpm. The isolated plasmid DNA was then in the resultant eluate which was stored at -20°C until further use in additional cloning procedures, plant/agrobacterium transformations and/or further verification with restriction digest or sequencing.

2.6 Transformation of *Arabidopsis thaliana* with *Agrobacterium tumefaciens*

2.6.1 Transformation of *Agrobacterium tumefaciens* with plasmid DNA

50 µl of *A. tumefaciens* (GV101::pMP90RK) electrocompetent cells were thawed on ice. 1 µl of plasmid DNA was added and mixed with the cells on ice and transferred to a pre-chilled sterile Eppendorf electroporation cuvette which was then subjected to 5 msec pulse of capacitance 25 µF, resistance 200 Ω and field strength 2.5 $kVcm^{-1}$ on a Bio-Rad Gene Pulser. 1ml of low salt LB broth (1 % w/v tryptone, 0.5 % w/v yeast extract, 0.5 % w/v NaCl, adjusted to pH 7.0) was then immediately added to the cuvette and the bacterial suspension was transferred to 10 ml of low salt LB broth and incubated for four hours at 28°C with shaking at 150 rpm. 50-200 µl of the bacterial broth was then plated on low salt LB agar plates containing 50 µg/ml gentamicin, 100 µg/ml rifampicin, 50 µg/ml kanamycin and 100 µg/ml spectinomycin. The plates were then incubated for 2-3 days at 28°C and then stored at 4°C.

2.6.2 Preparation of *Agrobacterium tumefaciens* for floral dipping

A modified version of the floral dipping method described by Clough and Bent (1998) was used for the transformation of *A. thaliana*. 5 ml of low salt LB broth containing the antibiotics described in section 2.6.1 was inoculated with an antibiotic-resistant *A. tumefaciens* colony from an LB plate which was then cultured overnight at 28°C in a sterile 50 ml Falcon tube with shaking at 150 rpm. 500 µl of the culture was added to 50 ml of antibiotic-free low salt LB broth in a sterile conical flask and cultured further overnight at 28°C with shaking at 150 rpm. Cells were then pelleted by centrifugation for 10 minutes at 5,000 rpm in a Heraeus centrifuge. The resultant supernatant was discarded and the *A. tumefaciens* pellet was resuspended, by way of gentle mixing, in 200 µl of 5 % sucrose solution to which 100 µl of silwet L-77 was added.

2.6.3 *Agrobacterium tumefaciens*-mediated transformation of *Arabidopsis thaliana* by floral dipping

Arabidopsis thaliana plants were grown until they flowered. The initial floral bolt was cut to promote the growth of multiple secondary stems. After 5-7 days, the plants were transformed by submerging flower buds in the *A. tumefaciens* sucrose/silwet solution (prepared as described in section 2.6.4) for 10-15 seconds. The plants were then placed in the dark and kept in high humidity for one hour. Dipping was repeated 2-3 more times, with 3-4 day intervals, on freshly bolted inflorescences. The plants were maintained until they set seed. Once the seed had been collected transformants were determined by the detection of seed-expressed green fluorescent protein (GFP) (Fig 2.7) with a Leica MZFLIII stereo microscope with GFP3 and B filters. Transformed plants (T_1 lines) were grown and PCR verification of the insertion was conducted using genomic DNA. Transgene expression was confirmed by RT-PCR using RNA extracted from flowers.

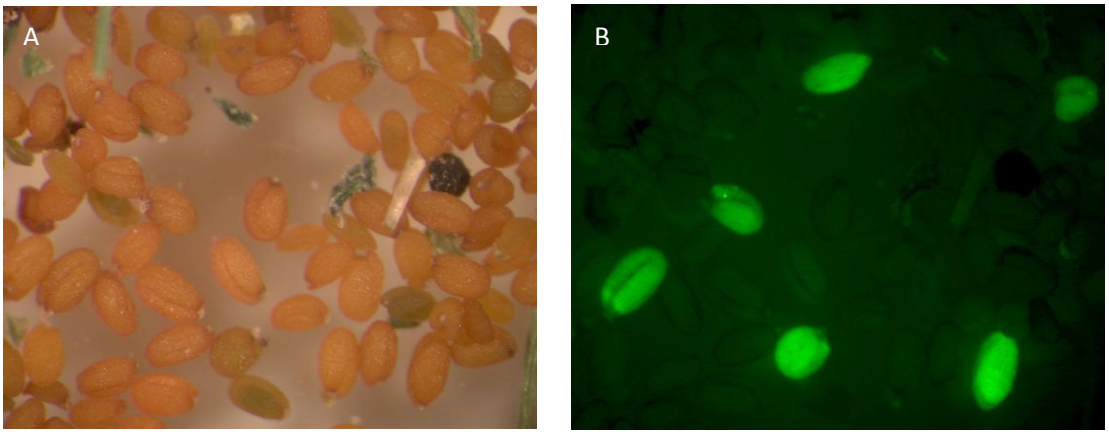

Figure 2.7. Detection of seed-expressed GFP in transformed *A. thaliana* plants. A, Brightfield seed. B, GFP seed.

2.6.4 Polyethylene glycol(PEG)-mediated transformation of *Physcomitrella patens*

Six day old wildtype *P. patens* protonemal tissue cultured on a BCDA agar plate covered by cellophane was scraped off the plate and transferred into 5 ml 1 % Driselase/8 % mannitol solution and gently stirred at room temperature for 30-40 minutes until the filamentous tissue was no longer visible and a protoplast suspension

had therefore formed. The protoplast suspension was then carefully applied to a 100 μm filter. The filtered protoplast suspension was transferred to a 25 ml plastic bottle and centrifuged at 700 rpm for four minutes. The resultant supernatant was removed leaving only a small volume (~0.2 ml) of the supernatant. The protoplasts were then initially resuspended in the remaining supernatant to loosen the pellet and then with the addition of 10 ml of sterile 8 % mannitol. At this point a 0.2 ml aliquot of the protoplast suspension was taken to ascertain protoplast density using a haemocytometer (mean number per 1 mm^2, n = 8). The centrifugation and resuspension steps were then repeated. The protoplasts were resuspended in sterile 8 % mannitol at 2x the required density for transformation (optimal density for transformation is $1.6x10^6$/ml). 150 μl of the protoplast suspension was then pipetted with wide-bored tips into 2 ml tubes with sterile 2xMaMg (for 100 ml - 6.1 g $MgCl_2 \cdot 6H_2O$, 8 g mannitol, 0.2 g MES) and gently mixed well with the pipette tip. 12-15 μg of DNA (in 30 μl of sterile water) was quickly added to the mix with further gentle mixing. The 2xMaMg/protoplast/DNA mix was then transferred to a 10 ml tube containing sterile PEGcms (for 10 ml – 0.236 g $Ca(NO_3)_2 \cdot 4H_2O$, 0.0476 g HEPES, 0.728 g mannitol, 4 g PEG6000) using a Pasteur pipette. The whole mix was pipetted gently once, returned to the tube, and heat-shocked for five minutes at 45°C. The PEG/protoplast mix was then diluted with sterile 8 % mannitol over a period of 30-60 minutes to allow the protoplasts a chance to recover from a high concentration PEG condition to a lower one, eg. 300 μl x 1, 600 μl x 2, 1 ml x 2, then volume brought up to 9 ml. In each dilution step the protoplasts were thoroughly, but gently, mixed by tilting and rolling the tubes. The diluted protoplasts were then centrifuged for four minutes at 700 rpm. Whilst centrifugation was taking place 50 μl of $CaCl_2$ was added to 5 ml of liquid protoplast regeneration medium-top layer (PRM-L) (BCDA + 6 % mannitol + 10 mM $CaCl_2$). The supernatant from the centrifuged diluted protoplast mix was then removed and the 5.05 ml of PRM-L was added and mixed gently with the protoplasts. The suspension was then incubated in the dark at 25°C overnight.

The following morning the protoplasts had sunk to the bottom of the tube and the supernatant was removed. Warm ≥45°C protoplast regeneration medium-top layer (PRM-T) (PRM-L + 0.4 % agar) was then quickly added and gently mixed and pipetted onto protoplast regeneration medium-bottom layer (PRM-B) (PRM-L + 0.55

% agar) plates overlaid with cellophane. The plates were then incubated under continuous light at 25°C. After 3-4 days the cellophane(s) attached to the PRM-T and cultures were transferred using sterile forceps to BCDA plates supplemented with adequate appropriate antibiotics. These plates were then incubated under continuous light at 25°C. Two weeks later, the same cellophane(s) were transferred to antibiotic-free BCDA plates and incubated under continuous light at 25°C. Two further weeks later the cellophane(s) were transferred to fresh antibiotic-supplemented BCDA plates for a second round of selection to eliminate transient transformants. After one week of incubation surviving colonies were deemed to be stable putative positive transformants and grown on antibiotic-free media for tissue collection, nucleic acid extraction, genotyping and phenotyping.

2.7 Phenotypic analyses

2.7.1 Scanning electron microscopy (SEM)

For SEM examination without fixation fresh spore capsules (punctured) and dehisced anthers were mounted on 12.5 mm diameter specimen stubs using adhesive carbon tape. Samples were then coated with 25 nm of gold in an Edwards S150B sputter coater and then viewed and imaged with a Phillips XL-20 microscope at an accelerating voltage of 10 Kv.

For SEM examination with fixation the specimens were primarily fixed in 3 % glutaraldehyde in 0.1 M phosphate buffer for four hours at 4°C. The specimens were then washed in 0.1 M phosphate buffer twice (15 minutes each time) at 4°C. Secondary fixation was carried out in 2 % aqueous osmium tetroxide for 60 minutes at room temperature. The wash step was then repeated. Specimens were then dehydrated in a graded series of ethanol at room temperature (75 % ethanol for 15 minutes, 95 % ethanol for 15 minutes, 100 % ethanol for 15 minutes x 2, 100 % ethanol dried over anyhydrous copper sulphate for 15 minutes). The specimens were then critical point dried and mounted, coated and viewed as previously described.

2.7.2 Transmission electron microscopy (TEM)

Spore capsules and anthers were fixed and dehydrated using the method described in section 2.7.1 although samples were incubated in primary fixative overnight. After dehydration the samples were transferred to glass vials to which 2-3 ml of the solvent, propylene oxide, was added. The sample was incubated for 15 minutes at room temperature after which the propylene oxide was decanted. This solvent step was then repeated. Samples were then infiltrated with a 50:50 Araldite/propylene oxide resin overnight at room temperature. The following morning samples were transferred to 100 % Araldite resin and incubated for 6-8 hours at room temperature. The samples were then embedded in fresh 100 % araldite resin, supplemented with BDMA (benzyl dimethylamine) accelerator, in an appropriate mould. The embedded samples were baked in an oven at 60°C for 48-72 hours. Once the resin blocks had set 85-90 nm sections were cut with a diamond knife, using a Reichert-Jung Ultracut E ultramicrotome, and mounted on copper TEM grids. Sections were then stained for 10 minutes with uranyl acetate in the dark and then with Reynold's lead citrate for a further 10 minutes. The sections were then viewed and imaged using a FEI Tecnai G2 Spirit TEM.

2.7.3 Spore germination test

Spore capsules were harvested and air dried for 3-5 days. Spores were germinated using the method described in section 2.2.5. Using a Leica dissection microscope the number of germinated spores were counted each day (for five days) after the spores were plated. The percentage of spores which germinated was calculated for each day (three replicates per *P. patens* line). A minimum of 200 spores per replicate were included in the analysis.

2.7.4 Acetolysis

A minimum of 200 spores per *P. patens* line were harvested in a small quantity of water in 1.5 ml Eppendorf tubes. Approximately 1 ml of glacial acetic acid was added to each sample which were then centrifuged for one minute at 13,000 rpm. The supernatant was decanted and ~1 ml a 9:1 (v/v) mixture of acetic anhydride and sulphuric acid was added to each sample tube. The samples were then incubated at ~70°C for 20-25 minutes. After incubation the samples were centrifuged for three minutes at 13,000 rpm. The acetic anhydride/sulphuric acid mix was then diluted with

water and decanted. The spores were then mounted on a glass slide and observed and counted using an Olympus compound light microscope.

2.7.5 Raman microspectroscopy

Spores of wildtype and mutant *P. patens* lines were placed on calcium fluoride slides with a drop of water. For each measurement a single spore was selected and spectra were acquired with a confocal Raman microscope (100 μm aperture pinhole). The linear polarised laser beam (λ = 532.25 nm) was targeted on spores using a charge-coupled device camera monitor and a motorised XY stage (0.1 - μm step). The acquisition time for one spectrum was 8-10 seconds. Spectra were processed for baseline correction and normalisation by LabSpec 5 software (Horiba Jobin Yvon Ltd., UK). Principle components analysis (PCA) was performed using SIMCA (v. 8.0, Umetri AB, Sweden).

CHAPTER 3. **The development of the *Physcomitrella patens* sporophyte**

3.1 Introduction

The ephemeral bryopsid moss *P. patens*, a member of the Funariaceae, is distributed widely throughout temperate zones, particularly in the northern hemisphere, where development is initiated in late summer by the germination of overwintered spores. It typically grows on the banks of rivers, lakes and ponds exposed by falling water levels (Prigge and Bezanilla 2010). Sporophytes develop in the autumn or early winter prompted by decreasing temperatures and shortening days (Hohe *et al*. 2002).

In common with vascular plants *P. patens* exhibits alternation of generations where it undergoes two distinct stages in its life cycle: a haploid stage (gametophyte) capable of producing gametes by way of mitosis, and a diploid stage (sporophyte) characterised by the ability of the moss to generate haploid spores via meiosis (Fig. 3.1). As with other bryophytes, the gametophyte in *P. patens* is the larger, longer-lived and nutritionally independent generation and is therefore dominant. The sporophyte does not become free-living and is nutritionally dependent on the gametophyte and is permanently attached to it (Haig and Wilczek 2006; Prigge and Bezanilla 2010).

Physcomitrella patens germinates from a haploid spore giving rise to protonemal filaments, the first component of the dimorphic gametophyte, which develop by growth of stem cells at the apex of each filament (Menand *et al*. 2007). Chloronemal cells with large and abundant chloroplasts (50-100 in number) are the first to emerge. As development continues the apical cells transition to caulonemal cells which are associated with fast growth. Side branching in chloronemal filaments eventually becomes modified to enable the emergence of gametophores, the second gametophyte component, which at their apex give rise to both antheridia and archegonia (*P. patens* is monoicious). The antheridia generate motile flagellate sperm (spermatozoids) which, when conditions are moist, swim to fertilise egg cells within archegonia (Prigge and Bezanilla 2010). Following gamete fusion, the zygote develops into the diploid generation, the sporophyte, which materialises as a proto-shoot structure

which remains relatively small and connected to the gametophore (Glime 2007). The sporophyte consists of a short seta and a spore capsule (sporangium) within which cells undergo meiosis to form haploid, unicellular spores which are ultimately dispersed into the environment.

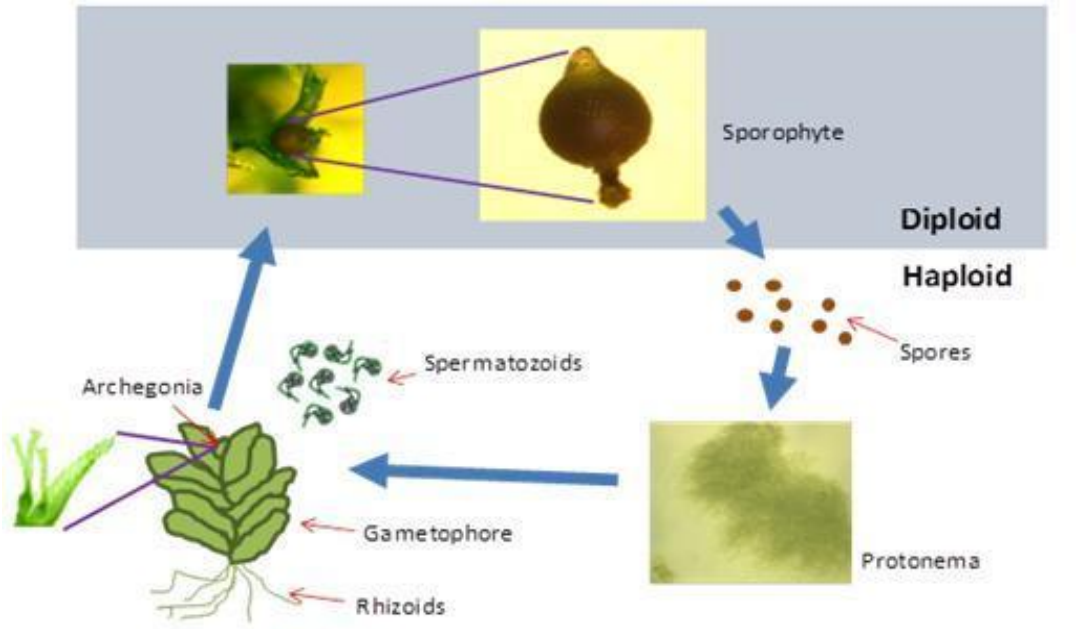

Figure 3.1. The life cycle of *P.patens*. In common with all embryophytes the life cycle of *P. patens* alternates between two morphologically and physiologically distinct generations, the haploid gametophyte and the diploid sporophyte.

Whilst there has been a significant increase in our understanding of many of the developmental processes associated with *P. patens* in recent years, only minimal progress has been achieved with regard to the development of its spore wall. Therefore the primary focus of this chapter is on spore wall formation in *P. patens* and how closely the wall construction processes in this moss conform to that of other embryophytes, particularly bryophytes, as described in section 1.2.3 of chapter 1. In order to illuminate these processes, such as layer deposition, timing and origin, wall ultrastructure is examined with the use of TEM. TEM analysis also allows the determination of wall development with respect to sporogenesis and the morphology

of the spore capsule. The following sporogenesis/spore capsule developmental stages in *P. patens* have been speculatively proposed (S. Schuette, University of Southern Illinois, USA, pers. comm. 2009):

1. Archesporial – Early sporophyte; spore capsules likely to be torpedo-shaped.
2. Pre-meiotic free spore mother cells – Spore capsules ellipsoid and translucent.
3. Free spore mother cells undergoing meiosis; spore capsules ovoid and translucent.
4. Post-meiotic microspores – Early spores within spore mother cells; spore capsules spherical and slightly yellow.
5. Free spores – Spore capsules spherical and dark yellow to brown.

The same source suggests that spore wall formation takes place in stages four and five based on TEM analysis of ultrastructural features. Huang *et al*. (2009) have offered the only other attempt to characterise sporogenesis/spore capsule maturation and have subdivided the process into four stages which can be described as follows based on their TEM analysis (Fig. 3.2):

1. Archesporial/spore mother cells – Spore capsules ovoid, lime green and slightly translucent.
2. Pre-meiotic free spore mother cells – Spore capsules spherical and dark green.
3. Post-meiotic microspores in tetrad – Spore capsules spherical and brown.
4. Free spores - Dehisced brown capsules.

This chapter therefore also aims to test and refine these proposed characterisations of spore wall development with respect to sporogenesis and spore capsule morphology. The basic general development of selected *P. patens* ecotypes is also compared with the current knowledge regarding its life cycle. Three ecotypes/lines were used in this study. The Gransden ecotype, collected in a field near Gransden Wood in Cambridgeshire, UK by H. Whitehouse in 1962 (Ashton and Cove 1977), is regarded as the standard laboratory strain and two Gransden lines, Gransden 2004 and GrD12, are included in this study. The Villersexel K3 ecotype, collected from Villersexel, Villers la Ville, France is also included. Both Gransden lines are derived from the original single isolate collected near Gransden Wood. Gransden 2004 is a direct self-

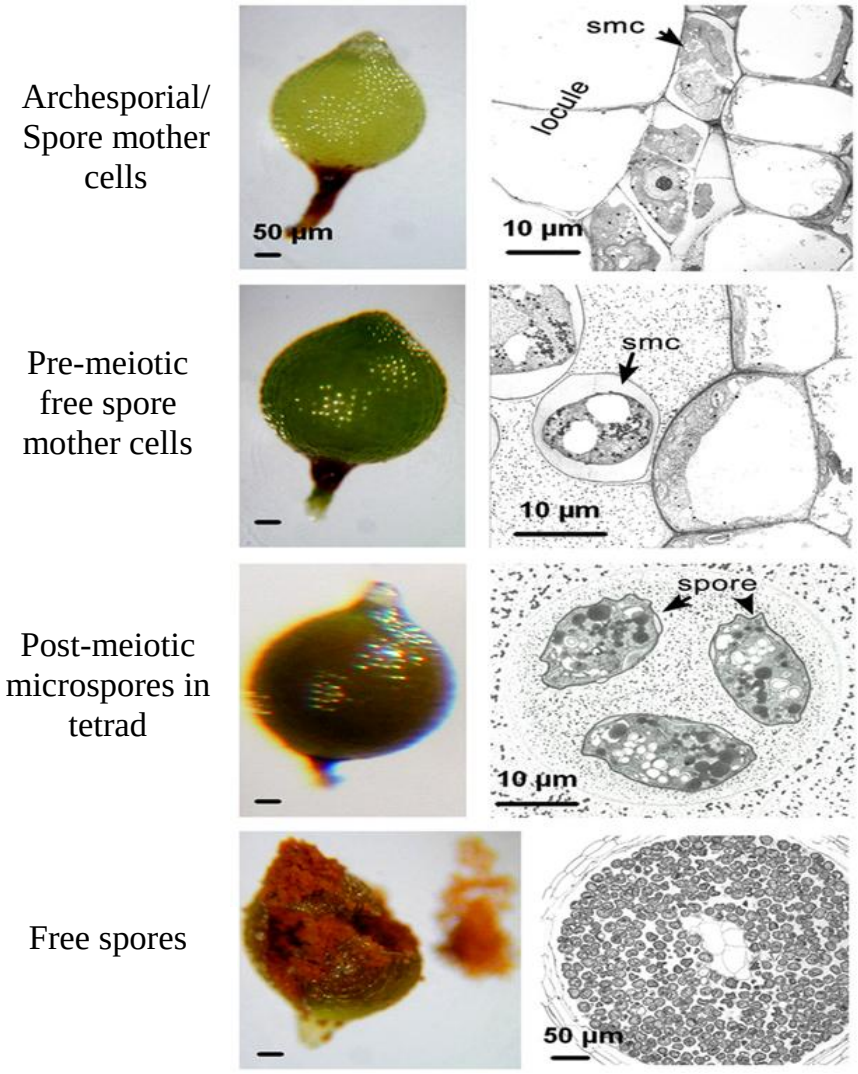

Figure 3.2. Proposed model by Huang *et al*. (2009) of sporophyte development with respect to sporogenesis in *P. patens*. Images in the left column show the entire sporophyte, and the right column consists of TEM images which show sporogenesis. Key: smc = spore mother cell. Modified from Huang *et al*. (2009).

fertilised descendant of the original isolate (derived from a single spore) and was the line used to sequence the *P. patens* genome. GrD12 was regenerated from a single spore of Gransden 2004 and is therefore a direct self-fertilised descendant of Gransden 2004. Given this history, there are likely to be very few genetic differences between these two Gransden lines although it is possible that there are epigenetic differences (A. Cuming, University of Leeds, UK, pers. comm. 2013).

3.2 Results

3.2.1 The life cycle of *Physcomitrella patens*

Spores from Gransden 2004, GrD12 and Villersexel K3 ecotypes/lines germinated 36-48 hours after being plated. Gransden 2004 and Villersexel K3 germinated spores were observed for five days after plating. In each ecotype 74-75 % of spores had germinated after five days (Fig. 3.3). In all three ecotypes/lines densely branched

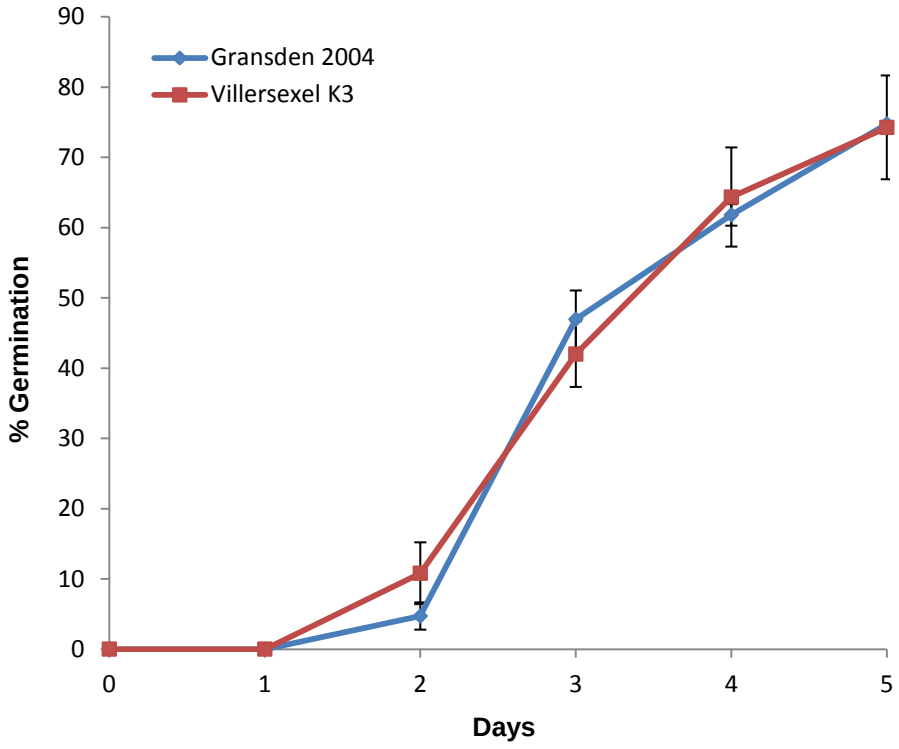

Figure 3.3. Spore germination for two ecotypes of *P. patens* (Gransden 2004 and Villersexel K3) under controlled axenic conditions (n=3).

protonemal tissue subsequently developed, followed by the formation of gametophores after approximately 14 days. Gametophore growth in Gransden 2004 was less vigorous than observed in the other two ecotypes/lines and took longer to reach full maturity whereby it could be possible for gametangia development to be induced. With GrD12 and Villersexel K3, cultures could be transferred to sporophyte induction conditions (see chapter 2, section 2.2 for full details of *P. patens* culturing conditions) approximately 14 days after initial gametophore development with abundant fully formed gametangia observed after approximately 7-14 days exposure to inductive conditions. Sporophyte development was initiated 7-14 days after gametangia maturation and abundant mature spore capsules (~0.6ml in diameter) could be observed after a further 21 days above and below water. Sporophytes which developed below the water surface were reduced in size and were approximately two-thirds of the size of those which developed above water. In total, the life cycles of GrD12 and Villersexel K3 take around 3-4 months to complete.

With Gransden 2004 gametophores took 2-3 weeks longer to reach full maturity and even after subsequent prolonged exposure to inductive conditions (more than one month), few gametangia were observed and very few sporophytes (typically less than ten) developed. The life cycle of Gransden 2004 therefore took 4-5 months to complete and exhibited greatly reduced fertility. The approximate durations of each life cycle stage for all three ecotypes/lines are summarised in Table 3.1.

Table 3.1. Summary of life cycle stages duration in three *P. patens* ecotypes/lines.

	Spore Germination (days)	Gametophore Initiation (days)	Gametophore Maturation Period (days)	Gametangia Initiation (days)*	Sporophyte Initiation (days)†	Sporophyte Maturation Period (days)	Total (months)
Gransden 2004	2	14	21-28	21-28	14-21**	21	4
GrD12	2	14	14-21	14	7-14	21	3
Villersexel K3	2	14	14	7-14	7-10	21	3

***** No. of days after transfer to inductive conditions (15˚C, 8 hour photoperiod).
† No. of days after gametangia maturation; **low frequency of sporophyte intiation (typically <10).

3.2.2 Sporogenesis and spore wall development in *Physcomitrella patens*

TEM images of spore wall ultrastructure were collated with TEM data acquired from analysis of early developmental stages of sporogenesis conducted by Huang *et al*. (2009) (Fig. 3.4). Attempts were made to acquire early stage images in-house. However, these attempts were unsuccessful as samples did not appear to fix and/or infiltrate well with Araldite or Spurr's resin (Electron Microscopy Supplies, USA) and as a result, post sectioning, they were severely misshapen and no cell detail could be discerned.

The TEM data allowed for the increased clarification of sporogenesis with respect to spore capsule morphology and the process could be characterised by six developmental stages (Fig. 3.4A). The first stage is termed, archesporial, at which point the spore capsules are torpedo-shaped, translucent and shrouded by calyptrae, and archesporial cells are in the process of giving rise to spore mother cells. The second stage is described as meiotic where the spore mother cells begin to undergo meiotic cell division which eventually produces four haploid microspores. On completion of meiosis the four microspores are joined together in a tetrad and TEM observation suggests that at this stage tetrads are still surrounded by the primary cell wall of the spore mother cell. The microspores also appear to have a distinct wall consisting of one layer, the exine, which is reasonably advanced in terms of development suggesting that the wall construction process may have begun as early as the meiotic stage. These early stages of sporogenesis occur over a period of 10-14 days. Very shortly after the completion of meiosis the microspores separate from their tetrad states and spore capsules at this stage are almost fully expanded, ovoid to spherical in shape, and lime green in colour. Approximately one week after this the spore capsules are fully expanded and yellow. At this point spore wall construction is nearing completion. After a further 4-5 days the capsules turn dark brown and spores are fully mature and ready for dispersal when the spore capsule eventually dehisces.

TEM analysis of the spore wall of *P. patens* suggests that wall formation most likely commences immediately after meiosis. The sporopolleninous exine is the first wall layer to form and seems to ultimately comprise two layers, an initial homogenous inner layer which when complete is approximately 0.2 µm thick, and a much thinner electron-dense outer layer which is around 25 nm thick. Both exine layers are

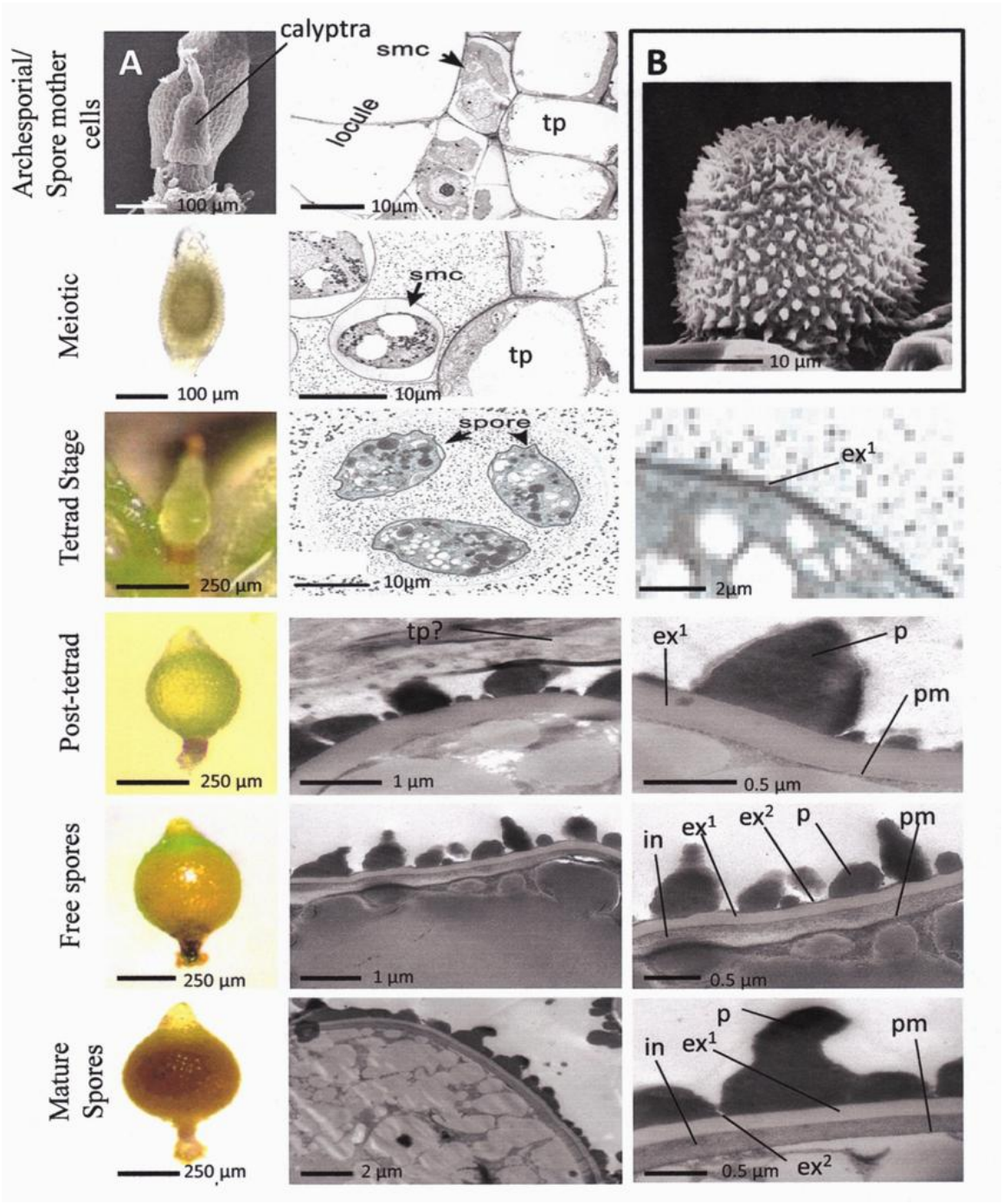

Figure 3.4. Sporophyte development in *P. patens*. A, Left column shows the entire sporophyte, and the middle and right columns consist of TEM images which show sporogenesis and spore wall development. The top four TEM images (archesporial – tetrad stage) were obtained by Huang *et al*. (2009). The remaining TEM images (post-tetrad (n=2), free spores (n=3) and mature spores (n=3)) were obtained in this study. The top three spore capsule images are included courtesy of C. Chater (University of Sheffield, UK). Key: smc = spore mother cell; pm = plasma membrane; p = perine; ex^1 = inner exine; ex^2 = outer exine; in = intine; tp = tapetum; smc = spore mother cell. B, SEM image of a mature spore.

uniform in thickness. The inner exine is the first layer to develop and is well advanced whilst the spores are in tetrads and is fully formed shortly after the microspores are released from the tetrad state. At the same stage, following tetrad release, the perine layer is rapidly deposited on the exine and consists of electron-dense sporopolleninous material most likely discharged from a degenerating tapetum layer, although the tapetum could not be definitively identified due to the previously described fixation and/or infiltration problems associated with this type of tissue. These problems meant that the sporophyte wall layers could only be clearly observed in a fully developed sporophyte (Fig. 3.5), at which point the tapetum would be expected to have completely degenerated.

The outer exine layer is only discernable shortly afterwards, at which point the final wall layer to develop, the fibrillar intine, has begun to form and is already near completion although not yet uniform in thickness. The perine then reaches completion forming the spore ornamentation consisting of dense pointed projections which can be up to 1µm in length (Fig. 3.4B). The completed perine conceals the outer exine layer which is presumably still present. The intine layer then becomes fully formed (~0.25 µm thick) and this concludes the process of spore wall formation. Mature spores range in size from 25-30 µm in diameter.

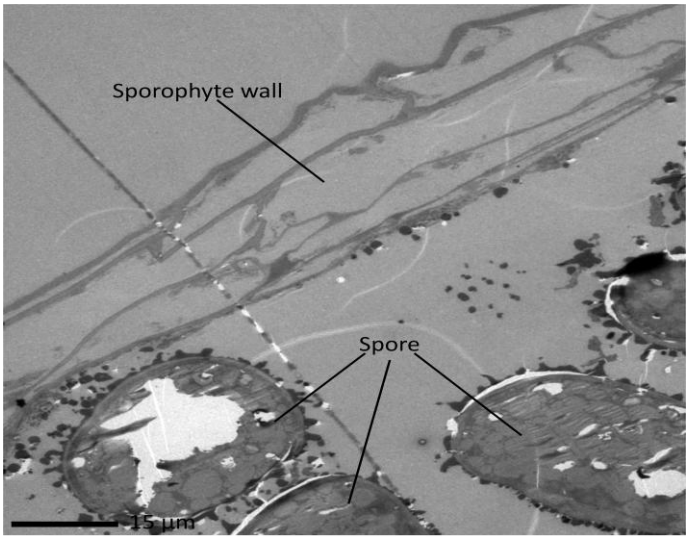

Figure 3.5. TEM image of a mature *P. patens* sporophyte section. Sporophyte wall structure can be clearly observed. The tapetum would appear to be completely, or mostly, degenerated at this stage.

3.3 Discussion

3.3.1 Life cycle variation among *Physcomitrella patens* ecotypes

The optimisation of the controlled conditions, using BCDA medium, for culturing the Gransden and Villersexel K3 ecotypes of *P. patens* enabled their life cycles to be completed in 3-4 months after subculture. The time periods associated with each developmental stage were also mostly consistent with previous studies (Nakosteen and Hughes 1978; Collier and Hughes 1982; Schaefer and Zryd 2001). However, these previous studies demonstrated that the life cycle duration of the Gransden strain could be reduced to around two months provided cultures were transferred to sporophyte induction conditions when only a very limited number of gametophores had matured (~15 days after spore germination). This modification to culture conditions meant that, whilst sporulation initiation was quicker, sporophyte abundance was greatly reduced which was not a practical approach for the studies conducted in this thesis.

One of the Gransden lines included in the study, Gransden 2004, did not consistently complete its life cycle as the sporophyte generation could not be easily induced. It is likely that further attempts to optimise culturing conditions would not improve sporophyte induction consistency in this line as years of culture in the laboratory appear to have considerably reduced its fertility, particularly as the limited amount of study conducted with regard to the sporophyte generation of *P. patens* suggests that Gransden 2004 has mostly been maintained vegetatively. It is possible that allowing cultures to regularly undergo sexual reproduction, and therefore regularly complete their life cycles, helps to maintain the reproductive vigour of a line. (A. Cuming, University of Leeds, UK, pers. comm. 2013). The levels of fertility exhibited by these lines should influence the choice of strain when embarking upon physiological and reverse genetic approaches involving the sporophyte generation.

3.3.2 Revision of developmental staging of sporogenesis

The TEM analysis conducted for this study suggests that previous propositions regarding developmental staging of sporogenesis with regards to spore capsule morphology require revision. In particular, this new data greatly contradicts the staging advocated by Huang *et al*. (2009). The TEM images presented here (Fig. 3.4) conclusively demonstrate that the intimation by Huang *et al*. (2009), that the spore

capsule has reached an advanced stage in its development (close to full expansion, ovoid and lime green) before the spore mother cells have undergone meiosis, is inaccurate. The results are somewhat more consistent with the staging proposed by S. Schuette (University of Southern Illinois, USA, pers. comm. 2009) although once again the speed of spore capsule development is overestimated with respect to spore development. When all data and proposals are considered the following model of sporogenesis with respect to spore capsule morphology can now be put forward:

1. Archesporial/spore mother cells – Early sporophyte; spore capsule at intial stage of expansion; formation of spore mother cells.
2. Free spore mother cells undergoing meiosis – spore capsules likely to be torpedo-shaped and mostly translucent/lime green. Spore wall construction initiated.
3. Early microspores/tetrad stage – spore capsules ellipsoid, mostly translucent/lime green.
4. Immediately post-tetrad/free spores - spore capsules ovoid to spherical and lime green.
5. Maturing free spores – spore capsules spherical and yellow.
6. Mature spores – spore capsules spherical and brown.

Additional TEM analysis is required to confirm or clarify the early stages of sporogenesis and therefore the first three stages of the above model can only be regarded as a revised hypothesis of sporogenesis in *P. patens*. Given the problems encountered in this study with regards to the fixation and infiltration of early stage spores, TEM preparation protocols need to be optimised further or different techniques need to be explored. Araldite resin was replaced with Spurr's resin, used successfully by Huang *et al*. (2009), in later attempts at obtaining TEM sections. Spurr's resin is considerably less viscous than Araldite resin and may therefore improve tissue infiltration. However, in this instance the use of Spurr's resin did not improve the quality of the sections which perhaps suggests that fixation is the primary problem. If further optimisation with resin and various fixatives does not yield improved results then the application of cryo-TEM could be investigated whereby the freezing of hydrated samples replaces traditional fixing and infiltration.

Despite the potential for further clarification, the updated characterisation and staging of sporophyte/spore development presented here increases our understanding of the maturation of the diploid stage in the life cycle of *P. patens*. This revision can also aid functional genomic approaches by assisting the pinpointing of which component or aspect of sporogenesis sporophyte-upregulated genes, or sporogenesis candidate genes, may be involved in based upon the morphology of the spore capsule.

3.3.3 Development of the *Physcomitrella patens* spore wall

The process of spore wall morphogenesis in *P. patens* is summarised in Fig. 3.6. Wall construction most likely begins immediately after meiosis at the early tetrad stage with the formation of the inner exine layer. However, TEM analysis shows that this layer already exhibits considerable thickness at this stage which suggests that it is not inconceivable that wall building commences even earlier during meiosis. The inner exine appears to lack the conspicuous lamellae seen in other early land plant groups and is of medium electron density and homogenous throughout its development, and at no point does it appear to be stratiform in character, although TEM images at early stages of wall development, particularly the tetrad stage, are required to confirm this as observations in other species have noted that lamellae are only briefly visible during wall development. The thinner outer exine is also homogenous and, in agreement with Schuette *et al*. (2009), forms a very minor part of the eventual ornamentation of the spore. Schuette *et al*. (2009), by way of their own TEM analysis, suggest that the inner exine is fibrillar. However, the TEM images presented in this thesis do not concur with this observation and conform to the observations of a non-fibrillar exine presented in the pioneering study on moss wall ultrastructure by McClymont and Larson (1964). Brown and Lemmon (1990) have previously noted the occurrence of an initial exine foundation layer in bryopsid moss spore walls which forms by the accumulation of sporopollenin on WLCL. This foundation layer was not observed in this study although, given that this layer is described as inconspicuous, it is likely that it is not easily detectable and, once again, further TEM images obtained at additional developmental stages may be required to confirm the presence or absence of this layer.

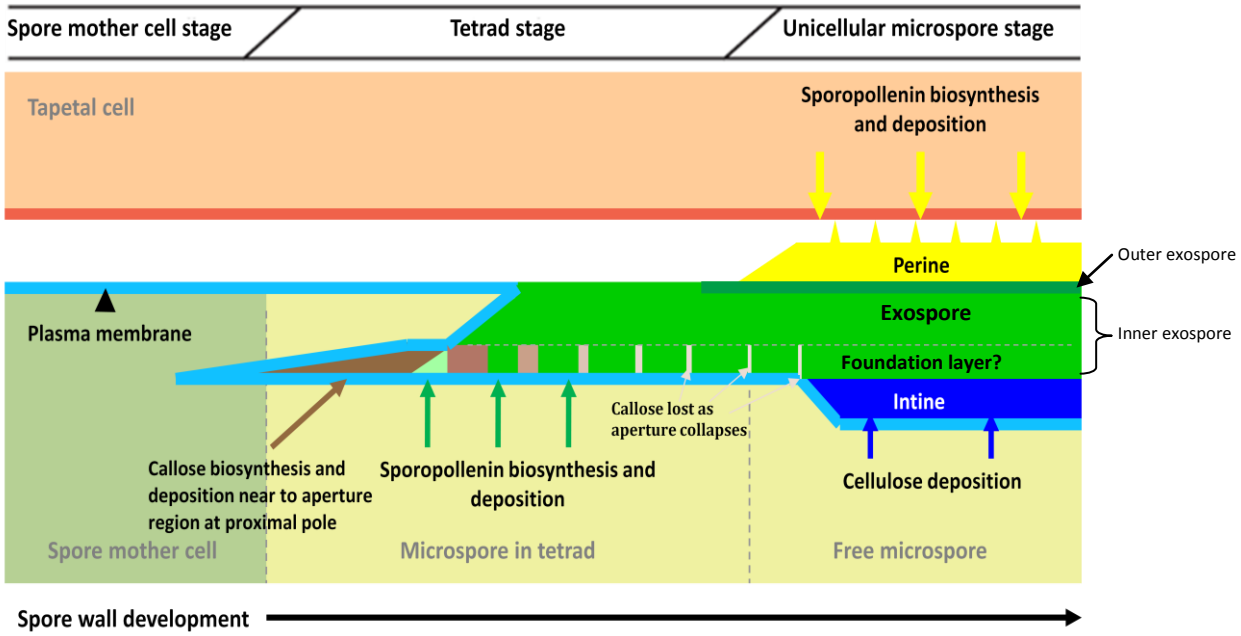

Figure 3.6. Proposed model of spore wall development in *P. patens*. The exine foundation layer is laid down first by way of sporopollenin accumulation on WLCL. The rest of the exine layer is deposited outside of the foundation layer centrifugally. Note the appearance of callose in the inner exine which is confined to the expanded aperture region at the proximal pole.

In addition to sporopollenin, Schuette *et al*. (2009) observed the accumulation of callose in the inner region of the exine in developing and mature spores and postulated that it was involved in aperture expansion and spore germination. Callose appears to play a major role in pollen wall development in gymnosperms and angiosperms, where a callose wall surrounds the tetrad and serves as a template for exine development. The role of callose in wall development in other groups is less well defined. In some bryophytes (Hepaticopsida: *Anthoceros*, *Geothallus*, *Riccia*; Bryopsida: *Mnium*) (Waterkeyn and Bienfait 1971), callose has been identified around the spore mother cell but its link to wall development, if any, is not well understood. It could be the case that, in 'lower' land plants, callose is relictual as it is involved in the reproductive systems of some algal groups (Gabarayeva and Hemsley 2006).

There continues to be much debate with regards to the source of the materials used to construct both spore and pollen exospores. In 'higher' land plants it is generally accepted that the tapetum provides most of the precursors required for the sporopolleninous exospore and therefore the diploid sporophyte is chiefly responsible

for the sporopollenin component of the pollen wall (Crang and May 1974; Piffanelli *et al*. 1998; Suzuki *et al*. 2008), and recent studies have demonstrated that several enzymes associated with sporopollenin synthesis are mostly localised to the endoplasmic reticulum of tapetal cells (Lallemand *et al*. 2013). Similar assertions have also been made with respect to 'lower' land plants (Uehara *et al*. 1991). The TEM analysis presented here suggests that much of the exine layer has already formed prior to the degeneration of the tapetum. This implies that the exine layer is most likely derived from the haploid spore and that the tapetum is probably solely responsible for providing sporopolleninous material for perine formation. It has been observed in gymnosperms and angiosperms that spherical vesicles, possibly consisting of fatty acids and synthesised by the endoplasmic reticulum in the cytosol (Gabarayeva and Hemsley 2006), can pass through the plasma membrane and secrete and add a sporopolleninous contribution to the exine (Dickinson and Bell 1970; Dickinson 1971; Zavada 1983; Gabarayeva 1996). These vesicles, or multimembrane inclusions, are involved in the processing, synthesis and/or transport of sporopollenin precursors (Pérez-Muñoz *et al*. 1993). Spherical vesicles are present and adjacent to the *P. patens* spore wall during the entirety of its development although further analysis is required to determine whether they pass and/or secrete material through the plasma membrane and therefore whether this mode and origin of sporopollenin synthesis is conserved in embryophytes. Chromatography has shown that many of these vesicles are lipidic oil bodies whose primary role is to store food for gluconeogenesis and subsequent germination (Huang *et al*. 2009), and affords spores remarkable longevity in ephemeral environments (Schuette *et al*. 2006).

Obvious sporopollenin precursor transport/secretory structures were not observed on the inner surface of the tapetum and this may suggest that the *P. patens* tapetum is probably not secretory and therefore it is likely that there is only a single and fairly rapid tapetal contribution to the spore wall where the electron-dense perine designated material is shed onto the near complete exine. The density and form of the resultant spinose perine projections are then possibly determined by a combination of a genetically controlled template system and self-assembly processes. The projections are very closely packed together, particularly when compared with the perines of other members of the Funariaceae such as *Physcomitrium pyriforme* and *Funaria hygrometrica* (Nakosteen and Hughes 1978). The non-secretory status of the tapetum

needs further confirmation and secretory tapeta have been observed in some mosses (Krystyna 1995). Once again, TEM artifacts associated with fixation/infiltration issues may have masked secretory structures and/or morphologies associated with secretory tapeta such as Ubisch bodies.

Finally, in common with many previously examined moss spores (McClymont and Larson 1964; Stetler and DeMaggio 1976) the intine layer of *P. patens* is fibrillar, lacking stratification and is the last wall layer to develop. A single-layered intine is not a constant feature of bryopsid mosses as stratification (up to three layers) has been reported in some species (Carrión *et al*. 1995; Estébanez *et al*. 1997). The fibrillar content of the *P. patens* intine is not obviously organised or specifically oriented and, in common with other embrypohytes, most likely consists of cellulose and pectin inclusions (Hess 1993; Suárez-Cervera *et al*. 2002). The intine is derived from the spore and in many land plants has been associated with the increased activity of dictyosomes in the cytoplasm (Heslop-Harrison 1968b; Echlin and Godwin 1969; Roland 1971).

The ultrastructural analysis presented here progresses understanding of spore wall development in this increasingly valuable model plant system. The results confirm that the formation of the spore wall is a relatively straightforward process, and given the greater complexity observed in the walls of 'higher' plants, is underpinned by flexible developmental processes which allow for swift evolution and specialisation in response to evolving lifestyles and changing environments.

3.4 Summary

The life cycles of three ecotypes/lines of *P. patens* were observed which enabled the determination of a tractable line(s) for use in research regarding sporophyte development. Essentially an ecotype/line in which abundant sporophytes could be consistently induced was sought and identified and used for the reverse genetics and gene expression analyses conducted in this study. TEM analysis of *P. patens* spore wall ultrastructure enabled wall development and sporogenesis, with respect to sporangium morphology, to be characterised, and previous propositions with regard to this to be substantially revised. The revised characterisation will better inform

experimental approaches, such as transcriptomic analyses, in future EvoDevo studies involving the *P. patens* sporophyte.

The wall ultrastructure data presented in this chapter further elucidates the processes which underpin wall formation. When this data is pooled with previous studies regarding wall development in mosses, updated hypotheses can be formed. It would appear that the sporopolleninous exine layer in *P. patens* is most likely predominately derived from the spore and the perine layer is entirely constructed from sporopolleninous material derived from a degenerating tapetum soon after tetrad release. A single-layered pectocellulosic intine derived from the spore is the final layer to develop. Increased understanding of wall construction processes will allow for improved understanding of phenotypic analyses conducted on spores of *P. patens* knock-out lines, as presented in later chapters in this thesis, and associated gene function.

CHAPTER 4. **Identification of candidate spore wall genes in *Physcomitrella patens***

4.1 Introduction

The data presented in chapter 3 add to the previous evidence gathered with regards to the spore walls of 'lower' land plants which suggest that, whilst their structure is considerably simpler than the walls of pollen grains, many of the developmental processes responsible for the formation of both spore and pollen walls are remarkably similar. This implies that the molecular mechanisms which underpin wall development in 'higher' plants may also be present, and function, in 'lower' land plants and therefore are conserved in embryophytes.

The developmental processes associated with pollen wall formation are controlled by intricate regulatory gene networks involving a number of structural proteins, metabolites and transcription factors. Additionally, in recent years a number of genes implicated in pollen wall development (genes identified in *A. thaliana* are described in chapter 1) have been linked to lipid metabolism (particularly fatty acids) and to polysaccharide metabolism (specifically callose, cellulose and pectin). Lipid metabolic pathways play a significant role in the synthesis of sporopollenin and most of the substances utilised for lipid metabolism are derived from acetyl-CoA of the tricarboxylic acid cycle (Ariizumi *et al*. 2011; Jiang *et al*. 2013). Whilst the biosynthetic route and genetics of sporopollenin are still not well understood a model of tapetum derived sporopollenin has been proposed. Fatty acids are synthesised in the plastids of the tapetal cells and transferred to the endoplasmic reticulum to be hydroxylated. The resultant hydroxylated fatty acids are then reduced to fatty alcohol groups and then covalently linked with phenylpropanoids to form sporopollenin precursors. These precursors are then translocated to the surface of the microspores via vesicular transport or an adenosine triphosphate binding cassette transporter, with the aid of lipid transfer proteins (Huang *et al*. 2011; Grienenberger *et al*. 2010; Ariizumi and Toriyame 2011; Jiang *et al*. 2013).

Polysaccharide metabolic pathways are strongly associated with intine formation, primexine formation, and the synthesis and degradation of the primary cell wall of the

pollen mother cell and the callose wall (Jiang *et al*. 2013). The synthesis of callose, a β-1,3-linked glucan (Dong *et al*. 2005; Jiang *et al*. 2013), involves the utilisation of UDP-glucose as a substrate, as does the synthesis of cellulose which consists of many β-1,4-linked D-glucose units (Updegraff 1969). The deposition of cellulose is catalysed by cellulose synthase complexes situated in the plasma membrane (Jiang *et al*. 2013). Pectin is mostly comprised of homogalacturan, rhamnogalacturan I and rhamnogalacturan II, and is synthesised in the Golgi apparatus. During the synthesis of pectin, which once again starts from UDP-glucose, the backbone of homogalacturan is in a methylesterified state and therefore consequently the pectins are fully methylesterified (Brett and Waldron 1996; Tucker and Seymour 2002).

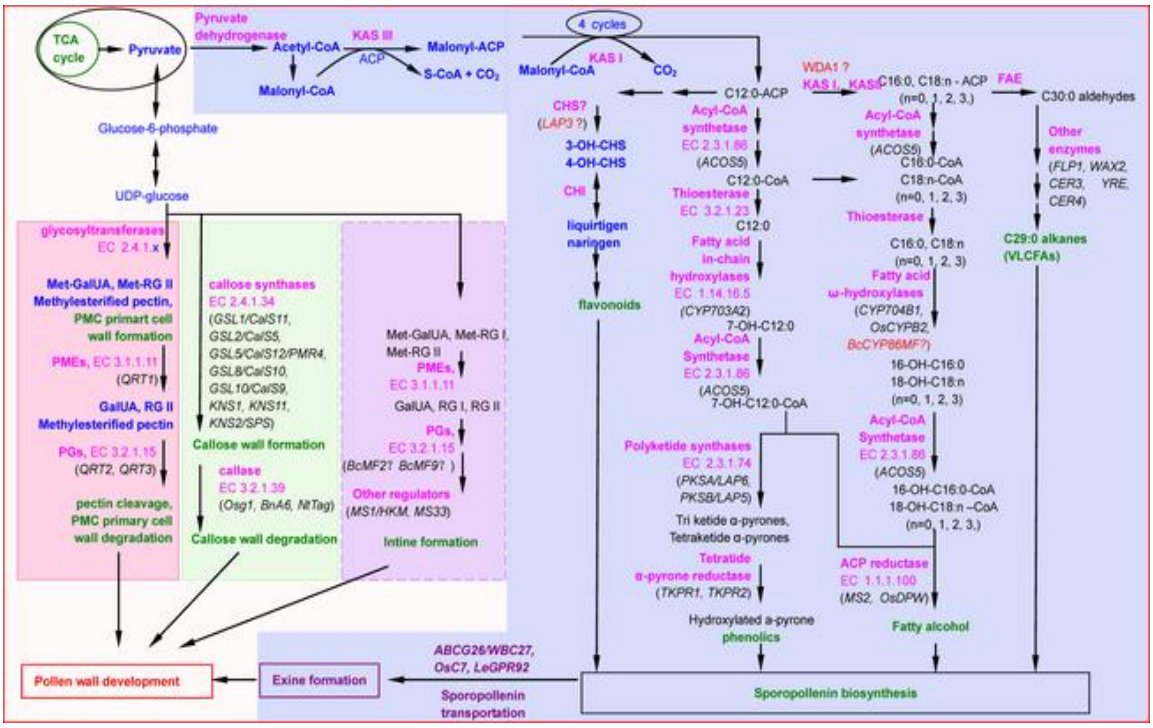

Figure 4.1. Schematic of metabolic pathways and associated enzymes involved in pollen wall development. The various pollen wall layers are shown in boxes. Putative genes which contribute in the metabolic pathways are displayed and the arrows indicate metabolic directions. The dashed box signifies a microspore origin for the intine. Other layers are proposed to be mostly synthesised in the tapetum. Key: CHS = chalcone synthase; CHI = chalcone isomerase; FAE = fatty acid elongation complex; KAS = 3-ketoacyl-ACP; PME = pectin methylesterase; PG = polygalacturonases. Taken from Jiang *et al*. (2013).

Jiang *et al*. (2013) recently proposed a model of pollen wall development in angiosperms which integrates the current knowledge regarding molecular genetic and metabolic pathway data (Fig. 4.1), much of which was introduced in chapter 1 and is described in greater detail later in this chapter. This model emphasises that the substrates involved and their associated products take part in metabolic pathways by way of a number of catalytic enzyme reactions. By considering this model alongside whole genome and transcriptome data of *P. patens* this chapter attempts to accumulate evidence to test the hypothesis that components of the pollen wall biochemical and developmental pathways are present in 'lower' land plants and have therefore been conserved across 400 million years of land plant evolution.

A bioinformatic strategy was taken to ascertain whether homologues of the *A. thaliana* pollen wall genes described in chapter 1 are potentially present in the genomes of *P. patens* and the emerging model lycophyte, *Selaginella moellendorffii*. A transcriptomic approach was then employed in order to obtain and compare gene expression profiles of the early gametophyte and two stages of the sporophyte generation of *P. patens* by way of microarray analysis, a sensitive technique for analysing gene expression across whole genomes, using RNA extracted from protonemal and dissected sporophyte tissue. Pre-expanded columnar spore capsules were used to represent the early developmental phase of sporophyte development (equivalent to the meiotic stage described in chapter 3), and ovoid to near spherical translucent lime green spore capsules were chosen to represent the mid developmental stage of the sporophyte (equivalent to the post-tetrad stage described in chapter 3) (Fig. 4.2). From this it was possible to identify whether potential homologues of *A. thaliana* pollen wall genes had significantly upregulated expression in the sporophyte and were therefore candidate genes likely to be involved in spore wall development of *P. patens*. The bioinformatic data associated with these candidate genes was then used to inform the selection of a single gene for further investigation by way of a reverse genetics approach (chapter 5).

The methods applied to conduct the experiments and analyses in this chapter, including BLAST parameters, microarray preparation and analysis, phylogenetic analyses and sq-RT-PCR, are outlined in detail in chapter 2.

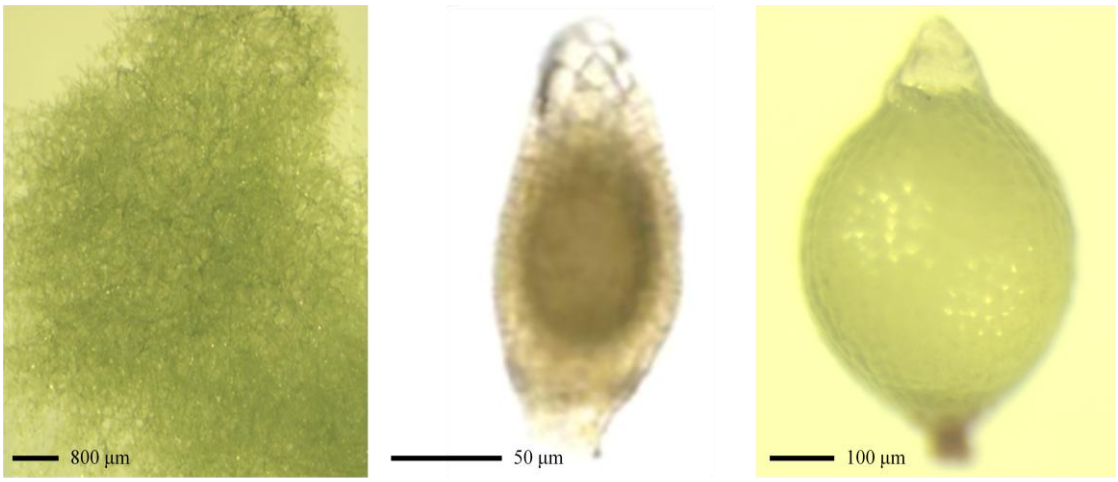

Figure 4.2. Developmental stages featured in the microarray experiment. mRNA was extracted from early gametophyte tissue (protonema), early (pre-expanded columnar capsules) and mid stage (ovoid to near spherical translucent lime green capsules) sporophytes for the microarray analysis. After hybridisation and normalisation the arrays were split into individual channels to allow the comparison of gametophyte vs. early sporophyte and gametophyte vs. mid sporophyte. Each comparison involved three replicate microarrays.

4.2 Results

4.2.1 *Physcomitrella patens* and *Selaginella moellendorffii* genome search results

Literature searches resulted in the identification of 37 *A. thaliana* genes implicated in the development of the pollen wall. At the time of writing of this thesis 26 of these genes had been annotated and their sequences were retrieved from the TAIR website. The protein sequences were used to search for homologous genes in the *P. patens* and *S. moellendorffii* genomes using TBLASTN. TBLASTN results suggest that homologues of all but one (FLA3) of the *A. thaliana* pollen wall associated genes are present in the *P. patens* genome with numbers of proposed homologues ranging from one for *NEF1*, *DEX1* and *TDE1/DET2* to in excess of 50 with *AtMYB103/MS188*. Similar results were observed in *S. moellendorffii* with homologues of almost all of the *A. thaliana* pollen wall associated genes present in its genome (with the exception of *QRT3*) ranging from two homologues in *DEX1*, *MS1* and *NEF1* to more than 50 once again for *CYP703A2*, *AtMYB103/MS188* and the callase related *A6* gene (Table 4.1).

4.2.2 Microarray analysis: expression profiles of spore wall candidate genes during sporophyte development

Microarray analysis indicated that a number of the *P. patens* pollen wall gene homologues are significantly upregulated at both early and mid sporophyte developmental stages. MA plots of each of the microarray replicates were used to determine a cut off value to initially guide the selection of genes for further investigation (Fig. 4.3). This cut off point was placed at the point at which outliers begin to appear on the MA plots (~1.25 – 1.4 log fold change in terms of upregulation). Corrected P-values were also considered although the Benjamini-Hochberg corrected p-value of $p \leq 0.05$ for significantly upregulated genes, the standard level of significance, is highly conservative and therefore results marginally in excess of this were not discounted.

Homologues of seven of the pollen wall associated genes, *QRT1*, *CYP703A2*, *CYP704B1*, *RPG1*, *MS2*, *ACOS5* and *QRT2*, have log fold change values in excess of the cut off boundary (Table 4.2). TBLASTN analysis suggested that homologues of *QRT1* comprise a large multigene family of 45 genes in *P. patens*.

Table 4.1. TBLASTN results of searches of the genomes of *P. patens* and *S. moellendorffii* with *A. thaliana* pollen wall genes. An e-value threshold of 1e-4 was used as an initial filter to determine number of homologues. Identity percentages (≥30%) and BLAST scores were then used to filter numbers further. Best match is defined as BLAST hit with the highest BLAST score.

General function in *A. thaliana*	*A. thaliana* gene	Gene reference	Proposed Gene class	No of proposed homologues in *P. patens* (no. significantly upregulated in the sporophyte)	% identity of best match in *P. patens*	BLAST score (bits) of best match in *P. patens*	No of proposed homologues in *S. moellendorffii*	% identity of best match in *S. moellendorffii*	BLAST score (bits) of best match in *S. moellendorffii*
Sporopollenin biosynthesis and exine formation	*MS2*	AT3G11980	Fatty acyl reductase	2(1)	48	1293	4	48	1221
	YRE/WAX2/FLP1/ CER3	AT5G57800	Aldehyde decarbonylase	4(0)	47	1528	9	49	1642
	CYP703A2	AT1G01280	Cytochrome P450	31(2)	46	1106	>50	46	1218
	CYP704B1	AT1G69500	Cytochrome P450	8(1)	57	1612	27	60	1514
	ACOS5	AT1G62940	Fatty acyl-CoA synthetase	11(2)	50	1378	26	51	1401
	RPG1	AT5G40260	Unknown Plasma membrane protein	6(3)	37	392	26	43	439
	NEF1	AT5G13390	Unknown plastid integral membrane protein	1(0)	44	2487	2	41	2168
	KNS5-10 (type 3)	-	Unknown	-	-	-	-	-	-
	KNS4 (type 2)	-	Unknown	-	-	-	-	-	-
	ABCG26	AT3G13220	ATP-binding cassette transporter	3(0)	46	1420	6	52	1593
	LAP5/PKSB	AT4G34850	Polyketide synthase	21(0)	57	1194	9	59	1149
	LAP6/PKSA	AT1G02050	Polyketide synthase	16(0)	50	944	9	47	932
	TKPR1/DRL1	AT4G35420	Oxidoreductase	7(0)	51	868	32	52	850

Continued

Table 4.1. ***Continued*.**

General function in *A. thaliana*	***A. thaliana* gene**	**Gene reference**	**Proposed Gene class**	**No of proposed homologues in *P. patens* (no. significantly upregulated in the sporophyte)**	**% identity of best match in *P. patens***	**BLAST score (bits) of best match in *P. patens***	**No of proposed homologues in *S. moellendorffii***	**% identity of best match in *S. moellendorffii***	**BLAST score (bits) of best match in *S. moellendorffii***
Sporopollenin biosynthesis and exine formation (cont.)	*TKPR2/CCRL6*	AT1G68540	Oxidoreductase	7(0)	52	881	31	52	879
	AtMYB103/MS188	AT5G56110	R2R3 MYB transcription factor	>50(0)	75	587	>50	66	482
	MS1	AT5G22260	PHD-type transcription factor	2(0)	37	1109	2	38	1124
	AtbZIP34	AT2G42380	bZIP transcription factor	13(0)	60	315	9	67	319
Exine formation (probaculae)	*DEX1*	AT3G09090	Unknown membrane protein	1(0)	70	1663	2	50	2210
	TDE1/DET2	AT2G38050	Unknown	1(0)	40	455	4	43	495
	KNS2, 3, 12 (type 4)	AT5G11110 (KNS2)	Sucrose phosphate synthase (KNS2)	2(0) (KNS2)	52 (KNS2)	2839 (KNS2)	4	53	2809
Intine formation	*FLA3*	AT2G24450	Fasciclin-like arabinogalactan	0(0)	n/a	n/a	5	33	221
	MS33	-	Unknown	-	-	-	-	-	-
	RGP1	AT3G02230	Reversibly glycosylated polypeptide	7(0)	83	1609	8	89	1656
	RGP2	AT5G15650	Reversibly glycosylated polypeptide	7(0)	84	1627	8	88	1657
Callose wall formation	*CALS5/LAP1*	AT2G13680	Callose synthase	12(0)	64	6575	13	64	6597
	KNS1,11 (type 1)	-	Unknown	-	-	-	-	-	-
Tetrad Separation	*QRT1*	AT5G55590	Pectin methylesterase	45(4)	47	804	45	54	821
	QRT2	AT3G07970	Pectin methylesterase	3(1)	41	733	20	44	823
	QRT3	AT4G20050	Endopolygalcturonase	2(0)	50	996	0	n/a	n/a
	A6	CAA49853	Callase	31(0)	43	982	>50	45	980

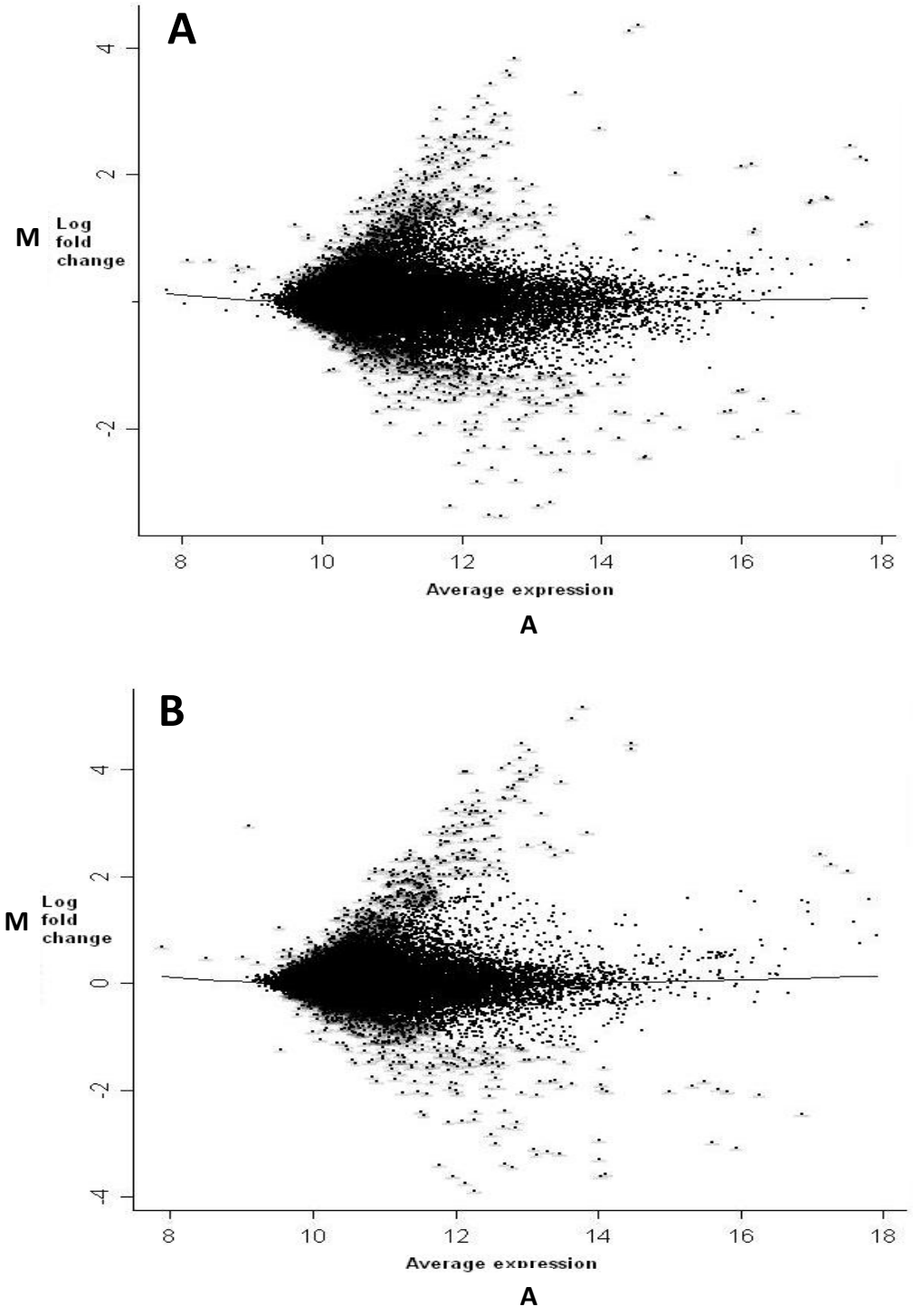

Figure 4.3. MA plots for *P. patens* microarray replicates. A, One replicate of gametophyte stage expression vs early sporophyte stage expression. B, One replicate of gametophyte stage expression vs mid sporophyte stage expression. Microarray data normalised within and between arrays. Plot shows level of up and down regulation of genes at early sporophyte stage compared to gametophyte stage. M represents log ratios (log (Cy3/Cy5) and A (logCy3+logCy5)/2 represents average log expression of each gene across the two developmental stages. Each spot represents a gene or control.

Four genes of this family (Pp_121276, Pp_135225, Pp_14944 and Pp_31639) are significantly upregulated during both early (1.66 – 2.57 log fold change from gametophyte stage) and mid (1.90 – 2.95) stages of sporophyte development. *CYP703A2* has 31 homologues in *P. patens*. Two members (Pp_201018 and Pp_186336) of this multigene family are significantly upregulated during early (1.44 – 1.58) and mid (1.58 – 1.74) sporophyte stages. *CYP704B1* has eight homologues in *P. patens*. One of these homologues (Pp_183927) has a log fold change value above the cut off boundary in both early (1.60) and mid (1.67) sporophyte stages. Six *RPG1* homologues are present in *P. patens*. One of these homologues (Pp_146196) is significantly upregulated at early and mid sporophyte stages (2.40 and 3.31) and two more (Pp_149962 and Pp_163268) are highly expressed (1.34 – 1.76) at the mid sporophyte stage. One of the two homologues of *MS2* in *P. patens* (Pp_11916) is significantly upregulated at early (1.70) and mid (1.41) sporophyte stages. 11 homologues of *ACOS*5 are present in *P. patens* and two of these genes (Pp_81614 and Pp_104959) are highly expressed in early (1.40 – 1.47) and mid (1.50 – 1.52) sporophyte stages. *QRT2* has three homologues in *P. patens*. One of these homologues (Pp_116593) is significantly upregulated at early (1.42) and mid (1.67) sporophyte stages. Microarray data for all *P. patens* homologues of *A. thaliana* pollen wall associated genes is presented in Appendices I and II.

The microarray data was validated by way of sq-RT-PCR experiments with a selection of genes using cDNA derived from RNA extracted from protonemal and mid sporophyte stage tissue (Figure 4.4). These genes consisted of four putative spore wall genes (Pp_11916, Pp_146196, Pp_163268 and Pp_149962), which the microarray data suggested were significantly upregulated at the mid sporophyte stage, and two genes (Pp_100530 (unannotated) and Pp_184189 (a leghemoglobin)), which exhibited the highest levels of downregulation in the mid sporophyte compared to the gametophyte in the whole of the microarray dataset. Additionally, one pollen wall homologue (Pp_120173), which was seemingly reasonably evenly expressed in both gametophyte and sporophyte tissue, and two control genes (rubisco and actin2) were included. The sq-RT-PCR experiments showed that all but one of these genes exhibited expression patterns which were strongly consistent with those suggested by the microarray analysis. This one exception was Pp_120173 which sq-RT_PCR showed was less evenly expressed than the microarray data predicted.

Table 4.2. Expression profiles of *P. patens* genes implicated in spore wall development derived from microarray analysis (gametophyte vs early sporophyte (GvsES) and gametophyte vs mid sporophyte (GvsMS)). Only genes with log fold change values in excess of the cut off boundary (1.25 (GvsES); 1.4 (GvsMS) log fold change) are included. Genes ranked by average expression log fold change (GvsMS). Average p-value for each gene in brackets.

Gene Name in *A. Thaliana*	Homologous Gene Transcript ID	Average Expression Log Fold Change GvsES	GvsMS
RPG1	Pp_146196	2.40 (5.82E-05)	3.31 (2.67E-05)
QRT1	Pp_121276	2.57 (0.0051)	2.95 (0.0016)
QRT1	Pp_14944	2.18 (0.0045)	2.50 (0.0016)
QRT1	Pp_135225	2.21 (0.0084)	2.45 (0.0017)
QRT1	Pp_31639	1.66 (0.0102)	1.90 (0.0030)
RPG1	Pp_163268	0.83 (0.0387)	1.76 (0.0017)
CYP703A2	Pp_201018	1.58 (0.0023)	1.74 (0.0004)
QRT2	Pp_116593	1.42 (0.0476)	1.67 (0.0178)
CYP704B1	Pp_183927	1.60 (0.0624)	1.67 (0.0409)
CYP703A2	Pp_186336	1.44 (0.0173)	1.58 (0.0043)
ACOS5	Pp_104959	1.40 (0.0211)	1.52 (0.0062)
ACOS5	Pp_81614	1.47 (0.0990)	1.50 (0.0830)
MS2	Pp_11916	1.70 (0.0321)	1.41 (0.0662)
RPG1	Pp_149962	0.92 (0.0031)	1.34 (0.0012)

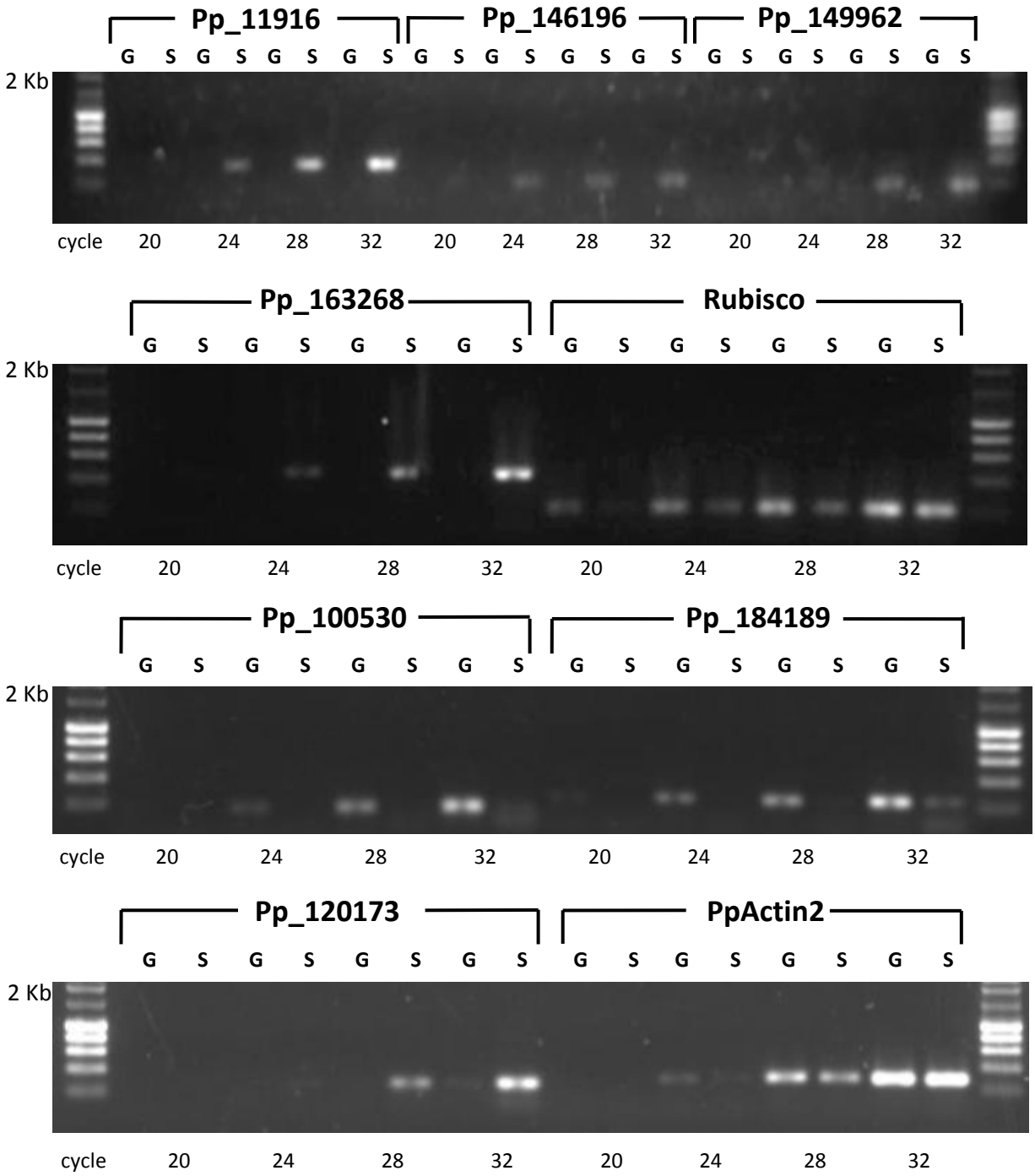

Figure 4.4. Sq-RT-PCR validation of microarray data. RNA was extracted from *P. patens* gametophyte (G) and sporophyte (S) tissue, reverse transcribed, then PCR was performed on spore wall candidate genes (Pp_11916, Pp_146196, 149962 and Pp_163268), and two genes (Pp_100530 and Pp_184189) which exhibited the highest levels of downregulation in the sporophyte. Additionally, one evenly expressed pollen wall homologue (Pp_120173) and two control genes (rubisco and actin2) were included. Amplified DNA was removed at different cycle numbers (20, 24, 28, 32 - as indicated) and run on an agarose gel.

4.2.3 Phylogenetic analyses

Maximum parsimony analysis was conducted using multiple alignments of protein sequences from putative land plant homologues of two *A. thaliana* pollen wall associated genes, *MS2* and *RPG1*, which in *P. patens* were deemed to be the strongest candidates for further investigation given the bioinformatic data presented in this chapter. With the *MS2* alignment, involving 24 protein sequences and a total of 709 positions, the most parsimonious tree recovered had a length of 3094 steps (Fig. 4.5A). This tree had a consistency index of 0.7116, a retention index of 0.7000, and a composite index of 0.4981 for parsimony informative sites. Putative *P. patens* homologues (Pp_11916 and Pp_120173) of *MS2* were resolved as monophyletic with very high bootstrap support (100%). The *RPG1* alignment involved 83 protein sequences and a total of 777 positions. The most parsimonious tree recovered was 5794 steps in length (Fig. 4.6) and had a consistency index of 0.3997, a retention index of 0.5752, and a composite index of 0.2299 for parsimony informative sites. The six putative *P. patens* homologues of *RPG1* were not resolved as monophyletic. Pp_146196, Pp_163268, Pp_149962 and Pp_136254 form a clade with strong bootstrap support (97%) and have a sister group relationship with four putative *S. moellendorffii RPG1* homologues. However, Pp_146546 is nested in a clade with four other putative *S. moellendorffii RPG1* homologues, and Pp_122188 is grouped with one putative *Populus trichocarpa RPG1* homologue albeit with very weak statistical support.

The tree with the highest log likelihood (-16441.4776) generated by maximum likelihood analysis of the *MS2* alignment is shown in Figure 4.5B. The tree exhibits a very similar topology to the tree generated by maximum parsimony analysis of the same dataset and once again the two putative *P. patens* homologues were resolved as monophyletic with very strong statistical support (bootstrap = 100%).

4.2.4 Electron microscope analysis of *Arabidopsis thaliana ms2* and *rpg1* pollen wall phenotypes

TEM analysis, in agreement with previous studies (Aarts *et al*. 1997; Dobritsa *et al*. 2009), shows that *A. thaliana ms2* mutants lack a normal exine layer which is replaced by arbitrarily deposited electron dense material (Fig. 4.7). A thin dark layer

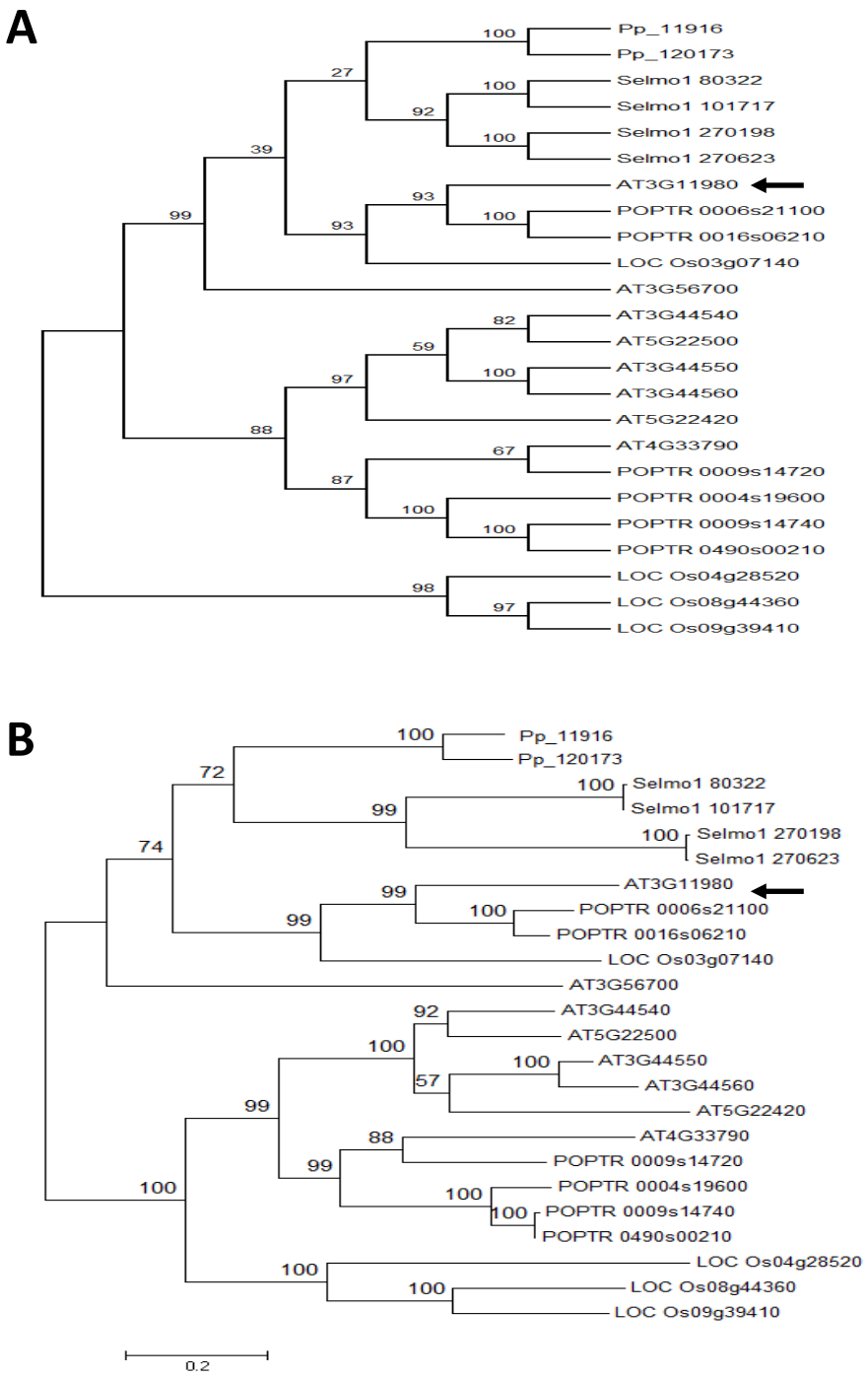

Figure 4.5. Phylogenetic analysis of *MS2* and homologous proteins. A, Maximum parsimony tree. Most parsimonious tree (length = 3094 steps) is shown. The consistency index is 0.7116, the retention index is 0.7000 and the composite index is 0.5102 for all sites and 0.4981 for parsimony informative sites. Bootstrap support values, based on 1000 replications, are shown above branches. B, Maximum likelihood tree based on the Whelan and Goldman model. The tree with the highest log likelihood (-16441.4776) is shown. The tree is drawn to scale, with branch lengths measured in the number of amino acid substitutions per site, with a scale provided at the bottom of the tree. Bootstrap support values, based on 1000 replications, are once again shown above branches. The arrow indicates *MS2* (AT3G11980).

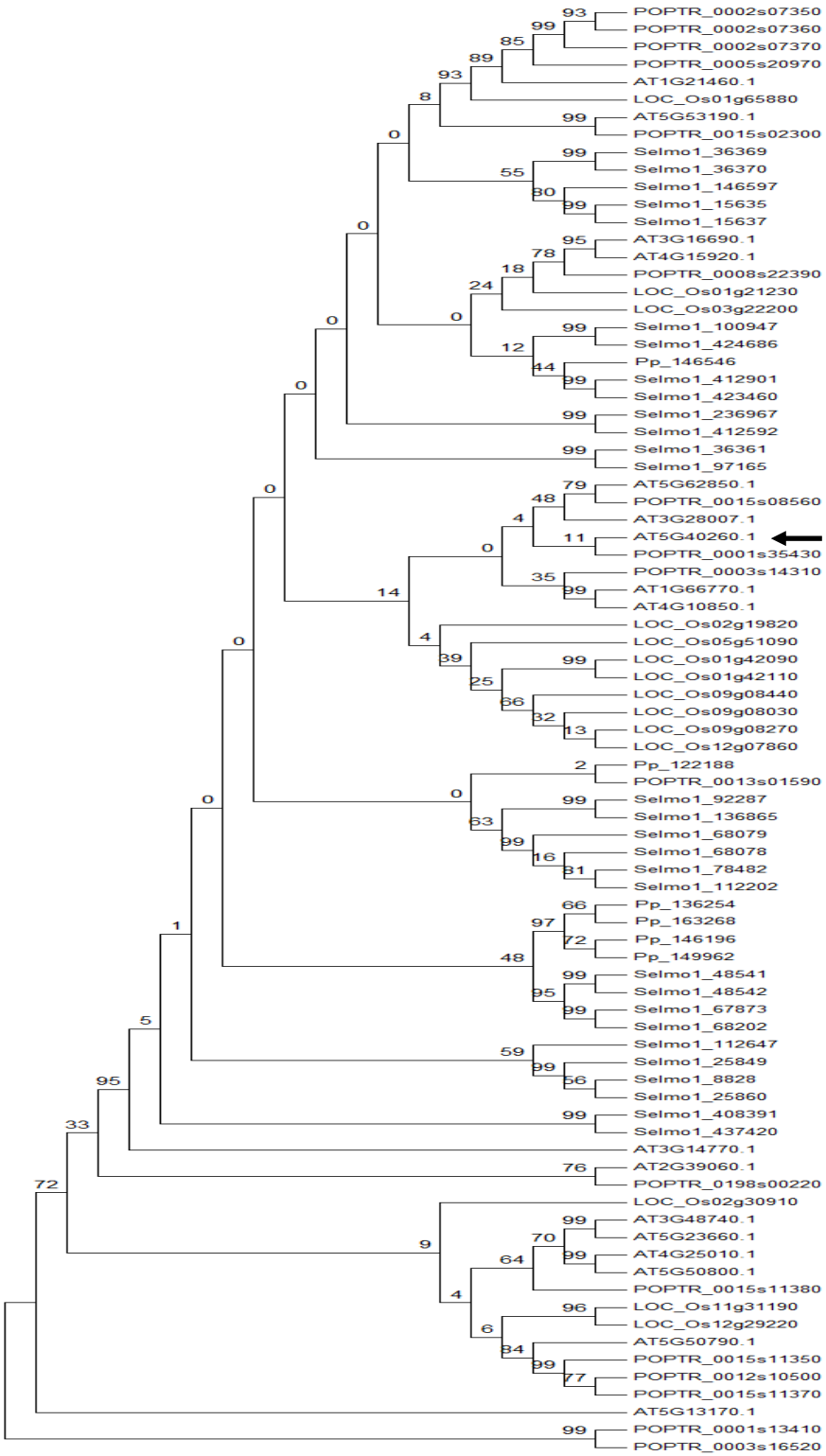

Figure 4.6. Maximum parsimony phylogenetic analysis of *RPG1* and homologous proteins. Most parsimonious tree (length = 5794 steps) is shown. The consistency index is 0.3997, the retention index is 0.5752 and the composite index is 0.2431 for all sites and 0.2299 for parsimony informative sites. Bootstrap support values, based on 1000 replications, are shown above branches. The arrow indicates *RPG1* (AT5G40260).

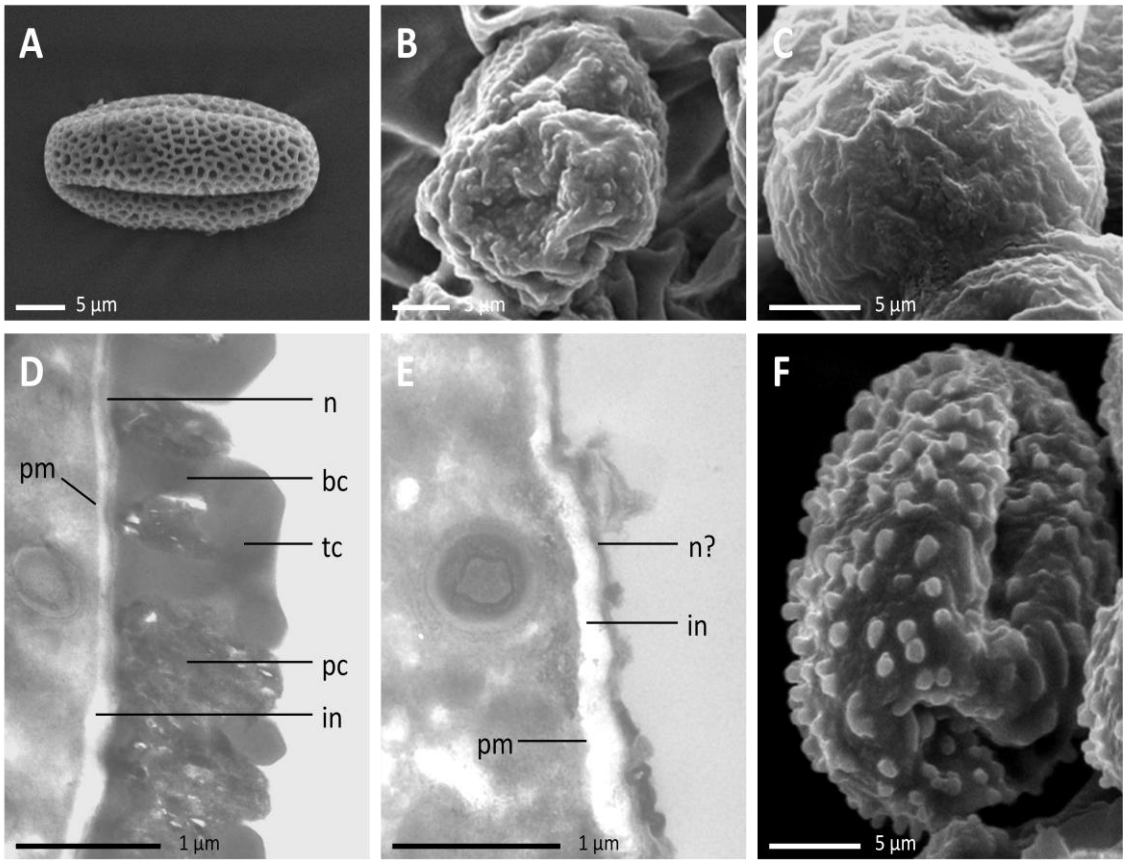

Figure 4.7. Electron microscope analysis of *ms2* and *rpg1* pollen wall phenotypes in *A. thaliana*. A (SEM without fixation) and D (TEM), Col-3 wildtype. B (SEM without fixation), C (SEM with fixation) and E (TEM), *ms2* (SAIL_75_E01). F (SEM without fixation), *rpg1* (SALK_142803). Key: n = nexine; bc = baculae; tc = tecta; pc = pollen coat; in = intine; pm = plasma membrane.

(<0.1µm) covering the intine, which may possibly be the nexine, can also be observed. SEM analysis demonstrated that mature unfixed *ms2* pollen grains collapse under the vacuum condition of the SEM. Fixed mature *ms2* pollen grains lacked the characteristic apertures of wildtype pollen and were much more spherical in shape.

SEM analysis of *A. thaliana rpg1* mutants was also in consensus with previous studies (Guan *et al*. 2008) by showing that most *rpg1* pollen grains were ruptured and/or collapsed and exhibited defective exine patterning with sporopollenin seemingly deposited randomly on the pollen surface resulting in a spotted exine phenotype (Fig. 4.7F).

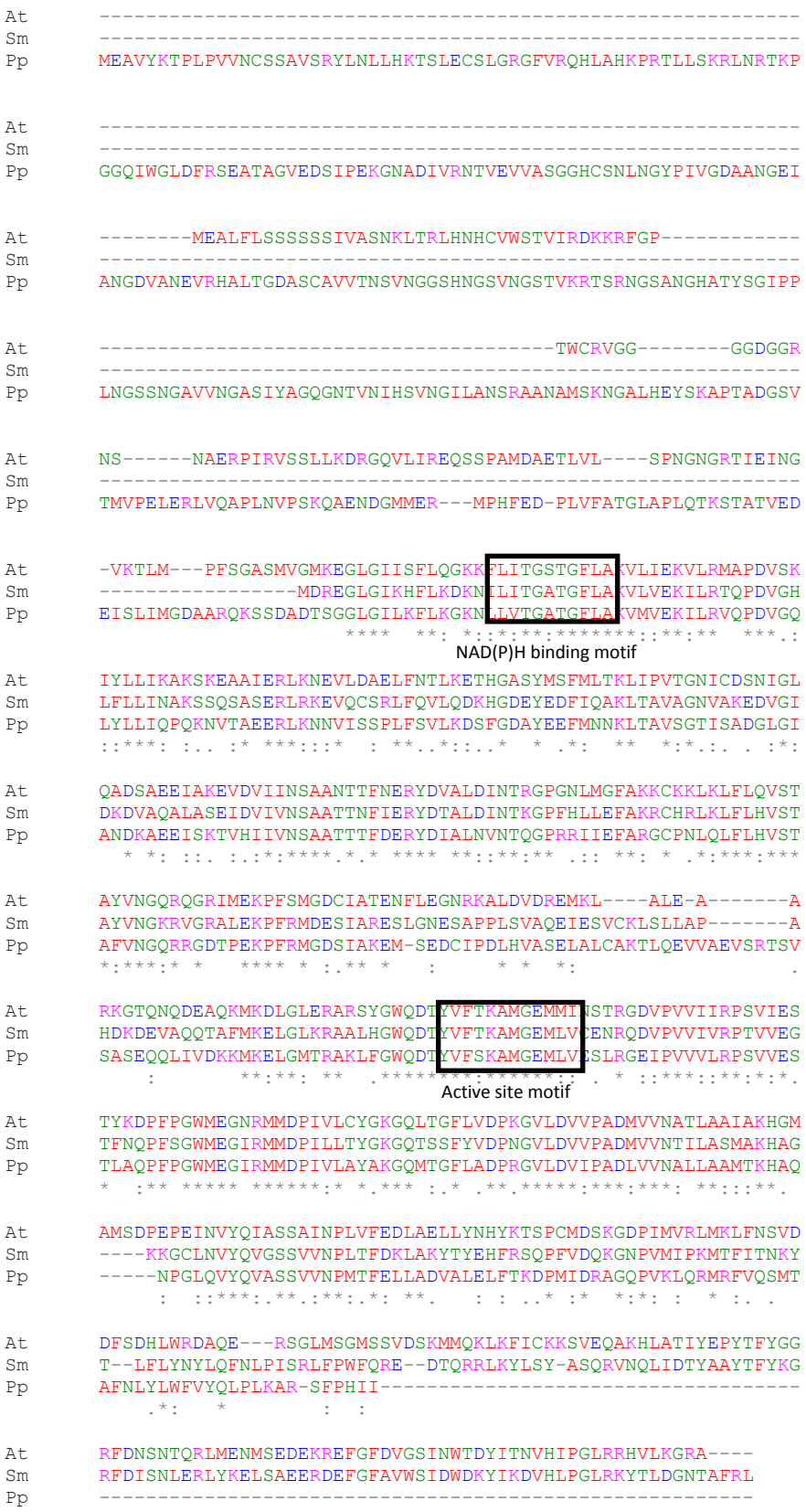

Figure 4.8. Alignment of *A. thaliana* (At) *MS2* protein sequence (AT3G11980) with putative homologues identified in the 'lower' land plant species, *P. patens* (Pp) and *S. moellendorffii* (Sm). Proposed NAD(P)H binding and active site motifs are indicated with square boxes. Key: "*" = residues identical in all sequences; ":" = conserved substitutions; "." = semi-conserved substitutions.

The *A. thaliana ms2* (SAIL_75_E01 and SAIL_92_C07) and *rpg1* (SALK_142803) mutants were generated by way of T-DNA insertions (Fig 4.9). The positions of the *ms2* T-DNA insertions were confirmed by PCR genotyping (primers: SAIL_75_E01 - FP, 5'-GTTTTATGTTACGGGAAGGGG-3'; RP, 5'-GCATTACTATGAGAAGAGACTTTGCC-3'; LB2, 5'-GCTTCCTATTATATCTTCCCAAATTACCAATACA-3': SAIL_92_C07 - FP, 5'-GGACAATCACTAAATGACATTTAATTG-3'; RP, 5'-GTTTTATGTTACGGGAAGGGG-3'; LB2 (as above)). The genotyping also identified plants which were homozygous for each of these insertions.

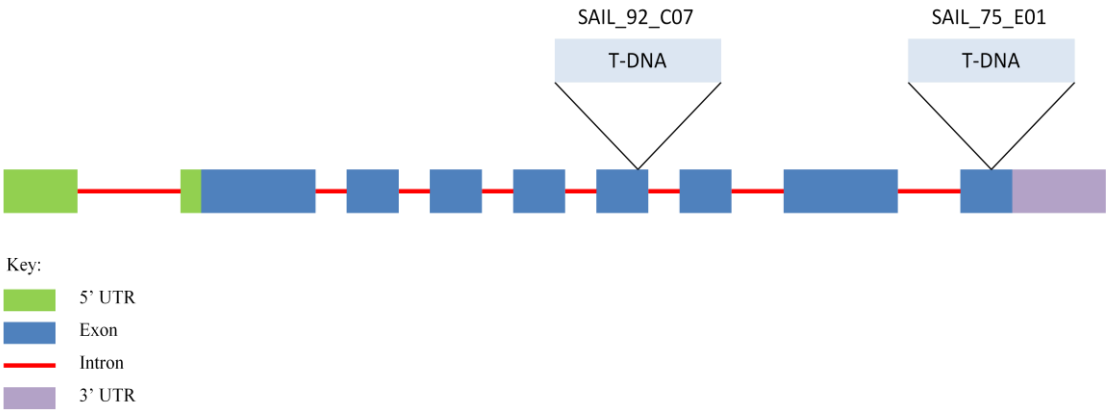

Figure 4.9. Schematic of *A. thaliana MS2* (AT3G11980) and location of SAIL_75_E01 and SAIL_92_C07 T-DNA insertion sites. With SAIL_75_E01 the T-DNA insertion is in exon 8 and with SAIL_92_C07 the T-DNA insertion site is located in exon 5.

4.2.5 Sequence alignment and transcript analysis of *MS2* homologues

A final ClustalW2 alignment of *A. thaliana*, *S. moellendorffii* and *P. patens MS2* homologues was 836 residues long (Fig. 4.8). 13 gaps, ranging from 1-51 residues in length were required to align the homologues.

Analysis of the transcripts of *A. thaliana MS2* and selected predicted *MS2* homologues (Fig. 4.10) revealed that the CDS of *A. thaliana MS2* and the *P. patens MS2*-like gene, Pp_11916, both consist of eight exons and seven introns. The CDS of the *Oryza sativa MS2*-like gene, LOC_Os03g07140, has nine exons and eight introns, and the CDS of the *S. moellendorffii MS2*-like gene, Selmo1_80322, is predicted to have ten exons and nine introns. In each of these homologues the length of exons two, three, four and six are conserved. Pp_11916 is predicted to have considerably longer introns than the other *MS2* homologues.

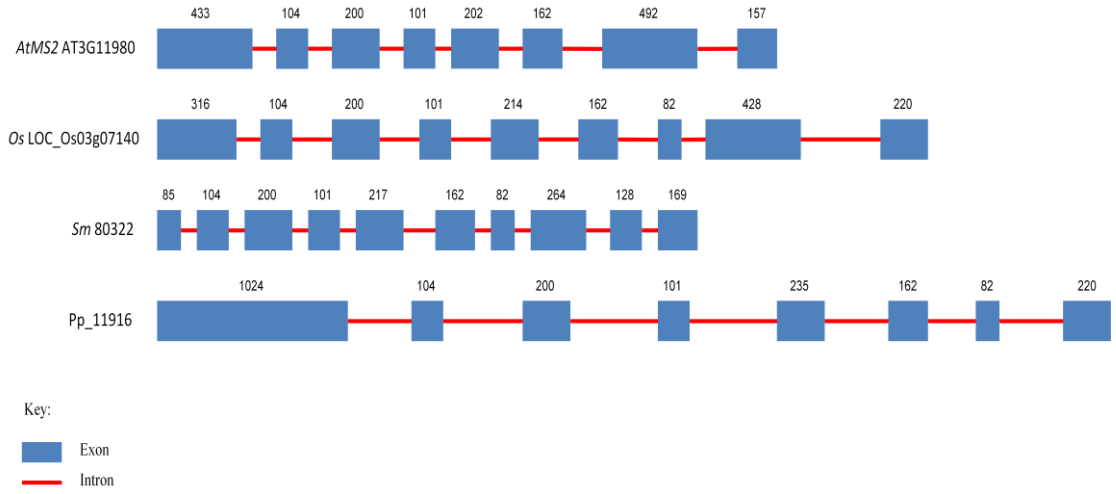

Figure 4.10. Exon-intron structure of *A. thaliana* (At) *MS2* and selected predicted land plant homologues (*Os* = *O. sativa*; *Sm* = *S. moellendorffii*; *Pp* = *P. patens*). Values above each exon represent exon length in base pairs.

4.3 Discussion

4.3.1 Flowering plant homologue genes for spore wall development are present in *Physcomitrella patens* and *Selaginella moellendorffii*

With genome search results suggesting that the vast majority of genes implicated in *A. thaliana* pollen development are also easily identifiable in the genomes of basal embryophytes, an initial group of spore wall target genes has been identified for potential further investigation by way of functional analyses. These results also indicate that the vast majority of these spore wall candidate genes belong to multigene families, and therefore, as with almost every developmental, signalling and metabolic context (Kafri *et al*. 2009), there is a high potential for genetic redundancy. Analyses of large collections of EST sequences have suggested that *P. patens* is a palaeopolyploid with a whole genome duplication having occured between 30 and 60 million years ago (Rensing *et al*., 2007), which may account for the presence of some of these gene duplications. Whilst the *S. moellendorffii* sequence data do not indicate any ancient whole genome duplication (Banks *et al*. 2011), the results here show that for most of the spore wall candidate genes numerous copies (greater in number than in the *P. patens* genome) are also present in the *S. moellendorffii* genome. This suggests the occurrence of many small-scale duplication events and a greater level of gene redundancy and/or number of pseudogenes in *S. moellendorffii* compared to *P. patens*.

4.3.2 Identification of lead genes for further investigation

Whilst the finding that homologues of angiosperm pollen wall associated genes are present in *P. patens* and *S. moellendorffii* opens the door to functional analyses of these genes, the potentially high levels of redundancy observed in these extant basal embryophytes present challenges to a functional approach. The *P. patens* sporophyte transcriptomic data presented in this chapter, by way of microarray analysis, helps circumvent some of these difficulties by allowing certain members of multigene families to be identified as the most likely to be involved in spore wall biogenesis. These genes can then be considered for gene knock-out and gene swap experiments.

The transcriptome profiles of spore wall candidate genes presented here imply that 16 homologues of seven of the *A. thaliana* pollen wall associated genes are significantly upregulated in the *P. patens* sporophyte. These candidate genes are homologous to *A.*

thaliana genes which can be divided into two discrete groups based upon their proposed general function (described in chapter 1 and summarised in Table 4.1). Five of these candidate genes are homologous to two *A. thaliana* genes which have been implicated in tetrad separation, specifically pectin degradation. The remaining eleven candidate genes are homologous to five pollen wall genes directly associated with sporopollenin biosynthesis and subsequent formation of the exine layer. None of the *P. patens* genes homologous to pollen wall genes associated with probaculae formation, intine construction and callose wall development were significantly upregulated at either sporophyte stage according to the microarray analysis and could therefore be promptly eliminated from the selection process for further investigation. Of course, the lack of significant upregulation exhibited by these genes does not necessarily mean that they do not play a role in spore wall development but the microarray experiment, backed up by sq-RT-PCR, represents an effective method of targeting spore wall candidate genes and therefore allows the selection of genes, for which functional analyses could potentially be conducted on, to be refined.

In addition to the transcriptomic data a number of other practical criteria were applied when selecting a gene or genes for functional analyses. Firstly, only candidate genes putatively identified as belonging to relatively small gene families in *P. patens* were considered in order to simplify knock-out experiments and maximise the likelihood of obtaining informative data from these experiments. Genetic redundancy is likely to be an issue with candidates which belong to sizeable gene families in *P. patens*, potentially masking the function of individual gene members and, therefore, increasing the likelihood that a number of family members may need to be knocked-out in order for an altered spore phenotype to be observed and/or easily measured. Secondly, *P. patens* spore wall candidate genes which are homologues to genes which have been identified as being involved in numerous functions and/or developmental processes in higher plants would not be considered due to the strong potential for many secondary phenotypes arising in knock-out mutants which could interfere with the primary study, and perhaps even be lethal to the study plant. Thirdly, preference would be given to candidate genes which, when knocked-out in *P. patens*, are likely to present distinct phenotypes, based upon observations and analysis of the corresponding mutants in *A. thaliana*.

4.3.2.1 Putative *Physcomitrella patens* tetrad separation genes

The *A. thaliana QUARTET* genes, *QRT1, QRT2* and *QRT3*, have significant numbers of homologues in *P. patens* and, as described in chapter 1, are associated with the timely degradation of pectic components of the pollen mother cell primary wall. The model proposed by Jiang *et al*. (2013) suggests that *QRT3* encodes an endopolygalacturonase (Rhee *et al*. 2003) which degrades polygalacturonan, an important carbohydrate component of the pectin network, by hydrolising the glycosidic bonds that covalently link galacturonic acid residues (Jones *et al*. 1972). In plants, this enzyme is employed in processes such as fruit softening, growth, organ abscission, root development and, of course, pollen development (Federici *et al*. 2001). Two putative *QRT3* homologues (Pp_227125 and Pp_198113 – both 50% amino acid homology) were identified in *P. patens* but neither of these genes are significantly upregulated in the sporophyte and therefore they were not selected for further investigation. However, four homologues of *QRT1* (33-42% homology), and one homologue of *QRT2* (39% homology) have significantly upregulated expression ($p<0.05$) at the sporophyte stage. The product of the *QRT2* gene has yet to be elucidated, although Jiang *et al*. (2013) have speculated that is also likely to be an endopolygalacturonase, but *QRT1* is proposed to encode a pectin methylesterase in *A. thaliana* (Francis *et al*. 2006). The changes in pectin structure brought about by pectin methylesterases are associated with alterations in the plasticity, pH, ionic contents and cellular adhesion of the cell wall and play a role in vegetative and reproductive processes (Pelloux *et al*. 2007). Therefore, the various complexities related to these genes, such as their roles in numerous developmental and physiological processes and associated potential secondary phenotypes, and the presence of large numbers of homologues of *QRT1* in *P. patens*, mean that they are not obviously suitable for the functional analyses proposed in this study. However, the high levels of expression of *QRT1* and *QRT2* homologues in the *P. patens* sporophyte does suggest that the degradation of the pectic components of the spore mother cell primary wall at the tetrad stage of sporogenesis may be necessary for microspore separation in early land plants, and aspects of the mechanism which underpin this process may therefore be conserved in embryophytes.

4.3.2.2 Putative *Physcomitrella patens* sporopollenin biosynthesis/exine genes

The majority of the genes identified and implicated in pollen wall development in *A. thaliana* to date, are directly associated with the biosynthesis of sporopollenin and/or exine formation, and all of these genes have homologues in the *P. patens* genome. Expression of homologues of five of these sporopollenin genes, *ACOS5*, *CYP703A2*, *CYP704B1*, *MS2* and *RPG1* are significantly upregulated in the *P. patens* sporophyte. The monomeric building blocks of sporopollenin are thought to be phenolics and derivatives of fatty acids. Functional analyses using *A. thaliana* have suggested that *ACOS5*, *CYP703A2*, *CYP704B1* and *MS2* and their associated enzymes may operate within a common fatty acid branch of the sporopollenin biosynthesis framework in tapetal cells (de Avezedo Souza *et al*. 2009; Dobritsa *et al*. 2009; Ariizumi and Toriyame 2011; Jiang *et al*. 2013). The precise composition of this pathway has yet to be confirmed, and further biochemical analyses are required, but a working model has been proposed (Fig. 4.11) based on the consensus of recent studies (de Avezedo Souza *et al*. 2009; Grienenberger *et al*. 2010; Ariizumi and Toriyame 2011), and has been summarised and incorporated into the larger Jiang *et al*. (2013) model of pollen wall formation. In this model *ACOS5* functions as a plastid localised acyl-CoA synthetase which is needed to produce a fatty acyl-CoA ester, from plastid generated lauric acids, which is then transferred to the endoplasmic reticulum (de Avezedo Souza *et al*. 2009). Hydrolysis by the specific thioesterase then occurs and once more lauric acids are generated in the endoplasmic reticulum (Ariizumi and Toriyame 2011). These lauric acids are then monohydroxylated by *CYP703A2* to create a 7-hydroxylauric acid which acts as a substrate for *ACOS5* resulting in the generation of 7-hydroxylaurel-CoA (Morant *et al*. 2007). Recent studies have shown that *CYP704B1* metabolises longer fatty acids, again synthesised in plastids, which suggests that two types of hydroxylated fatty acids, both CoA-esterified by *ACOS5*, serve as monomeric sporopollenin building blocks (Dobritsa *et al*. 2009), and that *CYP704B1* may operate along a separate branch of the sporopollenin fatty acid pathway. The liberated hydroxylated fatty acids are then reduced by *MS2* to fatty alcohol monomeric components which can then link with phenylpropanoids to form sporopollenin precursors (Morant *et al*. 2007; Ariizumi and Toriyame 2011). The phenotypes in *A. thaliana CYP703A2*, *CYP704B1* and *MS2* mutants are extremely similar and this, along with biochemical analysis, provided the main basis for the hypothesis that they are members of the same fatty acid branch, with the knock-out of any of them

resulting in the breakdown of this branch (or these branches) of sporopollenin biosynthesis. However, the phenotype of *ACOS5* mutants is distinct in that, whilst the exine layer would appear to be similarly defective, the pollen grains subsequently collapse and the mutants are completely male sterile, unlike the low levels of fertility exhibited by the other mutants (de Azevedo Souza *et al*. 2009). This may indicate that *ACOS5* plays a more central role in the sporopollenin biosynthetic pathway compared to *CYP703A2*, *CYP704B1* and *MS2*, and recent hypotheses have suggested that it may also operate within the phenylpropanoid branch as it shares its more severe phenotype with *LAP5*/*PKSB* and *LAP6*/*PKSA* mutants which have recently been implicated in the synthesis of phenylpropanoid constituents of sporopollenin (Dobritsa *et al*. 2010). The finding that homologues of *ACOS5*, *CYP703A2*, *CYP704B1* and *MS2* are significantly upregulated in the *P. patens* sporophyte suggests that they may be involved in synthesising the sporopollenin element of the *P. patens* spore wall and therefore participate in an ancient and conserved component of the sporopollenin biosynthesis pathway in embryophytes. The remainder of this section includes an assessment of the suitability of these homologues for functional analyses.

ACOS5 has 11 putative homologues in *P. patens* and two of these genes (36-50% homology) are significantly upregulated in the sporophyte. However, the potential for functional redundancy meant that genes with fewer homologues would be preferred for further investigation. Similar issues can be ascribed to the two cytochrome P450 genes, *CYP703A2* and *CYP704B1*, which again have relatively numerous homologues (31 and eight respectively) and belong to subfamilies of the large and diverse cytochrome P450 superfamily which in plants are involved in a wide range of biosynthetic pathways in primary and secondary metabolism (Morant *et al*. 2003; Duan and Schuler 2005). *CYP703A2* has two significantly upregulated homologues (both 33% homology) and *CYP704B1* has one (57% homology). Given the potential complications associated with these characteristics, and the likely difficulties in creating loss-of-function phenotypes, neither of these genes were considered for further functional analysis.

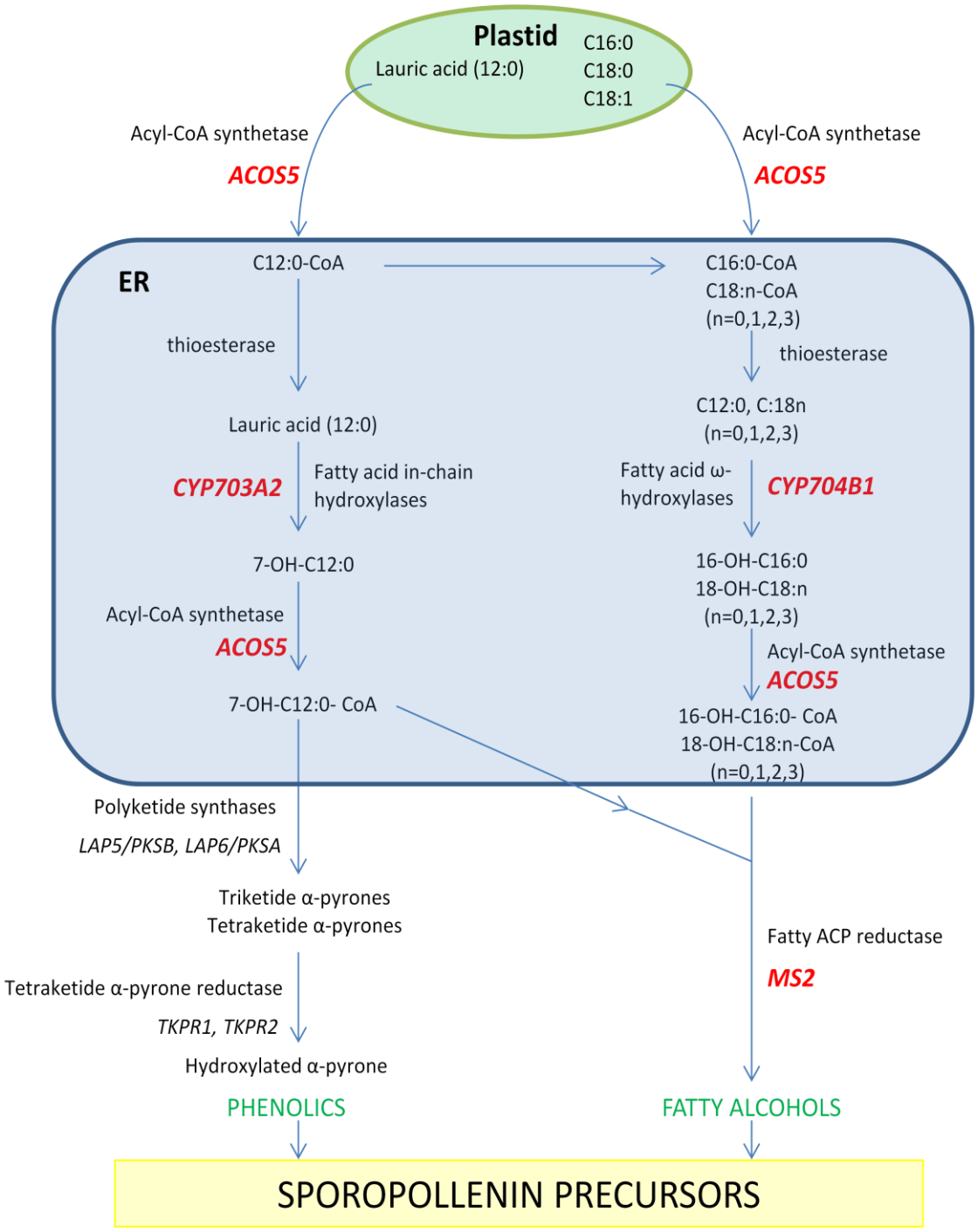

Figure 4.11. Model of sporopollenin monomer biosynthesis in *A. thaliana* tapetal cells. Genes which have homologues in *P. patens* that exhibit significantly upregulated expression in the sporophyte generation are in bold red text. Key: ER = endoplasmic reticulum. Modified from de Azevedo *et al*. 2007, Huang *et al*. 2011, Ariizumi and Toriyame 2011 and Jiang *et al*. 2013.

Only two homologues of *MS2*, which has been predicted to encode a plastid-localised fatty acyl carrier protein reductase (Chen *et al*. 2011), were identified in *P. patens* (both 48% homology). Electron microscope analysis has shown that *A. thaliana MS2* mutants possess a highly defective, and mostly absent, exine layer. As previously discussed in the introductory chapter, in *A. thaliana*, *MS2* converts fatty acids to the corresponding fatty alcohols and the apparent inability of *MS2* mutants to carry out this conversion indicates that this reaction is an essential stage in the biosynthesis of sporopollenin (Aarts *et al*. 1997; Ariizumi *et al*. 2008; Dobritsa *et al*. 2009). Biochemical analysis has demonstrated that recombinant *MS2* enzyme can convert palmitoyl-Acyl Carrier Protein to the corresponding C16:0 alcohol with NAD(P)H as the favoured electron donor, and the NAD(P)H-binding domain was shown, by way of genetic complementation experiments, to be essential for the function of *MS2* in pollen exine formation (Chen *et al*. 2011). The conserved NAD(P)H-binding and active site motifs (Doan *et al*. 2009) are also present in *P. patens* and *S. moellendorfii MS2* homologues (Fig. 4.8). Additionally, as a whole, the exon structure of *MS2* and its homologues, particularly in terms of number and length, appears to be quite conserved (Fig. 4.10) with no obvious suggestion of a pattern of intron gains and increasing length in more recently evolved embryophytes as has been often noted in various plant lineages (Babenko *et al*. 2004).

Fatty alcohols are important cellular components and have also been identified as key components of the lipidic anther cuticle (Jung *et al*. 2006; Li and Zhang 2010), and it is possible that pollen exine and cutin share a common lipidic biosynthetic pathway (Li and Zhang 2010; Zhang *et al*. 2010; Chen *et al*. 2011). Despite this, fatty alcohols are not associated with as many developmental and physiological processes as some of the other gene candidates described in this section. When this is considered alongside the fact that *MS2* is linked with a distinct wall phenotype in *A. thaliana*, and has just two homologues in *P. patens*, lower than any of the other gene candidates with transcriptomic analysis providing strong evidence as to which member of this gene family is functional (Pp_11916), it would seem that the putative *P. patens MS2*-like gene(s) represents a practical and intriguing option for further investigation.

Six putative homologues of *RPG1*, an unknown plasma membrane protein, were identified in *P. patens* (35-37% homology). *RPG1* has been shown to be a member of

the MtN3/saliva gene family which, in plants, is generally related to reproductive development. The putative intracellular region of the MtN3/saliva domain is conserved in *RPG1* and exhibits phosphorylation motifs which suggests *RPG1* may be involved in protein regulatory networks (Guan *et al*. 2008). TEM (Guan *et al*. 2008) and SEM analysis has demonstrated that primexine deposition was irregular in *A. thaliana RPG1* mutants. Phylogenetic analysis of *RPG1* and homologous proteins, identified in selected embryophyte model species, implies that the *P. patens RPG1* homologues form a complex family, but does not provide any strong indications as to which of these homologues are likely to be functional in the sporophyte. However, microarray analysis suggests that Pp_146196, Pp_149962 and Pp_163268 are the only homologues that are significantly upregulated ($p<0.05$) at the sporophyte stage. These three putative *P. patens RPG1*-like genes should therefore be considered the prime candidates for any proposed knock-out experiments investigating the conservation and function of *RPG1* which overall represents a realistic choice for further investigation given the relatively low number of homologues present in *P. patens*, and its easily defined phenotype in *A. thaliana*.

Of all the pollen wall associated genes with significantly upregulated homologues in the *P. patens* sporophyte, *RPG1* and *MS2* come closest to satisfying the criteria set out earlier in this discussion section. The potential role of the *P. patens RPG1*-like genes in the development of the spore wall poses intriguing questions given the absence of a primexine in 'lower' land plants. Was this gene recruited from another wall component and therefore a key element in driving the increase in complexity observed in pollen walls? Or is it simply the case that *RPG1* and other genes associated with more specialist wall elements, such as the primexine, are less well conserved than other pollen wall genes? However, given the time constraints associated with this study, the *MS2*-like genes are more likely to deliver easily measurable and informative data in a shorter period of time and were therefore selected for initial gene knock-out and gene swap experiments described in chapter 5. The *MS2*-like genes also have higher amino acid homology to *MS2* than *RPG1*-like genes have to *RPG1*. Additionally, the direct connection between *MS2* and sporopollenin biosynthesis, the key component of spore and pollen walls in terms of affording plants the ability to survive in terrestrial environments, makes it an attractive option for testing

conservation of gene function in the spore/pollen wall and its relevance to the colonisation of the land by plants.

4.4 Summary

In this chapter, genome searches have revealed that the vast majority of genes strongly associated with pollen wall development in *A. thaliana* have homologues in *P. patens* and *S. moellendorffii*. This finding raises the prospect that the molecular mechanisms responsible for pollen wall formation are ancient and conserved, and justifies further investigation by way of functional analyses of these genes. Transcriptomic data derived from microarray analysis showed that homologues of seven pollen wall associated genes exhibit significant upregulated expression in early and mid developmental stages of the *P. patens* sporophyte. From this refined pool of spore wall candidate genes certain practical criteria were applied to select genes which were likely to be highly suitable for gene knock-out and gene swap experiments in *P. patens*. *MS2*-like and *RPG1*-like genes in *P. patens* were the only two genes which sufficiently satisfied the selection criteria. The *MS2*-like genes were chosen for further investigation by way of functional analysis (described in chapter 5) primarily due to the presence of just two homologues in *P. patens*, strong transcriptomic evidence as to which homologue is functional, and the direct association of *MS2* with sporopollenin biosynthesis in *A. thaliana*.

CHAPTER 5. **Functional analysis of the *MS2*-like gene in spore wall morphogenesis in *Physcomitrella patens***

5.1 Introduction

Whilst expression analysis of putative spore wall genes in *P. patens* has proven to be illuminating, it essentially only provides a platform for generating new hypotheses and directing future experimental approaches. In order for a selected hypothesis regarding a candidate gene's involvement in spore wall development to be verified, a much more targeted approach is required whereby the candidate gene is disrupted, knocked-out or knocked-down, or is exchanged with a proposed homologous gene in another species, followed by analysis of the resultant phenotypes. This chapter describes the results obtained from a gene knock-out experiment, where the *MS2*-like gene identified in the previous chapter was deleted from *P. patens*, and a gene swap experiment where the same gene was transformed into *A. thaliana ms2* mutants to determine whether the moss gene could restore the wildtype pollen wall phenotype.

A model of the *P. patens MS2*-like gene, which from here onwards will be referred to as *PPMS2-1*, has been proposed and presented on the Cosmoss database. However, this model has been produced by way of gene prediction algorithms and as of yet there is no complete EST evidence to support it. The model suggests *PPMS2-1* consists of eight exons and seven introns with a long 5' untranslated region consisting of 1351 base pairs and a 3' UTR of 472 base pairs in length. The CDS is predicted to be 2202 base pairs in length (encoding a 733 residue protein). This CDS region was deleted from *P. patens* in the knock-out experiments, and also amplified and transformed into *A. thaliana MS2* mutants, under the control of the native *MS2* promoter, to effectively generate a gene swap experiment.

As previously discussed, *P. patens* displays a very high level of gene targeting efficiency and successful knock-outs of spore wall associated genes have been achieved previously with the generation of stable *PPGAMYB1* and *PPGAMYB2* loss-of-function transformants (Aya *et al*. 2011). Given the *P. patens* life cycle data presented in chapter 3, the Villersexel K3 and Gransden GrD12 wildtypes were

selected as the background lines for generating *PPMS2-1* knock-out mutants by way of PEG-mediated protoplast transformation.

In order for gene swap, or complementation, experiments to be conducted, it was necessary to generate or obtain *A. thaliana ms2* mutant plants. Conveniently, three *A. thaliana ms2* mutant lines are available from the European Arabidopsis Stock Centre. The *MS2* pollen wall phenotype was first reported in a transposon excision mutant produced by Aarts *et al*. (1993, 1997) which also exhibited male sterility due to the collapse of the microspores towards the latter stages of their development. The mutation did not completely eradicate the production of viable pollen but the plants could only yield approximately 1 % of the wildtype seed set (Aarts *et al*. 1997). This lack of fertility presents practical difficulties for gene swap experiments. However, two *MS2* T-DNA insertion lines (SAIL_75_E01 and SAIL_92_C07) have recently been made available from the Syngenta Arabidopsis Insertion Library (SAIL) (Sessions *et al*. 2002). These T-DNA insertion lines still seemingly have the same defective pollen wall phenotype but observations of their life cycles have shown that they produce large amounts of pollen and are much more fertile than the transposon excision mutant (Dobritsa *et al*. 2009). The reasons for these phenotypic differences are unclear but Dobritsa *et al*. (2009) postulated that it is possible that the differences in the wildtype backgrounds (Landsberg *erecta* for the transposon excision mutant and Col-3 for the two SAIL lines), and the potential for second site mutations with transposon mobilisation, may be responsible. Given their more practical levels of fertility, the two SAIL lines were therefore used for the gene swap experiments carried out in the study presented here.

A gene swap experiment involving an *MS2* homologue has been conducted previously where a predicted homologue in the monocot rice, *DEFECTIVE POLLEN WALL (DPW)*, was shown to be able to complement an *A. thaliana ms2* mutant (a dicot) by restoring the wildtype pollen wall phenotype (Shi *et al*. 2011). This suggested that the fatty alcohol synthesis step in pollen wall development is conserved in monocots and dicots. The complementation of an *A. thaliana ms2* mutant by a *P. patens* homologue would provide greater insights regarding the evolutionary development of the spore/pollen wall and land plant evolution due to the large evolutionary gulf between the two species, and would provide compelling evidence for the conservation of *MS2*

function in spore/pollen walls. Therefore, the primary aim of the *A. thaliana* gain-of-function and *P. patens* loss-of-function experiments is to further elucidate the function of PPMS2-1 in the *P. patens* sporophyte and determine the conservation of a key component of the spore/pollen wall biochemical and developmental pathway throughout land plant history. The materials and methods required/applied to conduct these experiments and subsequent analyses, including plant transformation, SEM, TEM, acetolysis and Raman microspectroscopy, are described in chapter 2.

5.2 Results

5.2.1 Generation and molecular analysis of *Physcomitrella patens PPMS2-1* knock-out lines and *Arabidopsis thaliana PPMS2-1* gain-of-function lines

Physcomitrella patens mutant lines lacking the *PPMS2-1* CDS were successfully created, in both Villersexel K3 and Gransden GrD12 ecotypes, by way of PEG-mediated protoplast transformation. Transformation efficiency was greater with GrD12 with many more stable putative positive transformants observed after antibiotic selection than with Villersexel K3. The deletion of *PPMS2-1* was confirmed in five transformants, obtained using Villersexel K3, by genotyping (Fig. 5.1). Genotyping was also carried out on three of the numerous putative positive transformants obtained with GrD12 which confirmed the deletion of *PPMS2-1* in two of these transformants (Fig. 5.2). Southern blot analysis confirmed that three of the five genotyped transformants obtained with Villersexel K3 were single-copy replacement transformants (*ppms2-1* KO1, KO2 and KO3) (Fig. 5.1), therefore these lines were primarily used for phenotypic analysis. RT-PCR confirmed the absence of a *PPMS2-1* gene product in one of these lines (*ppms2-1* KO3) and demonstrated that the deletion of *PPMS2-1* does not affect *PPMS2-2* (Pp_120173) expression. However, the *PPMS2-1* gene product was observed in *ppms2-1* KO1 and KO2 (Fig. 5.1) confirming the occurrence of ectopic reintegration whereby the replaced wildtype DNA has reintegrated elsewhere in the genome (Puchta 2003). RT-PCR also confirmed the absence of *PPMS2-1* gene product in a genotyped transformant (*ppms2-1* Gr77) derived from GrD12 (Fig. 5.2). The cDNA used for RT-PCR verification was derived from mid sporophyte tissue as expression of *PPMS2-1* could not be detected

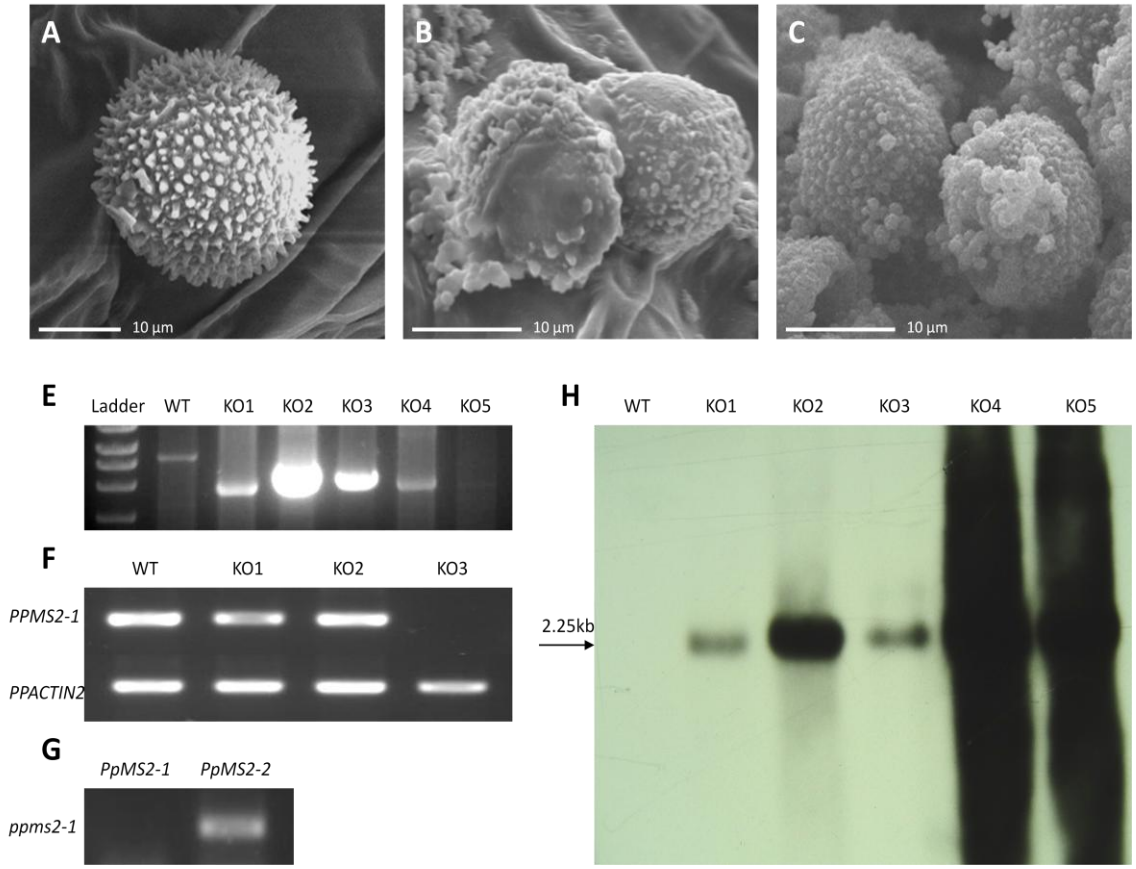

Figure 5.1. Generation and SEM analysis of *P. patens PPMS2-1* knock-out lines obtained with Villersexel K3. SEM examination of wildtype (A) and *ppms2-1* spores (unfixed (B) and fixed (C)). E, confirmation of the deletion of *PPMS2-1* in five *P. patens* transformants (albeit with a faint band observed with *ppms2-1* KO5). The smaller product sizes (3878 base pairs) confirm that the *PPMS2-1* CDS has been replaced by the smaller *npt*II selection cassette. F, RT-PCR Confirmation of lack of expression of *PPMS2-1* in *ppms2-1* KO3 and ectopic reintegration of the replaced wildtype DNA in *ppms2-1* KO1 and KO2. *PPACTIN2* included as a control. G, RT-PCR analysis demonstrating that the deletion of *PPMS2-1* has no effect on *PPMS2-2* expression in *ppms2-1*. H, Southern blot confirmation that *ppms2-1* KO1, KO2 and KO3 are single-copy replacement transformants.

in wildtype gametophyte tissue. Given the small size of the *P. patens* sporophyte, and the lengthy time period required to harvest sufficient sporophyte tissue for cDNA synthesis, RT-PCR verification could only be conducted on a limited number of *ppms2-1* lines.

Successful transformation of *Arabidopsis thaliana ms2* mutants with *PPMS2-1* (*ATMS2pro::PPMS2-1*) was initially determined by detection of seed-expressed GFP (see chapter 2, section 2.6.3), a component of the same destination vector carrying *PPMS2-1*. Once GFP fluorescent seeds (T_1 lines) were identified they were sown and cultivated, and PCR confirmation of the *PPMS2-1* and *PPMS2-1* splice variant insertions in T_1 and T_2 lines was conducted using genomic DNA extracted from leaves. The pollen phenotype of mature T_1 and T_2 lines was then analysed.

5.2.2 Phenotypic analysis of *ppms2-1* spores

SEM analysis of *ppms2-1* spores revealed a distinct phenotype (Fig. 5.1). Mature *ppms2-1* spores typically range from 14-21 µm and are therefore mostly around two thirds of the size of wildtype spores (Table 5.1). The projections which form the perine layer are much less dense, pointed and regular than those observed in the wildtype and therefore the outer surface of *ppms2-1* spores generally comprise a mosaic of blunted, incomplete perine projections and smooth areas seemingly devoid of perine material. The material for the perine is still seemingly synthesised normally but would appear to be unable to adhere properly to the surface of the spore and therefore large quantities of perine material are scattered throughout the spore capsule. This phenotype was observed in knock-out lines generated using both Villersexel K3 and Gransden GrD12 ecotypes, and in all lines exhibiting ectopic reintegration, with a particularly pronounced phenotype in *ppms2-1* KO1. TEM analysis of *ppms2-1* KO1 and KO3 confirmed the irregular nature of the perine and showed that in mature spores an entire layer of the wall is absent (Fig. 5.3). Given the homogenous nature of both the exine and intine layers, and their similar thicknesses in the wildtype, it is difficult to determine which of these is missing in *ppms2-1* although, at 0.5-0.7 µm thick, the remaining layer is approximately twice the thickness of both the wildtype intine and exine. In addition to an altered wall, mature *ppms2-1* spores exhibited an abnormal cytoplasmic organisation with the characteristic spherical vesicles, or oil bodies, associated with the wildtype greatly reduced in number. Post-tetrad stage

Table 5.1. Average diameter of *P. patens* wildtype and *ppms2-1* spores (n=12).

Line	Average Spore Diameter (µm) (± SD)*
Villersexel K3 wildtype	28.45 ± 1.64
ppms2-1	18.05 ± 2.69

*$P<0.0001$; unpaired two tailed Student's *t*-test (two-tailed).

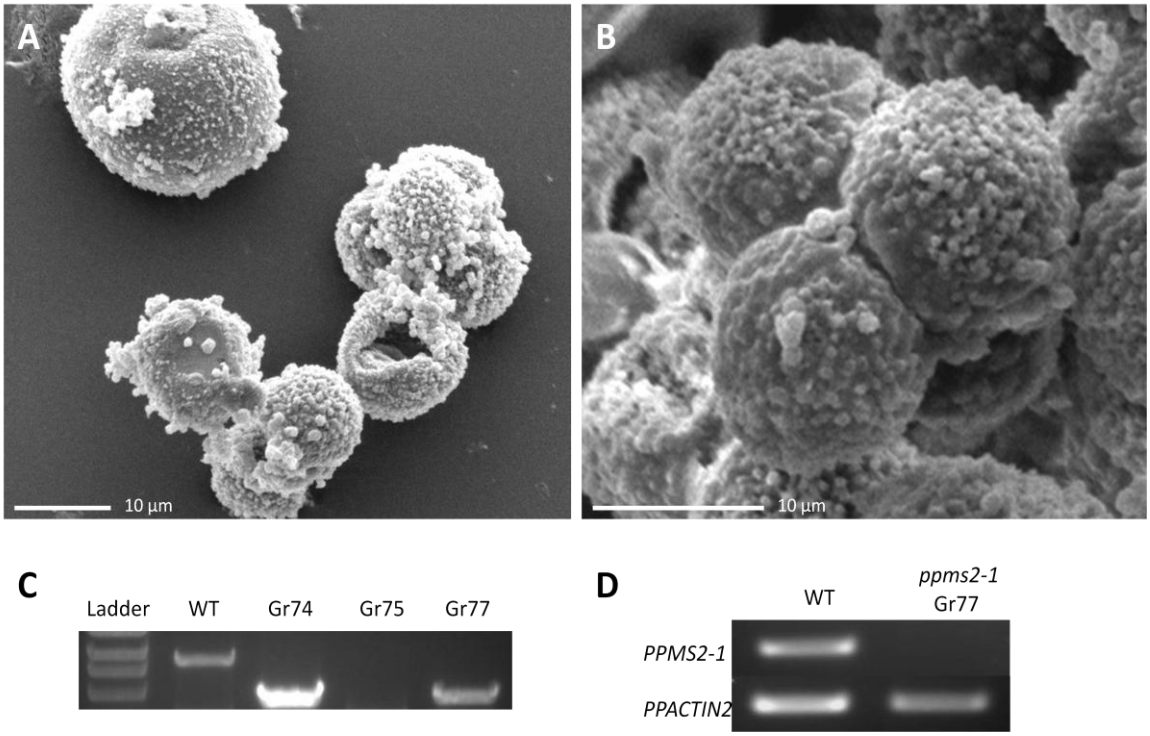

Figure 5.2. Generation and SEM analysis of *P. patens PPMS2-1* knock-out lines obtained with Gransden GrD12. SEM examination of spores in *ppms2-1* Gr74 (A) and Gr77 (B) knock-out lines. C, Confirmation of the deletion of *PPMS2-1* in two *P. patens* transformants (Gr74 and Gr77). The smaller product sizes (3878 base pairs) confirm that the *PPMS2-1* CDS has been replaced by the smaller *npt*II selection cassette. D, RT-PCR Confirmation of lack of expression of *PPMS2-1* in *ppms2-1* Gr77. *PPACTIN2* included as a control.

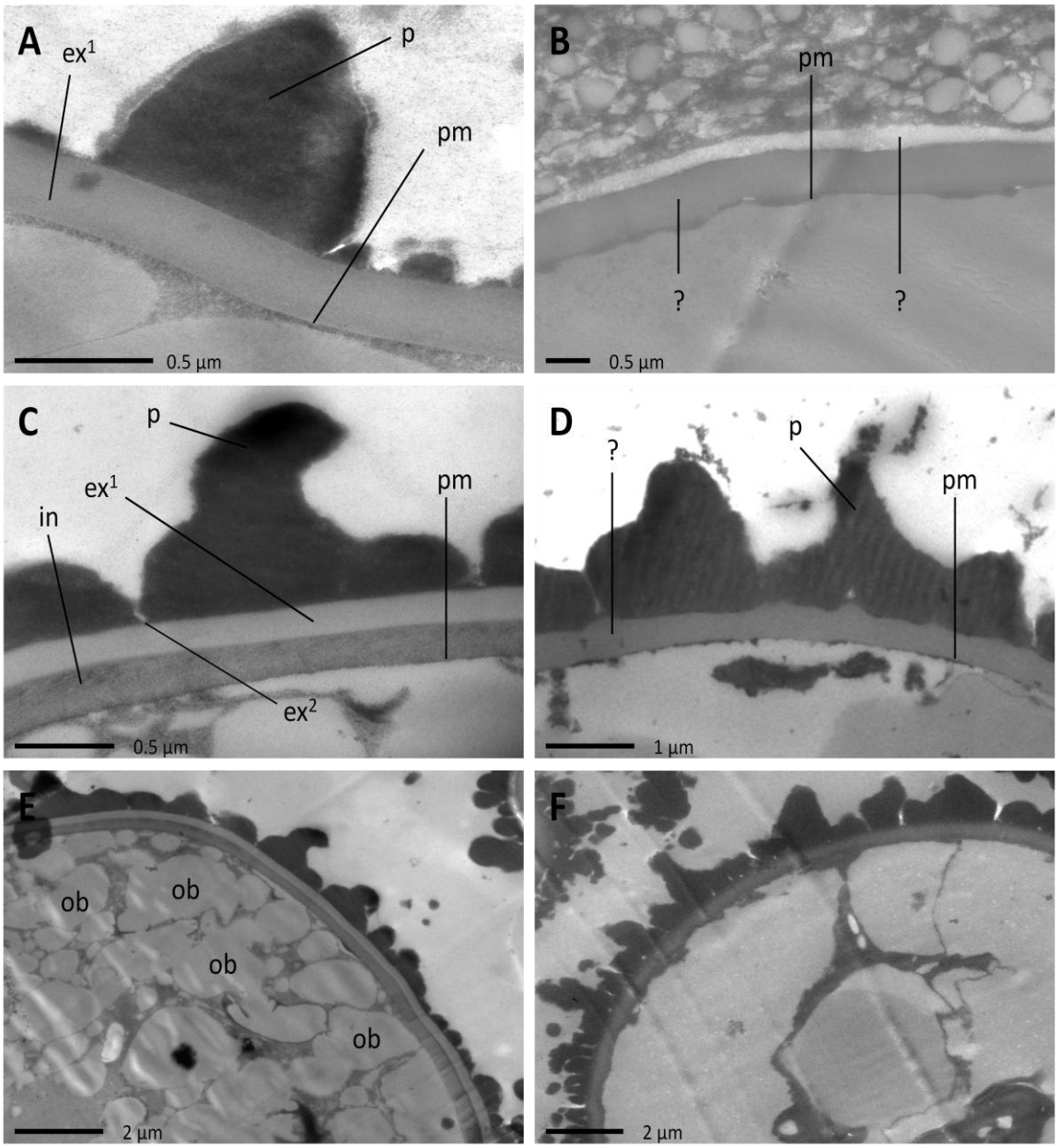

Figure 5.3. TEM analysis of wildtype (A, C and E) and *ppms2-1* (B, D and F) spore ultrastructure. A, wildtype spore wall ultrastructure at the post-tetrad developmental stage. B, *ppms2-1* (KO3) spore wall ultrastructure at the post-tetrad stage. C and E, mature wildtype spore ultrastructure. D and F, mature *ppms2-1* (KO3) spore ultrastructure. Key: pm = plasma membrane; p = perine; ex^1 = inner exine; ex^2 = outer exine; in = intine; ob = oil body.

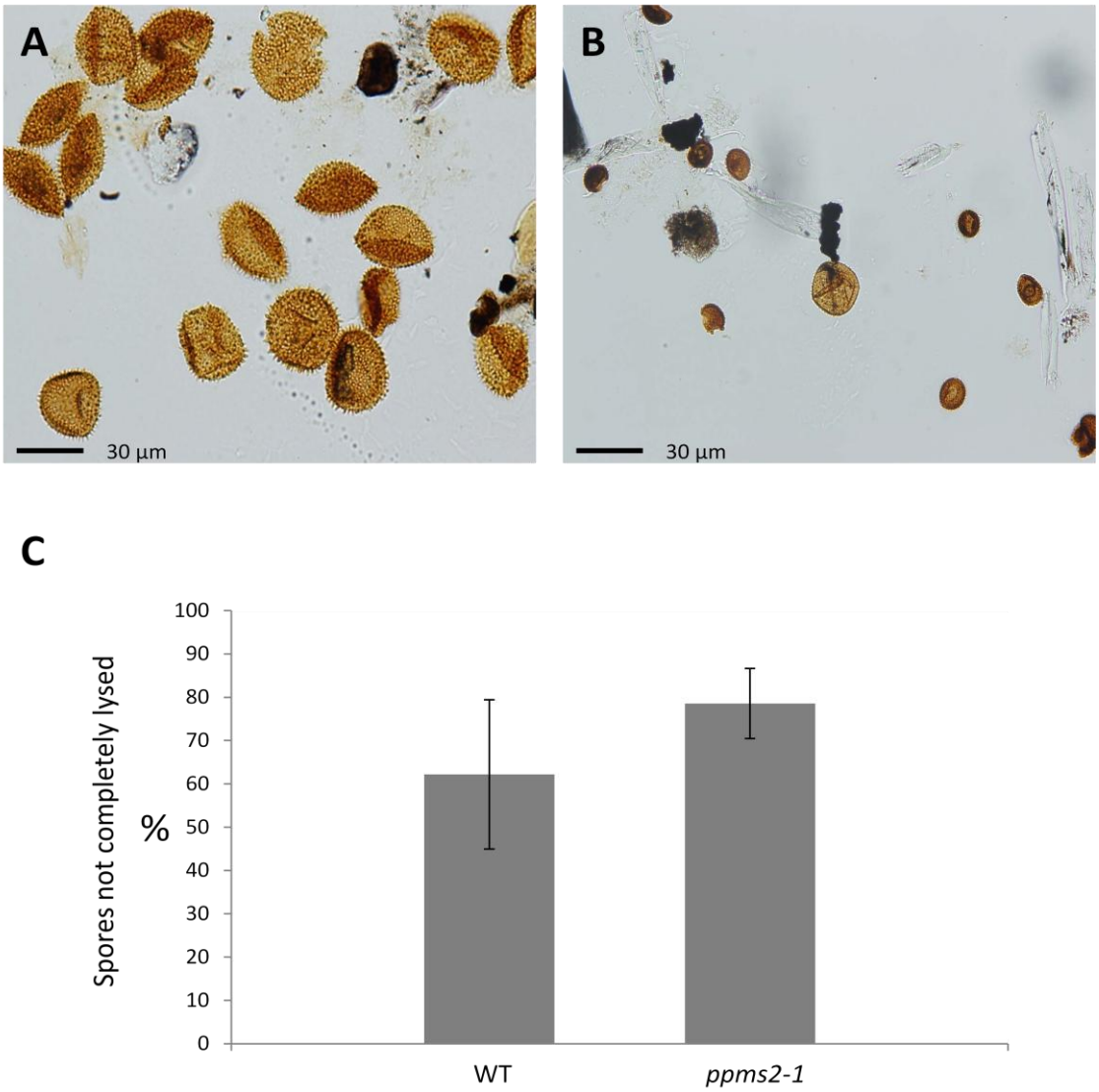

Figure 5.4. Acetolysis of wildtype and *ppms2-1* spores. Light microscope images of wildtype (A) and *ppms2-1* (B) spores after acetolysis. C, Quantitative analysis of acetolysed wildtype and *ppms2-1* spores. Chart shows the percentage of spores remaining (not completely lysed) after acetolysis. *P*=0.4378 (unpaired two tailed Student's *t*-test (two-tailed)).

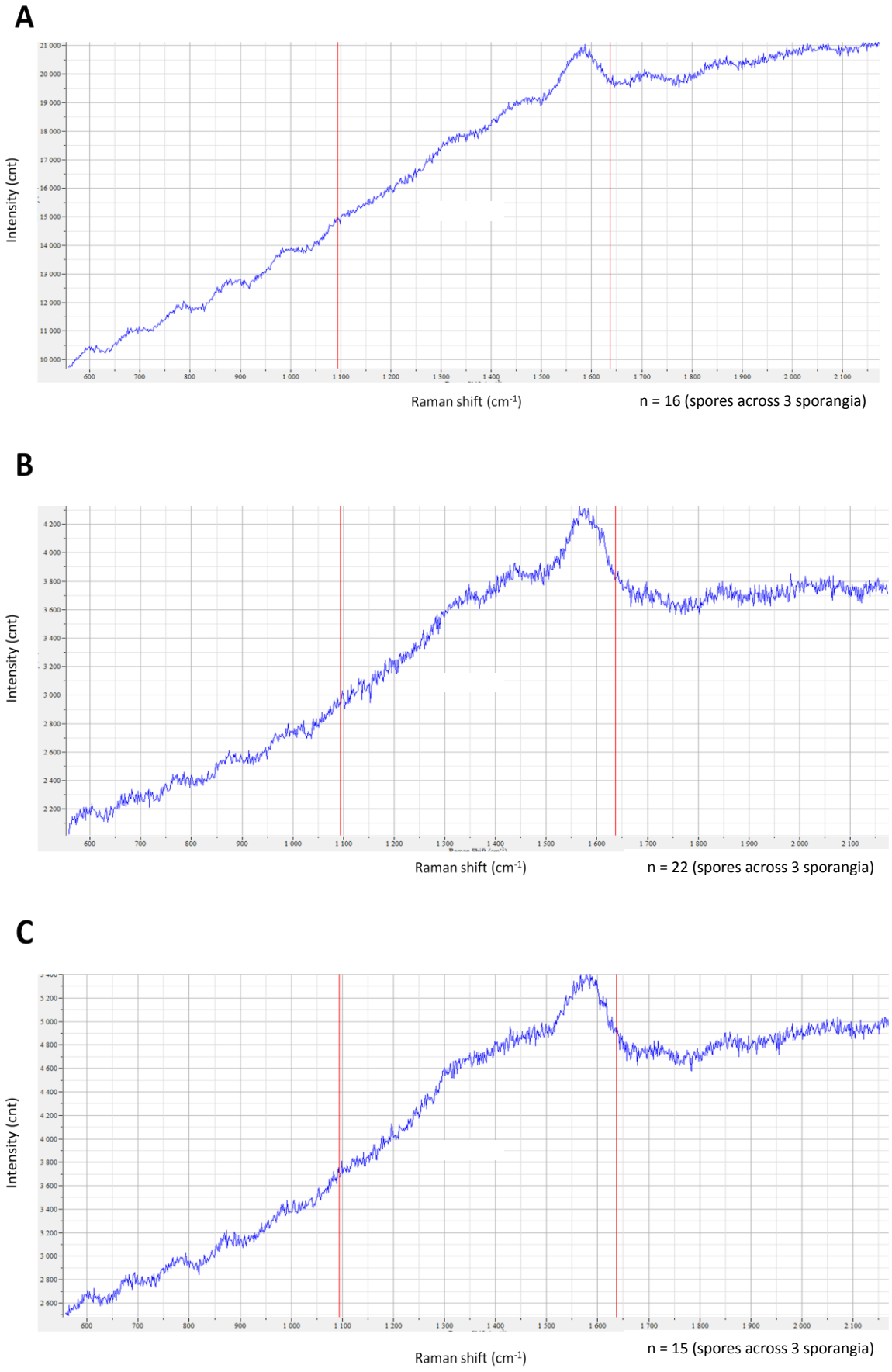

Figure 5.5. Raman spectra of one representative replicate each of wildtype (A), *ppms2-1* KO1 (B) and KO3 (C) spores. Spectra were produced with LabSpec 5 software.

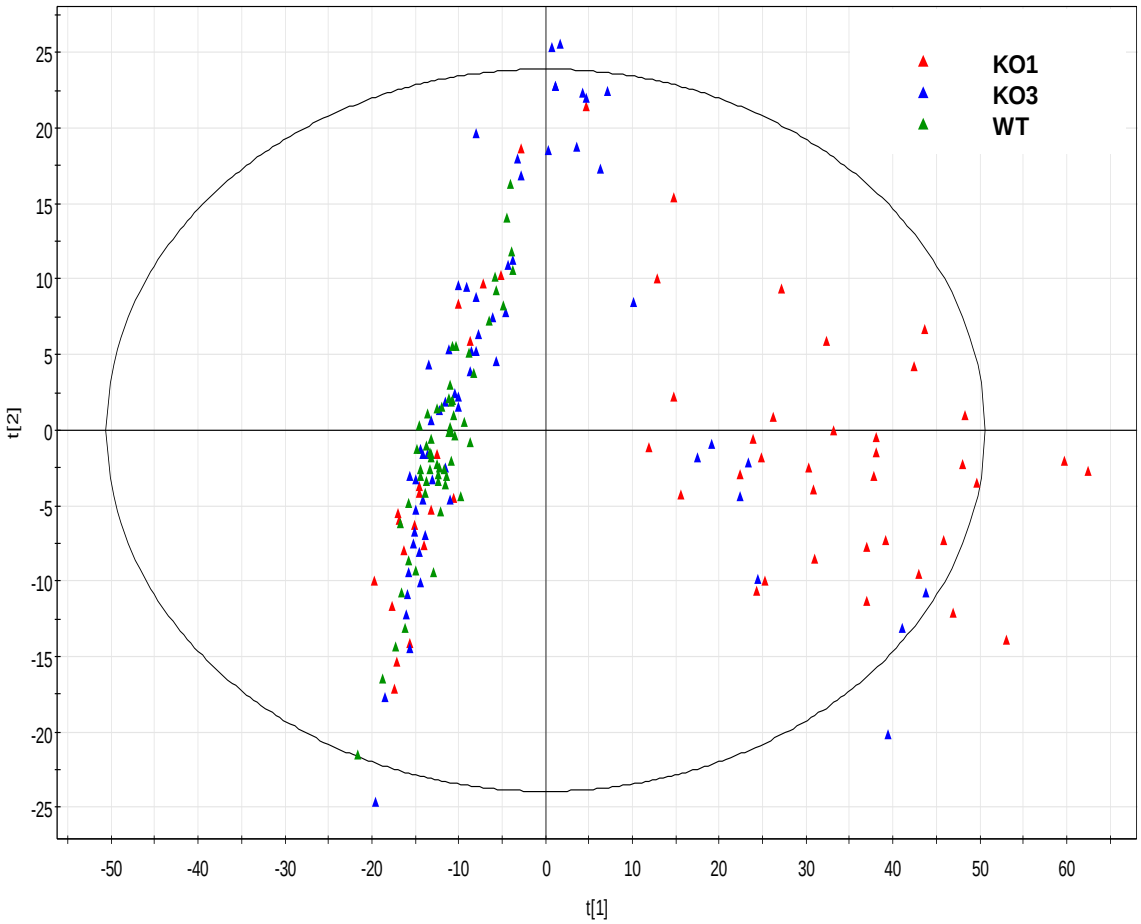

Figure 5.6. PCA analysis (baseline corrected and normalised) of Raman spectra obtained from wildtype, *ppms2-1* KO1 and KO3 spores. PCA and resultant plots were conducted and produced using SIMCA (v. 8.0). The circle represents the 95% confidence level.

ppms2-1 spores possess two wall layers although the outer layer does not resemble the perine present in wildtype spore walls at the same developmental stage. Instead this layer is thin and light and is replaced, by the time the spores mature, by the perine. *ppms2-1* spores also exhibit a disorganised cytoplasm at this stage.

Previous studies have shown that some exine mutants in both *P. patens* and *A. thaliana* (Aarts *et al.* 1997; Ariizumi *et al.* 2003; Aya *et al.* 2011) are sensitive to acetolysis, a procedure which involves incubating spores/pollen in a solution of acetic anhydride and sulphuric acid which generally degrades all spore/pollen

material except for the exospores (Erdtman 1960). However, *ppms2-1* spores were not more sensitive to acetolysis treatment than wildtype spores and slightly more mutant spores were observed after acetolysis than wildtype spores (Fig. 5.4), albeit percentages of remaining spores (62.18 % wildtype and 78.55 % *ppms2-1*) were within margin of error. Next, in order to discern differences in spore chemistry, Raman microspectroscopy, a rapid technique for biochemical analysis of cells by way of measurement of the vibrational energies of molecules by the inelastic scattering

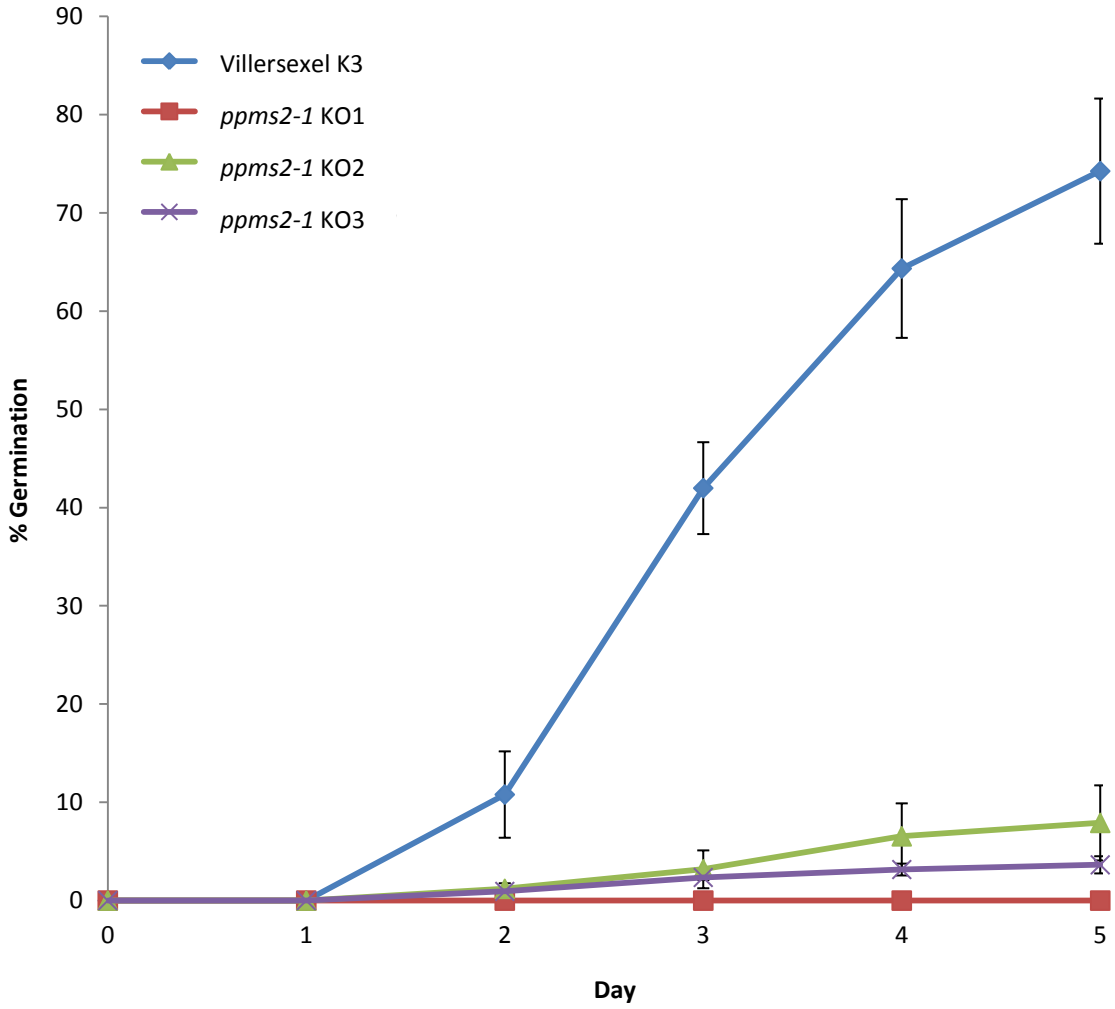

Figure 5.7. Spore germination for *P. patens* Villersexel K3 wildtype and *ppms2-1* KO1, KO2 and KO3 knock-out lines under controlled axenic conditions (n=3).

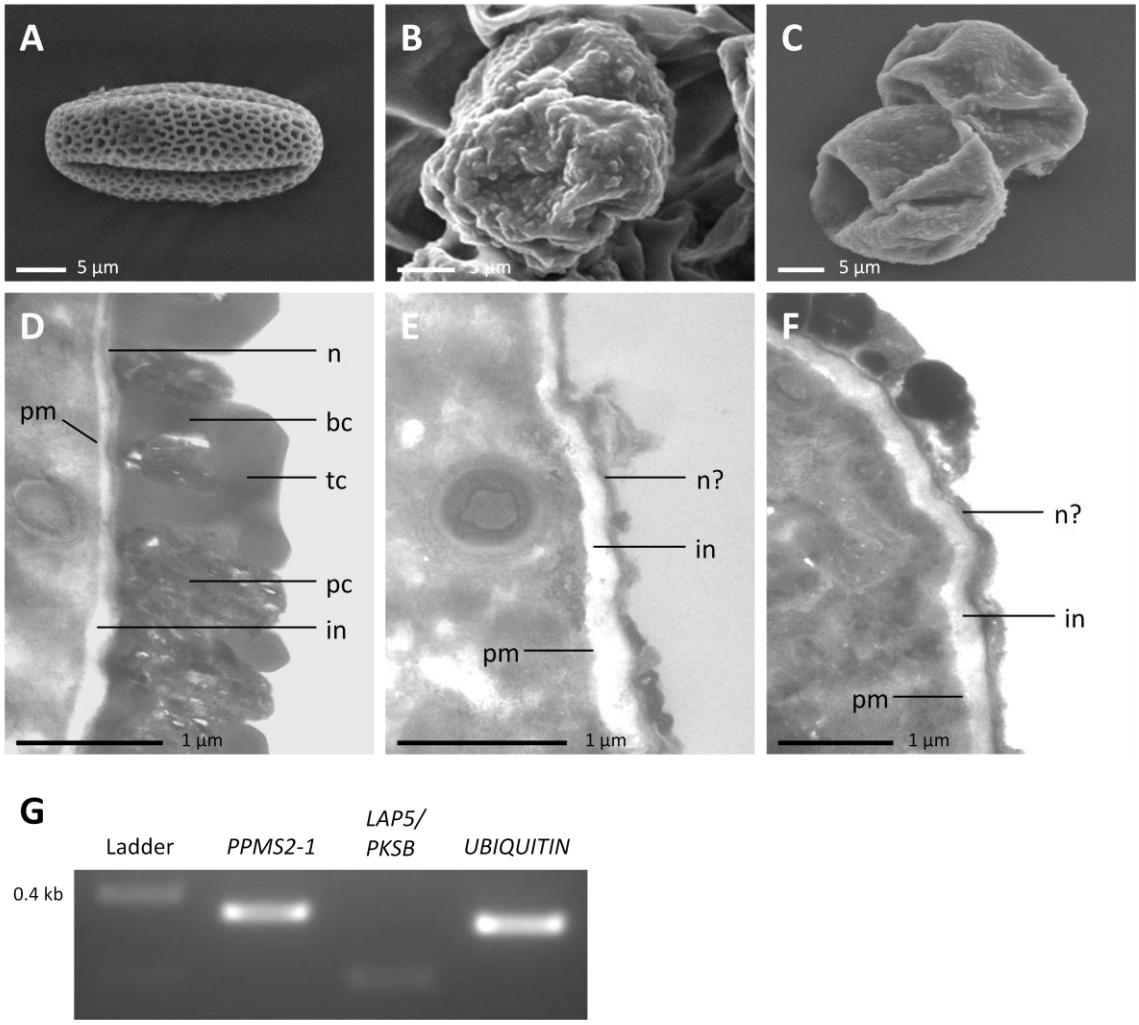

Figure 5.8. Electron microscope analysis of the *ATMS2pro*::*PPMS2-1* pollen phenotype. A (SEM) and D (TEM), mature wildtype pollen. B (SEM) and E (TEM), *ms2* (SAIL_75_E01) mature pollen. C (SEM) and F (TEM), *ATMS2pro::PPMS2-1* T_2 mature pollen. G, RT-PCR confirmation of expression of *PPMS2-1* in *ATMS2pro::PPMS2-1* flowers. *UBIQUITIN* and the tapetum specific *LAP5/PKSB* included as controls. Key: n = nexine; bc = baculae; tc = tecta; pc = pollen coat; in = intine; pm = plasma membrane.

of photons (De Gelder *et al*. 2007; Huang *et al*. 2010), was applied to wildtype, *ppms2-1* KO1 and KO3 spores. However, PCA of the resultant Raman spectra could not distinguish the three lines (Figs. 5.5 and 5.6). Replicates of the two *ppms2-1* lines did scatter widely on the PCA plot and form two groups within each line, but many of the mutant replicates formed a grouping with the wildtype replicates.

Given their distinct phenotype the functionality of *ppms2-1* spores was examined by the application of a spore germination test (Fig. 5.7). Five days after plating very few *ppms2-1* KO2 and KO3 lines spores had germinated (KO2 – 7. 91 %; KO3 – 3.64 %) compared to the wildtype (74.25 %). In *ppms2-1* KO1 germination percentage was 0 % and therefore this line was completely infertile.

5.2.3 Phenotypic analysis of *Arabidopsis thaliana ms2* mutants transformed with *PPMS2-1*

Once RT-PCR had confirmed the expression of *PPMS2-1* in the flowers of the plants transformed with the *ATMS2pro::PPMS2-1* construct (Fig. 5.8G), phenotypic analysis was conducted. SEM and TEM analysis of mature T_1 and T_2 *A. thaliana ms2* mutants (SAIL_75_E01 and SAIL_92_C07 backgrounds), transformed with *PPMS2-1* expressed under the control of the *A. thaliana MS2* promoter, showed that the moss gene could not restore the wildtype pollen wall phenotype and the same highly defective exine layer observed in *A. thaliana ms2* mutant pollen walls was therefore still present (Fig. 5.8). Transformations with the *PPMS2-1* splice variant described in section 2.5.1 of chapter 2 also yielded the same unaltered *ms2* defective exospore phenotype.

5.3 Discussion

5.3.1 Role of *PPMS2-1* in spore wall development in *Physcomitrella patens*

The results from the phenotypic analysis of *ppms2-1* mutant spores presented here demonstrate that, as in flowering plant pollen (Aarts *et al*. 1997; Shi *et al*. 2011), *MS2* is essential for the normal development of the spore wall and the spore as a whole in the bryophyte *P. patens*. Whilst the function of *MS2* in *P. patens* can be directly

associated with the spore wall, definitively linking it to a specific component, or layer, of the wall is difficult.

The electron microscope analysis indicates that despite the appearance of a defective perine in *ppms2-1* knock-out lines, the perine material is still synthesised by the tapetum in the same way as the wildtype, and the aberrant nature of the perine in mature spores is a consequence of a defect in another layer, which perhaps has a template system associated with it, and does not allow the perine material to adhere to the spores in the normal manner. Additionally, or alternatively, the absence of this layer may simply disrupt molecular interactions associated with previously described self-assembly processes in exospores (Hemsley *et al*. 1992; Gabarayeva 1993; Collinson *et al*. 1993; Gabarayeva and Hemsley 2006; Hemsley and Gabarayeva 2007) which may possibly be involved in normal perine development in *P*. *patens*. Either way, the electron microscope evidence implies that *PPMS2-1* is not directly associated with the synthesis of perine designated sporopollenin.

The protein sequence homology of PPMS2-1 with *A*. *thaliana* MS2 suggests that it is involved with the biosynthesis of the sporopolleninous exine layer of the moss spore wall, and therefore the layer missing in the mature spore walls of *ppms2-1* is the exine. However, data obtained from TEM analysis and acetolysis tests contradict this. In *P*. *patens* wildtype spores, at the post-tetrad stage, the exine is fully formed and a rapidly developing perine is present. Therefore, if the deletion of *PPMS2-1* results in the absence of the exine then in *ppms2-1* spores at the same stage it would be expected that the only potentially observable wall layer would be the perine. However, the post-tetrad *ppms2-1* TEM image presented here (Fig. 5.3B) shows two homogenous layers of different thicknesses which tentatively suggests that the exine layer, or an exine-like layer, is still present in *ppms2-1*, and the intine is the absent layer in mature *ppms2-1* spore walls. Further credence is added to this suggestion by the finding that *ppms2-1* spores are no more sensitive to acetolysis than wildtype spores (Fig. 5.4). A role of *PPMS2-1* in intine development would represent a remarkable finding as it would imply a major switch in the function of MS2 in spore/pollen wall development from an involvement in polysaccharide synthesis in 'lower' land plants, to playing a key role in sporopollenin synthesis in 'higher' land plants. However, the TEM evidence underpinning this proposition consists of just one image. Further

images/replicates could not be obtained in the time frame allocated for this study due to the fixation and infiltration problems associated with early to mid developmental stage spores/sporophytes described in chapter 3. Therefore further replicates are required to validate or invalidate this proposition. It could be the case that if the intine is still present then the deletion of *PPMS2-1*, in addition to severely compromising exine formation, affects the timing of intine development. An undetectable exine may still be present in some form and capable of affording *ppms2-1* spores resistance to acetolysis. If further investigations were to confirm that the missing, or highly defective, wall layer in *ppms2-1* mature spores is the exine then it would strongly suggest that *PPMS2-1* plays a homologous role to *A. thaliana MS2* in *P. patens* exine formation and spore wall formation as a whole.

Spore germination tests show that whichever layer is missing/undiscernable, the distinct and severe wall phenotype exhibited by *ppms2-1* renders the spores mostly inviable (Fig. 5.7), and one line (*ppms2-1* KO1) is completely infertile and cannot produce any spores of wildtype size. The reason for the discrepancy between *ppms2-1* KO1 and the other knock-out lines is unclear. It is feasible that this difference is due to a second site mutation occurring during the transformation process, and it would be interesting to determine, with inverse PCR, where the replaced wildtype DNA has recombined in the *P. patens* genome since RT-PCR showed that *ppms2-1* KO1 exhibited ectopic reintegration. Of course, phenotypic variation has often been observed with targeted mutagenesis and it is possible that mutant phenotypes are associated not only with specific functional effects, but also interference with wildtype networks resulting in the expression of numerous unrelated genes being affected (Featherstone and Brodie 2002; Bergman and Siegal 2003; Pouteau *et al*. 2004).

The abnormal cytoplasmic arrangement of *ppms2-1* spores indicates that *PPMS2-1* may be expressed in the spore itself and that the missing wall layer is derived from the spore. Of course, it is not inconceivable that this defect of the cytoplasm may in some part be due to the degradation observed in a number of the mutant spores. In order to determine the expression of *PPMS2-1* in haploid spores the transformation of *P. patens*, with a construct consisting of the GUS reporter gene under the control of the *PPMS2-1* promoter (*PPMS2-1::GUS*) (see chapter 2, section 2.5.3), was conducted. However, at the time of writing this thesis, putative positive transformants had not yet

been acquired. Once positive transformants are analysed in the near future, the specific location of *PPMS2-1* expression may be clarified and further illuminate its role in wall formation.

Attempts at determining differences in wildtype and mutant spore chemistry using Raman microspectroscopy were unsuccessful due to the lack of separation between sample sets with PCA. The wide scattering of replicates from *ppms2-1* on the PCA plot is possibly due to the ruptured nature of many of the mutant spores resulting in some spectra being representative of the outer surface of spores, and others representative of spore contents. Given these inconclusive data it would appear that Raman microspectroscopy is not a practical approach for the *ppms2-1* spore phenotype and other techniques, such as mass spectrometry where samples are ionised, should be explored.

There were no obvious morphological or growth defects at the protonemal or gametophore stages of the *ppms2-1* KO lines and sporophyte production appeared normal, although further analyses should be undertaken to detect any possible subtle phenotypes. In particular, given that a recent study has shown that moss calyptrae are covered by a cuticle (Budke *et al*. 2011), analysis of the *P. patens* calyptra cuticle may shed further light on which type of enzymatic pathway *PPMS2-1* is involved in since it is has been proposed that exine and cutin possibly share a common lipidic biosynthetic pathway. Additionally, it would be interesting to discover if a double knock-out of *PPMS2-1* and *PPMS2-2* (Pp_120173) would produce an even more pronounced spore phenotype.

Nevertheless, the observation of a highly defective spore wall with *PPMS2-1* loss of function suggests that the *MS2*-linked enzymatic pathway required for pollen wall development in angiosperms is present in some form in the sporophyte/spores of *P. patens* and therefore is most likely shared by all embryophytes.

5.3.2 Lack of complementation of *Arabidopsis thaliana ms2* mutants by *PPMS2-1*

The observation that *PPMS2-1* is unable to rescue the defective pollen wall of *A. thaliana ms2* suggests that the *MS2* gene has evolved in 'higher' land plants in concert with the increased complexity of their pollen walls. This is supported by the relatively

low protein sequence homology (48%) of the *MS2* homologues which is not particularly unexpected given the large evolutionary gulf between *A. thaliana* and *P. patens*. The same experiment was attempted using a *PPMS2-1* splice variant containing three introns (Fig. 5.9), as gene expression is often enhanced by the presence of introns, and in some instances the presence of multiple introns has been shown to be essential for gene expression (Karve *et al*. 2011). However, the same unrestored phenotype in the *A. thaliana ms2* background was also observed in this instance.

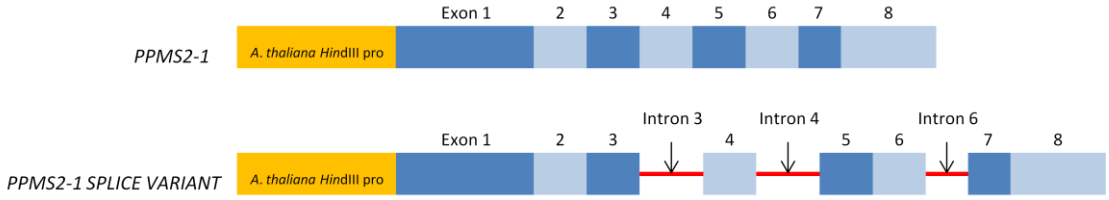

Figure 5.9. Schematic of *ATMS2pro::PPMS2-1* and a *ATMS2pro::PPMS2-1* splice variant constructs used for the attempted complementation of *A. thaliana ms2* mutants. The promoter is the *A. thaliana Hin*dIII *MS2* promoter fragment (1,077 base pairs) identified by Aarts *et al*. (1997). The splice variant consisted of the full *PPMS2-1* (Pp136_166V6; alias Pp_11916) CDS proposed and presented on the Cosmoss database, and three proposed introns.

It is possible that electron microscope analysis may not be sufficient to detect subtle partial rescues and future analysis should at least examine the functionality of *ATMS2pro::PPMS2-1* pollen with pollen germination tests. A partial rescue would indicate a conserved role of *MS2* in exine formation in land plants, but would also suggest that the interaction of PPMS2-1 protein with other elements of the sporopollenin biosynthesis pathway is less efficient than with the *A. thaliana* MS2 protein. Additionally, whilst the expression of *PPMS2-1* was verified in the flowers of *ATMS2pro::PPMS2-1*, this study did not attempt to confirm whether the *PPMS2-1* gene can actually produce a protein in the *A. thaliana ms2* background, and future analyses of this line should examine this by way of epitope tagging and/or western blot. Furthermore, the *PPMS2-1* model used for the complementation experiment has been produced using gene prediction algorithms with limited EST evidence to support

it. Therefore, some doubt remains as to whether the correct start codon has been identified (the start codon in the Cosmoss model has an adequate Kozak consensus) and consequently, whether the correct CDS has been used. Further mRNA sequencing and genetic characterisation should clarify the *PPMS2-1* CDS. Future complementation attempts may also look to use a different *A. thaliana MS2* promoter fragment. The *A. thaliana MS2 Hin*dIII promoter fragment employed here was originally used for a *MS2* promoter-*GUS* gene fusion by Aarts *et al*. (1997). The gene swap experiment which demonstrated that a rice *MS2* homologue, *DPW*, could complement *A. thaliana ms2* mutants, used a ~1,100 base pair *A. thaliana MS2* promoter fragment amplified directly upstream of the start codon (Shi *et al*. 2011), unlike the *Hin*dIII promoter fragment which was a 1,077 base pair fragment amplified 127 base pairs upstream of the start codon. It would be interesting to see if the use of this promoter fragment may yield a more obvious rescue, or partial rescue, in *A. thaliana ms2* mutants with *PPMS2-1*.

Complementation attempts were also made with *PPMS2-1* under the control of the constitutive *A. thaliana UB14* promoter (*ATUBQ14pro::PPMS2-1*) (see chapter 2, section 2.5.1) and positive transformants were identified. However, analysis of *ATUBQ14pro::PPMS2-1* pollen had not yet been conducted at the time of writing this thesis.

When these gene swap results are considered alongside the data from the *P. patens* knock-out experiments it would appear that the role of *MS2* in spore/pollen wall development is conserved across land plants. However, the lack of complementation of *A. thaliana MS2* with *PPMS2-1* suggests that, although *MS2* is conserved, it has evolved in 'higher' land plants as their pollen walls have increased in complexity.

5.4 Summary

The knock-out experiment results presented in this chapter have demonstrated that *PPMS2-1* is essential for normal *P. patens* spore wall development and the viability of spores as a whole which indicates that the involvement of *MS2* in spore/pollen wall formation is conserved in land plants. *PPMS2-1* deletion results in a defective perine and the absence of a spore wall layer. *ppms2-1* spores also exhibit a highly

disorganised cytoplasm which suggests that *PPMS2-1* is expressed in the spore itself and the absent layer is spore derived. Analysis of *ppms2-1* spores could not definitively determine which wall layer is absent and therefore two roles for *PPMS2-1* in spore wall development are hypothesised. First, the absent wall layer is the intine and therefore *PPMS2-1* is involved in intine formation which would infer that *MS2* has switched from playing a role in polysaccharide synthesis in 'lower' land plant spores to being recruited to play a role in sporopollenin synthesis and exine formation in the pollen grains of 'higher' land plants. Second, *PPMS2-1* is involved in exine formation and a highly defective and undetectable exine is present in *ppms2-1* spores, along with the intine, and enables the spores to still mostly resist acetolysis. Should this be subsequently proven, it would strongly suggest that the role of *MS2* in exine formation in angiosperms, and associated sporopollenin synthesis, has been conserved across 400 million years of land plant evolution. Additionally, the apparent inability of *PPMS2-1* to complement *A. thaliana ms2* mutants suggests that, whilst *MS2* is conserved, it has evolved in 'higher' land plants as pollen walls have accumulated greater complexity.

CHAPTER 6. **General discussion**

This chapter consolidates the findings from previous chapters so that the principle conclusions are discussed and put in context with existing research conducted in the field of spore and pollen wall development, and land plant evolution as a whole. Additionally, potential future works required to resolve some of the enduring unanswered questions are also considered. The principle conclusions are summarised first.

6.1 Principle conclusions

- *Physcomitrella patens* spore walls receive a sporopollenin input from both the spore and the tapetum, and therefore exospore development is controlled by both the diploid sporophyte and the haploid spore.

- *Physcomitrella patens* spores only reach full maturity at the latter stages of spore capsule development, a finding which contradicts previous propositions regarding sporogenesis with respect to spore capsule development put forward by Huang *et al*. (2009) and S. Schuette (University of Southern Illinois, USA, pers. comm.. 2009).

- Perine designated sporopollenin in *P. patens* appears to be supplied by a degenerating tapetum rather than a secretory tapetum.

- The vast majority of pollen wall associated genes identified in *A. thaliana* have homologues in *P. patens* and *S. moellendorffii*, and these homologues largely belong to multigene families indicating a high potential for genetic redundancy.

- Homologues of seven *A. thaliana* pollen wall associated genes (specifically implicated in tetrad separation and sporopollenin biosynthesis/exine formation) exhibit significantly upregulated expression in the *P. patens* sporophyte at stages when spore walls develop.

- *PPMS2-1* is essential for normal spore wall development and spore viability in *P. patens* and therefore, the involvement of *MS2* in spore and pollen wall development appears to be conserved in land plants.

- *PPMS2-1* cannot complement *A. thaliana ms2* mutants in the experiments conducted in this study which suggests that *MS2*, although conserved, may have evolved in higher plants as pollen walls have increased in complexity.

6.2 Spore wall development in *Physcomitrella patens*

Previous studies have emphasised how remarkably conserved the processes associated with sporogenesis and spore/pollen wall formation are within land plants (Owen and Makaroff 1995; Renzaglia *et al*. 2000; Scott *et al*. 2004; Blackmore *et al*. 2007), whereby contributions from diploid and haploid generations result in the formation of a sporopolleninous exospore shortly after meiosis at the tetrad stage, followed by the development of a pectocellulosic, microspore derived intine layer upon the release of the microspores from the tetrad. The observations presented in chapter 3 confirm that sporogenesis and spore wall formation in *P. patens* conforms to this paradigm. These observations also confirm the interplay between the diploid sporophyte and haploid microspores by identifying the main sources of sporopollenin for the perine and exine layers. Exine designated sporopollenin would appear to be derived from the spore (although the mechanisms for sporopollenin deposition in this instance remain unclear), and perine designated sporopollenin is provided by a rapidly degenerating tapetum. In 'higher' land plant pollen grains, which lack a perine, the tapetum contributes much of the exine sporopollenin (Ariizumi and Toriyama 2011; Dou *et al*. 2011). It seems highly feasible that the perine has become incorporated into the exine of 'higher' land plants which would mostly account for the tapetum assuming greater responsibility for exine sporopollenin and explain, to some degree, the increased complexity observed in pollen exines. In a number of *A. thaliana* pollen exine

mutants (Aarts *et al*. 1997; Morant *et al*. 2007; de Azevedo *et al*. 2009; Dobritsa *et al*. 2009), which exhibit highly aberrant exines due to the disruption in the synthesis of tapetally sourced sporopollenin, a thin layer which corresponds to the nexine, the internal part of the exine, is still present. The presence of this layer suggests that it may be microspore derived although an ongoing study has identified a tapetally expressed gene, named *NEXINE LAYER CONTROLLER* (*NLC*), which is thought to be involved in nexine development (Yang *et al*. 2012). Hopefully, the source of the nexine will be clarified further upon the conclusion of this study.

Consideration of these assertions allows propositions regarding spore/pollen wall component homology in land plants to be put forward. It would seem that the perine of 'lower' land plant spores may be homologous to the sexine division of the 'higher' land plant pollen exine. Additionally, should the nexine be shown to be microspore derived in some part then it would be reasonable to suggest that it is homologous to the exine of 'lower' land plant spores.

The study presented in chapter 3 has also further clarified spore development in *P. patens* with respect to spore capsule development. It has established a rudimentary developmental staging model which can more reliably aid and direct morphological and gene expression studies in the sporophyte than previously proposed schemes.

6.3 Identification of candidate spore wall genes in *Physcomitrella patens*

Through the combination of genome searches and transcriptomic analysis presented in chapter 4, a suite of candidate spore wall genes in *P. patens* has been identified and offers an insight into the biochemical and developmental pathways shared by the sporophytes and spores of mosses and anthers and pollen of 'higher' plants. Microarray analysis suggests that *A. thaliana* pectin degradation/tetrad separation and sporopollenin synthesis/exine gene homologues in *P. patens* are highly expressed during the spore wall building stages of sporophyte development. This implies that certain mechanisms required for pollen wall development in 'higher' land plants are conserved, and this conservation is due to similarites at the molecular level indicating that the proposed associated genetic pathways underpinning pollen wall development are ancient. Additionally, the finding that *P. patens* homologues of *A. thaliana* callose

wall genes are not significantly upregulated in the sporophyte is consistent with morphological observations which suggest that a callose wall only contributes to wall development in gymnosperms and angiosperms (Gabarayeva and Hemsley 2006). The callose wall can therefore be described as a more specialist element of pollen wall development and, as such, the genes and pathways associated with it are less well conserved and have evolved *de novo* or have been conscripted from existing callose networks involved with different cellular functions in 'lower' land plants.

6.4 A core component of the pollen wall developmental pathway appears to be ancient and highly conserved

The observations of abnormal spore walls with *PPMS2-1* loss of function, as presented in chapter 5, provides compelling evidence that the role of *MS2* in pollen wall development is highly conserved in land plants, and confirms that *MS2* is essential for normal spore and pollen wall development. Whilst this study does not definitively determine which aspect of spore wall formation *PPMS2-1* is involved in, a connection to sporopollenin synthesis seems most likely given the involvement of *MS2* in exine formation in angiosperms. This likely connection is reinforced by the significantly upregulated expression, during sporogenesis, of *P. patens* homologues of *A. thaliana* genes proposed to operate within the same fatty acid branch of the sporopollenin biosynthesis network as *MS2*.

The conservation of the biochemical and developmental pathway required for spore/pollen wall development is consistent with the findings from previous EvoDevo studies which have also found that core components of genetic networks, which underpin other evolutionary innovations which permitted the colonisation of land and subsequent diversification (leaf, root and stomata), are also ancient and highly conserved (Harrison *et al*. 2005; Menand *et al*. 2007; Chater *et al*. 2011; Ruszala *et al*. 2011). More specifically, the conservation of the genetic networks which control sporopollenin synthesis also meshes with the results obtained by a recent study which employed Fourier transform infrared spectroscopy (FT-IR) to demonstrate that the structure of sporopollenin has not changed since plants colonised land (Fraser *et al*. 2012).

The inability of *PPMS2-1* to complement *A. thaliana ms2* mutants suggests that the conservation of the *MS2* component of the sporopollenin biosynthesis framework is partial, and its evolution has been important in driving the increasing complexity observed in angiosperm pollen walls. Additionally, the abnormal cytoplasmic arrangement present in *ppms2-1* spores supports the electron microscope observations in chapter 3 that the sporopolleninous components (exine and perine) of the *P. patens* spore wall are most likely controlled by both the diploid sporophyte (perine) and the haploid spore (exine).

The support, provided in chapters 4 and 5, for the proposition that core components of the angiosperm pollen wall developmental pathway are operational in bryophyte spore walls suggests that these components were most likely co-opted from an existing network present in the last common ancestor of embryophytes, associated with the sporopolleninous zygote wall of algae. Therefore, the recruitment of parts of this genetic system represents a crucial step in the emergence of spore walls, an innovation which would endow the earliest 'prototypes' of land plants, or 'protoembryophytes', with the reproductive advantage of being able to manufacture desiccation-resistant spores (Brown and Lemmon 2011).

6.5 Future work

6.5.1 *Physcomitrella patens* spore wall development

Whilst the ultrastructural analysis presented in this thesis provides further insight and resolution with regards to spore wall ontogeny in *P. patens*, questions still remain with respect to key stages of its development. In particular, uncertainty persists as to whether lamellae are present and play a role in sporopollenin accumulation. The homogenous appearance of the mature *P. patens* spore exine may tempt observers to conclude that lamellae are not involved in its formation since their presence is often associated with observable substructure in embryophytes. However, sporopollenin deposition and/or compression can mask this substructure (Wellman 2004), and therefore, further and more exhaustive TEM analysis is required at early wall developmental stages to confirm their presence or absence. In addition to aiding future spore wall gene function studies, further elucidation of wall developmental

processes in this valuable model bryophyte may also assist in determining whether self-assembly processes are operative in the spore walls of basal land plants. The role of self-assembly in spore and pollen exine construction has been discussed by numerous authors (Heslop-Harrison 1972; Collinson *et al*. 1993; Hemsley *et al*. 1994, 2000, 2004; Borsh and Wilde 2000; Gabareyeva 2000; Gabarayeva and Hemsley 2006). The integration of EvoDevo studies and materials science, specifically colloid chemistry, which is central to studies of self-assembly in this context (Gabarayeva and Hemsley 2006), may clarify whether self-assembly processes are active in bryophyte spore walls and, if so, how these processes build upon the genetic control of wall development.

6.5.2 The fatty acid synthesis component of the sporopollenin biosynthesis framework

The finding that the function of *MS2* is conserved, or partially conserved, in embryophytes begs the question as to whether other genes proposed to function within a *MS2*-linked pathway in *A. thaliana* are also conserved, and as such potentially provide further evidence of a role in sporopollenin synthesis for *PPMS2-1*. These additional studies would indicate how much of the fatty acid synthesis component of the sporopollenin biosynthesis framework in higher plants is evolutionary conserved. The transcriptomic analysis presented in chapter 4 certainly suggests that all of the components of this proposed pathway may be similarly conserved and given this, verification by functional analyses of some of these genes is desirable. *P. patens* homologues of these genes, (e.g., *ACOS5*, *CYP703A2* and *CYP704B1*) were not investigated beyond the microarray analysis in this study due to their lack of obvious suitability for knock-out experiments, mostly because of the high potential for genetic redundancy. Therefore, different functional approaches could be investigated with these genes. For example, targeted gene silencing using RNA interference (RNAi) could be explored. Whilst this approach can be less definitive than knocking out genes, RNAi can enable multiple gene family members to be targeted and knocked-down with a single transgene. Additionally, if the conservation of the fatty acid synthesis pathway is to be further tested, the model proposed in *A. thaliana* (described in chapter 4) requires further verification. For example, clarification is required as to whether the two hydroxylation steps involving *CYP703A2* and *CYP704B1* operate within the same pathway. The results garnered from promising ongoing studies, using

FT-IR and pyrolysis to further elucidate the structure of sporopollenin (Fraser *et al*. 2012), should help to direct further propositions of models of sporopollenin synthesis.

6.5.3 The utilisation of emerging model systems and wider implications

Whilst much of the focus of this thesis has been on the bryophyte, *P. patens* (due to the availability of appropriate genetic resources), the development of novel 'lower' land plant experimental systems, such as *S. moellendorffii* and the liverwort, *Marchantia polymorpha*, will allow a deeper insight into the evolution of the spore and pollen wall, and more broadly, enable us to better assess whether the key mechanisms required for plant terrestrialisation have been conserved over 400 million years of embryophyte evolution. Additionally, comparisons of the genomes of these basal model plants with that of a genome of a charophycean green alga, the ancestral lineage from which embryophytes emerged, should further illuminate the evolution of sporopollenin encased propagules during the emergence of terrestrial plants, and perhaps confirm the direct evolutionary transfer of the algal zygote wall to the spores of embryophytes. Furthermore, as our understanding of the developmental processes which enabled plant terrestrialisation progresses, future research in this area may yield practical benefits. The rising global human population will further increase demand for natural resources, particularly water, and food. If crop plants can be genetically modified to use water more efficiently then an important contribution can be made towards ensuring that the demand for food and water does not outstrip supply.

References

Aarts MGM, Dirkse WG, Stiekema WJ, Pereira A. 1993. Transposon tagging of a male sterility gene in *Arabidopsis*. *Nature*, **363:** 715-717.

Aarts MGM, Hodge R, Halantidis K, Florack D, Wilson AZ, Mulligan BJ, Stiekema WJ Scott R, Pereira A. 1997. The *Arabidopsis* MALE STERILITY 2 protein shares similarity with reductases in elongation/condensation complexes. *The Plant Journal*, **12(3):** 615-623.

Abercrombie JM, O'Meara BC, Moffatt AR, Williams JH. 2011. Developmental evolution of flowering plant pollen tube cell walls: callose synthase (*CalS*) gene expression patterns. *EvoDevo*, **2:** 14.

Ahlers F, Thom I, Lambert J, Kuckuk R, Wiermann R. 1999. ^{1}H NMR analysis of sporopollenin from *Typha angustifolia*. *Phytochemistry*, **5:** 1095-1098.

Ariizumi T, Hatakeyama K, Hinata K, Inatsugi R, Nishida I, Sato S, Kato T, Tabata S, Toriyama K. 2004. Disruption of the novel plant protein NEF1 affects lipid accumulation in the plastids of the tapetum and exine formation of pollen, resulting in male sterility in *Arabidopsis thaliana*. *The Plant Journal*, **39:** 170-181.

Ariizumi T, Hatakeyama K, Hinata K, Sato S, Kato T, Tabata S, Toriyama K. 2003. A novel male-sterile mutant of *Arabidopsis thaliana*, *faceless pollen-1*, produces pollen with a smooth and an acetolysis-sensitive exine. *Plant Molecular Biology*, **53:** 107-116.

Ariizumi T, Hatakeyama K, Hinata K, Sato S, Kato T, Tabata S, Toriyama K. 2005. The HKM gene, which is identical to the MS1 gene of *Arabidopsis thaliana*, is essential for primexine formation and exine pattern formation. *Sexual Plant Reproduction*, **18:** 1-7.

Ariizumi T, Kawanabe T, Hatakeyama K, Sato S, Kato T, Tabata S, Toriyama K. 2008. Ultrastructural characterization of exine development of the transient defective exine 1 mutant suggests the existence of a factor involved in constructing reticulate exine architecture from sporopollenin aggregates. *Plant Cell Physiology*, **49(1):** 58-67.

Ariizumi T, Toriyama K. 2011. Genetic regulation of sporopollenin synthesis and pollen exine development. *Annual Review of Plant Biology*, **62:** 437-460.

Ashton NW, Cove DJ. 1977. The isolation and preliminary characterization of auxotrophic and analogue resistant mutants of the moss *Physcomitrella patens*. *Molecular and General Genetics*, **154:** 87-95.

Aya K, Hiwatashi Y, Kojima M, Sakakibara H, Ueguchi-Tanaka M, Hasebe M, Matsuoka M. 2011. The Gibberellin perception system evolved to regulate a pre-existing GAMYB-mediated system during land plant evolution. *Nature Communications*, **2:** 544.

Aya K, Ueguchi-Tanaka M, Kondo M, Hamada K, Yano K, Nishimura M, Matsuoka M. 2009. Gibberellin modulates anther development in rice via the transcriptional regulation of GAMYB. *Plant Cell*, **21:** 1453-1472.

Babenko VN, Rogozin IB, Mekhedov SL, Koonin EV. Prevalence of intron gain over intron loss in the evolution of paralogous gene families. *Nucleic Acids Research*, **32(12):** 3724-3733.

Banks JA, Nishiyama T, Hasebe M, Bowman JL, Gribskov M, De Pamphilis C, Albert VA, Aono N, Aoyama T, Ambrose BA *et al*. 2011. The *Selaginella* genome identifies genetic changes associated with the evolution of vascular plants. *Science*, **332:** 960-963.

Beerling DJ. 2007. *Emerald planet. How plants changed Earth's history.* Oxford: Oxford University Press.

Belin C. 2006. *Structure et fonctions de la protein kinase* OST1 *dans la cellule de garde d'Arabidopsis thaliana*. PhD Thesis. University of Paris-Sud: France.

Bergman A, Siegal ML. 2003. Evolutionary capacitance as a general feature of complex gene networks. *Nature*, **424:** 549-552.

Blackmore S, Barnes SH. 1987. Embryophyte spore walls: origin, development and homologies. *Cladistics*, **3:** 185-195.

Blackmore S, Takahashi M, Uehara K. 2000. A preliminary phylogenetic analysis of sporogenesis in pteridophytes. In: Harley MM, Morton CM, Blackmore S, eds. *Pollen and Spores: Morphology and Biology*. London: Royal Botanic Gardens, Kew, 109-124.

Blackmore S, Wortley AH, Skvarla JJ, Rowley JR. 2007. Pollen wall development in flowering plants. *New Phytologist*, **174:** 483-498.

Borsh T, Wilde V. 2000. Pollen variability within species, populations, and individuals, with particular reference to *Nelumbo*. In: Harley MM, Morton CM, Blackmore S, eds. *Pollen and Spores: Morphology and Biology*. London: Royal Botanic Gardens, Kew, 285-299.

Brett C, Waldron K. 1996. *Physiology and Biochemistry of Plant Cell Walls*. London: Chapman and Hall.

Brown RC, Lemmon BE. 1980. Ultrastructure of sporogenesis in a moss, *Ditrichum pallidum*. III. Spore wall formation. *American Journal of Botany*, **67(6):** 918-934.

Brown RC, Lemmon BE. 1984. Spore wall development in *Andreaea* (Musci: Andreaeopsida). *American journal of Botany*, **71(3):** 412-420.

Brown RC, Lemmon BE. 1985. Spore wall development in the liverwort, *Haplomitrium hookeri*. *Canadian Journal of Botany*, **64:** 1174-1182.

Brown RC, Lemmon BE. 1988. Sporogenesis in bryophytes. *Advances in Bryology*, **3:** 159-223.

Brown RC, Lemmon BE. 1990. Sporogenesis in bryophytes. In: Blackmore S, Barnes SH, eds. *Pollen and Spores: Patterns of Diversification*. The Systematics Association Special Volume No. 44. Oxford: Oxford Science Publications, 9-24.

Brown RC, Lemmon BE. 1993. Spore wall development in the liverwort *Fossombronia wondraczekii* (Corda) Dum. *Journal of the Hattori Botanical Laboratory*, **74:** 83-94.

Brown RC, Lemmon BE. 2011. Spores before sporophytes: hypothesizing the origin of sporogenesis at the algal-plant transition. *New Phytologist*, **190(4):** 875-881.

Brown RC, Lemmon BE, Carothers ZB. 1982. Spore wall development in *Sphagnum lescurii*. *Canadian Journal of Botany*, **60(11):** 2394-2409.

Brown RC, Lemmon BE, Renzaglia KS. 1986. Sporocytic control of spore wall pattern in liverworts. *American Journal of Botany*, **73(4):** 593-596.

Budke JM, Goffinet B, Jones CS. 2011. A hundred-year-old question: is the moss calyptras covered by a cuticle? A case study of Funaria hygrometrica. *Annals of Botany*, **107(8):** 1279-1286.

Carrión JS, Cano MJ, Guerra J. 1995. Spore morphology in the moss genus *Pterygoneurum* Jur. (Pottiaceae). *Nova Hedwigia*, **61:** 481-496.

Chater C, Kamisugi Y, Movahedi M, Fleming A, Cuming AC, Gray JE, Beerling DJ. 2011. Regulatory Mechanism controlling stomatal behavior conserved across 400 million years of land plant evolution. *Current Biology*, **12:** 1025-1029.

Chen X, Goodwin SM, Boroff VL, Liu X, Jenks MA. 2003. Cloning and characterization of the WAX2 gene of Arabidopsis involved in cuticle membrane and wax production. *Plant Cell*, **15:** 1170-1185.

Chen W, Yu X, Zhang K, Shi J, De Oliveira S, Schreiber L, Shanklin J, Zhang D. 2011. *Male Sterile2* encodes a plastid-localized fatty acyl carrier protein reductase required for pollen exine development in Arabidopsis. *Plant Physiology*, **157:** 842-853.

Clough SJ, Bent AF. 1998. Floral dip: A simplified method for Agrobacterium-mediated transformation of Arabidopsis thaliana. *Plant Journal*, **16:** 735-743.

Collier PA, Hughes KW. 1982. Life cycle of the moss, *Physcomitrella patens*, in culture. *Journal of Tissue Culture Methods*, **7(1):** 19-22.

Collinson ME, Hemsley AR, Taylor WA. 1993. Sporopollenin exhibiting colloidal organization in spore walls. *Grana*, **1, supplement:** 31-39.

Cove DJ. 2000. The moss, *Physcomitrella patens*. *Journal of Plant Growth Regulation*, **19:** 275-283.

Crang RE, May G. 1974. Evidence for silicon as a prevalent elemental component in pollen wall structure. *Canadian Journal of Botany*, **52(10):** 2171-2174.

Cronk Q. 2009. *The Molecular Organography of Plants*. Oxford: Oxford University Press.

De Avezado Souza C, Kim SS, Koch S, Kienow l, Schneider K, Mckim SM, Haugh GW, Kombrink E, Douglas CJ. 2009. A novel fatty acyl-CoA synthase is required for pollen development and sporopollenin biosynthesis in *Arabidopsis*. *The Plant Cell*, **21:** 507-525.

De Gelder J, De Gussem K, Vandenabeele P, Moens L. 2007. Reference database of Raman spectra of biological molecules. *Journal of Raman Spectroscopy*, **38:** 1133-1147.

Dickinson HG. 1971. The role played by sporopollenin in the development of pollen in *Pinus banksiana*. In: Brooks J, Grant PR, Muir MD, van Gijzel P, Shaw G, eds. *Sporopollenin*. New York: Academic Press, 31-65.

Dickinson HG, Bell PR. 1970. The development of the sacci during pollen formation in *Pinus banksiana*. *Grana*, **10:** 101-108.

Dickinson HG, Lewis D. 1973. The formation of the tryphine coating the pollen grains of *Raphanus*, and its properties relating to the self-incompatibility system. *Proceedings of the Royal Society of London*, **185:** 149-165.

Doan TT, Carlsson AS, Hamberg M, Bülow L, Stymne S, Olsson P. 2009. Functional expression of five *Arabidopsis* fatty acyl-CoA reductase genes in *Escherichia coli*. *Journal of Plant Physiology*, **166:** 787-796.

Dobritsa AA, Lei ZT, Nishikawa SI, Urbanaczyk-Wochniak E, Huhman DV, Preuss D, Sumner LW. 2010. LAP5 and LAP6 encode anther-specific proteins with similarity to chalcone synthase essential for pollen exine development in Arabidopsis. *Plant Physiology*, **153:** 937-955.

Dobritsa AA, Shresta J, Morant M, Pinot F, Matsuno M, Swanson R, Møller BL, Preuss D. 2009. CYP704B1 is a long-chain fatty acid ω-hydroxylase essential for sporopollenin synthesis in pollen of *Arabidopsis*. *Plant Physiology*, **151:** 574-589.

Domínguez E, Mercado JA, Quesada MA, Heredia A. 1999. Pollen sporopollenin: degradation and structural elucidation. *Sex Plant Reproduction*, **12:** 171-178.

Dong X, Hong Z, Sivaramakrishnan M, Mahfouz M, Verma DP. 2005. Callose synthase (CalS5) is required for exine formation during microgametogenesis and for pollen viability in *Arabidopsis*. *Plant Journal*, **42:** 315-328.

Dou XY, Yang KZ, Zhang Y, Wang W, Liu XL, Chen LQ, Zhang XQ, Ye D. 2011. WBC27, an adenosine tri-phosphate-binding cassette protein, controls pollen wall formation and patterning in Arabidopsis. *Journal of Integrative Plant Biology*, **53(1):** 74-88.

Drakakaki G, Zabotina O, Delgado I, Robert S, Keegstra K, Raikhel N. 2006. *Arabidopsis* reversibly glycosylated polypeptides 1 and 2 are essential for pollen development. *Plant Physiology*, **142:** 1480-1492.

Duan H, Schuler MA. 2005. Differential expression and evolution of the *Arabidopsis* CYP86A subfamily. *Plant Physiology*, **137:** 1067-1081.

Echlin P, Godwin H. 1969. The ultrastructure and ontogeny of pollen in *Helleborus foetidus* L. III. The formation of the pollen grain wall. *Journal of Cell Science*, **5:** 459-477.

Edgar RC. 2004. MUSCLE: multiple sequence alignment with high accuracy and high throughput. *Nucleic Acids Research*, **32(5):** 1792-1797.

Erdtman G. 1960. The acetolysis method. *Sven Bot Tidskr*, **54:** 561-564.

Estébanez B, Alfayate C, Ron E. 1997. Observations on spore ultrastructure in six species of *Grimmia* (Bryopsida). *Grana*, **36(6):** 347-357.

Featherstone DE, Broadie K. 2002. Wrestling with pleiotropy: genomic and topological analysis of the yeast gene expression network. *Bioessays*, **24:** 267-274.

Federici L, Caprari C, Mattei B, Savino C, Di Matteo A, De Lorenzo, Cervone F, Tsernoglou D. 2001. Structural requirements of endopolygalacturonase for the interaction with PGIP (Polygalacturonase-inhibiting protein). *Proceedings of the National Academy of Sciences*, **98(23):** 13425-13430.

Fei H, Zhang R, Pharis RP, Sawhney VK. 2004. Pleiotropic effects of the *males sterile33* (*ms33*) mutation in Arabidopsis are associated with modifications in endogenous gibberellins, indole-3-acetic acid and abscisic acid. *Planta*, **219:** 649-660.

Felsenstein J. 1985. Confidence limits on phylogenies: an approach using the bootstrap. *Evolution*, **39:** 783-791.

Francis KE, Lam SY, Copenhaver GP. 2006. Separation of *Arabidopsis* pollen tetrads is regulated by QUARTET1, a pectin methylesterase gene. *Plant Physiology*, **142:** 1004-1013.

Frankel R, Izhar S, Nitsan J. 1969. Timing of callase activity and cytoplasmic male sterility in *Petunia*. *Biochemical Genetics*, **3:** 451-455.

Fraser WT, Scott AC, Forbes AES, Glasspool IJ, Plotnick RE, Kenig F, Lomax BH. 2012. Evolutionary stasis of sporopollenin biochemistry revealed by unaltered Pennsylvanian spores. *New Phytologist*, **196(2):** 397-401.

Gabarayeva NI. 1993. Hypothetical ways of exine pattern determination. *Grana*, **33, supplement 2:** 54-59.

Gabarayeva NI. 1996. Sporoderm development in *Liriodendron chinense* (Magnoliaceae): a probable role of the endoplasmic reticulum. *Nordic Journal of Botany*, **16:** 307-323.

Gabarayeva NI. 2000. Principles and recurrent themes in sporoderm development. In: Harley MM, Morton CM, Blackmore S, eds. *Pollen and Spores: Morphology and Biology*. London: Royal Botanical Gardens, Kew, 1-16.

Gabarayeva NI, Hemsley AR. 2006. Merging concepts: The role of self-assembly in the development of pollen wall structure. *Review of Palaeobotany and Palynology*, **138:** 121-139.

Gibalová A, Reňák D, Matczuk K, Dupl'áková N, Cháb D, Twell D, Honys D. 2009. AtbZIP34 is required for *Arabidopsis* pollen wall patterning and the control of several metabolic pathways in developing pollen. *Plant Molecular Biology*, **70:** 581-601.

Glime JM. 2007. *Bryophyte Ecology*. Volume 1. Physiological Ecology. Ebook sponsored by Michigan Technological University and the International Association of Bryologists.

Graham LE. 1993. *Origin of Land Plants*. New York: Wiley.

Grienenberger E, Kim SS, Lallemand B, Geoffroy P, Heintz D, Souza CD, Heitz T, Douglas CJ, Legrand M. 2010. Analysis of TETRAKETIDE alpha-PYRONE REDUCTASE function in *Arabidopsis thaliana* reveals a previously unknown, but conserved, biochemical pathway in sporopollenin monomer biosynthesis. *The Plant Cell*, **22:** 4067-4083.

Guan Y, Huang X, Zhu J, Gao J, Zhang H, Yang Z. 2008. *RUPTURED POLLEN GRAIN1*, a member of the MtN3/saliva gene family, is crucial for exine pattern formation and cell integrity of microspores in *Arabidopsis*. *Plant Physiology*, **147:** 852-863.

Haig D, Wilczek A. 2006. Sexual conflict and the alternation of haploid and diploid generations. *Philosophical Transactions of the Royal Society B*, **361:** 335-343.

Harrison CJ, Corley SB, Moylan EC, Alexander DL, Scotland RW, Langdale JA. 2005. Independent recruitment of a conserved developmental mechanism during leaf evolution. *Nature*, **434:** 509-514.

Hemsley AR, Collinson ME, Brain APR. 1992. Colloidal crystal-like structure of sporopollenin in the megaspore walls of recent *Selaginella* and similar fossil spores. *Botanical Journal of Linnean Society*, **108:** 307-320.

Hemsley AR, Collinson ME, Kovach WL, Vincent B, Williams T. 1994. The role of self-assembly in biological systems: evidence from iridescent colloidal sporopollenin in *Selaginella* megaspore walls. *Philosophical Transactions of the Royal Society London, Series B*, **345:** 163-173.

Hemsley AR, Collinson ME, Vincent B, Griffiths PC, Jenkins PD. 2000. Self-assembly of colloidal units in exine development. In: Harley MM, Morton CM, Blackmore S, eds. *Pollen and Spores: Morphology and Biology*. London: Royal Botanic Gardens, Kew, 31-44.

Hemsley AR, Lewis J, Griffiths PC. 2004. Soft and sticky development: some underlying reasons for microarchitectural pattern convergence. *Review of Palaeobotany and Palynology*, **130:** 105-119.

Hemsley AR, Gabarayeva NI. 2007. Exine development: The importance of looking through a colloidal chemistry "window". *Plant Systematics and Evolution*, **263:** 25-49.

Heslop-Harrison J. 1963. An ultrastructural study of pollen wall ontogeny in *Silene pendula*. *Grana Palynologica*, **4:** 7-24.

Heslop-Harrison J. 1968a. The pollen grain wall. *Science*, **161:** 230-237.

Heslop-Harrison J. 1968b. Some fine structural features of intine growth in the young microspore of *Lilium henryi*. *Portugalie Acta Biologicae*, **10:** 235-246.

Heslop-Harrison J. 1972. Pattern in plant cell wall morphogenesis in miniature. *Proceedings of the Royal Institution of Great Britain*, **45:** 335-351.

Hess MW. 1993. Cell-wall development in freeze-fixed pollen: intine formation of *Ledebouria socialis* (Hyacinthaceae). *Planta*, **189:** 139-149.

Higginson T, Li SF, Parish RW. 2003. AtMYB103 regulates tapetum and trichome development in *Arabidopsis thaliana*. *Plant Journal*, **35:** 177-192.

Hill JP. 1996. Heterochrony in the anther. In: D'Arcy WG, Keating RC, eds. *The anther - form, function and phylogeny*. Cambridge: Cambridge University Press, 118-135.

Hird DL, Worrall D, Hodge R, Smartt S, Paul W, Scott R. 1993. The anther-specific protein encoded by the *Brassica napus* and *Arabidopsis thaliana* A6 gene displays similarity to β-1,3-glucanase. *The Plant Journal*, **4:** 1023-1033.

Hohe A, Rensing SA, Mildner M, Lang D, Reski R. 2002. Day length and temperature strongly influence sexual reproduction and expression of a novel MADS-box gene in the moss *Physcomitrella patens*. *Plant Biology*, **4:** 595-602.

Huang C, Chung C, Lin Y, Hsing YC, Huang AHC. 2009. Oil bodies and oleosins in *Physcomitrella* possess characteristics representative of early trends in evolution. *Plant Physiology*, **150:** 1192-1203.

Huang M, Hsing YC, Huang AHC. 2011. Transcriptomes of the anther sporopohyte: availability and uses. *Plant and Cell Physiology*, **52(9):** 1459-1466.

Huang WE, Li M, Jarvis RM, Goodacre R, Banwart SA. 2010. Shining light on the microbial world: the application of Raman microspectroscopy. In: Laskin AI, Sariaslani S, Gadd GM, eds. *Advances in applied microbiology*. Burlington: Academic Press, 153-186.

Ito T, Nagata, N, Yoshiba Y, Ohme-takagi M, Ma H, Shinozaki K. 2007. *Arabidopsis* MALE STERILITY1 encodes a PHD-type transcription factor and regulates pollen and tapetum development. *The Plant Cell*, **19:** 3549-3562.

Jones DT, Taylor WR, Thornton JM. 1992. The rapid generation of mutation data matrices from protein sequences. *Computer Applications in the Biosciences*, **8:** 275-282.

Jiang J, Zhang Z, Cao J. 2013. Pollen wall development: the associated enzymes and metabolic pathways. *Plant Biology*, **15(2):** 249-263.

Jones TM, Anderson AJ, Albersheim P. 1972. Hostpathogen interactions IV, Studies on the polysaccharide-degrading enzymes secreted by *Fusarium oxysporum f. sp. lycopersici*. *Physiological Plant Pathology*, **2:** 153-166.

Jung KH, Han MJ, Lee DY, Lee YS, Schreiber L, Franke R, Faust A, Yephremov A, Saedler H, Kim YW, *et al*. 2006. *Wax-deficient anther1* is involved in cuticle and wax production in rice anther walls and is required for pollen development. *Plant Cell*, **18:** 3015-3032.

Kafri R, Springer M, Pilpel Y. 2009. Genetic redundancy: new tricks for old genes. *Cell*, **136:** 389-392.

Kamisugi Y, Cuming AC, Cove DJ. 2005. Parameters determining the efficiency of gene targeting in the moss *Physcomitrella patens*. *Nucleic Acids Research*, **33(19):** e173.

Karve R, Liu W, Willet SG, Torii KU, Shpak ED. 2011. The presence of multiple introns is essential for ERECTA expression in Arabidopsis. *RNA*, doi:10.1261/ma.2825811.

Kasahara M, Hiwatashi Y, Ishikawa T, Suzuki Y, Kamisugi Y, Lang D, Cuming AC, Reski R, Hasebe M, Nishiyama T. 2011. Genetic map of *Physcomitrella patens* based on SNP identification with Illumina sequencing. In Moss 2011 (Freiburg, Germany).

Kenrick P, Crane PR. 1997. *The Origin and Early Diversification of Land Plants: A Cladistic Study*. Washington: Smithsonian Institution Press.

Kim SS, Grienenberger E, Lallemand B, Colpitts CC, Kim SY, Souza CD, Geoffroy P, Henitz, D, Krahn D, Kaiser M, Kombrink E, Heitz T, Suh DY, Legrand M, Douglas CJ. 2010. LAP6/POLYKETIDE SYNTHASE A and LAP5/POLYKETIDE SYNTHASE B encode hydroxyalkyl alpha-pyrone synthases required for pollen development and sporopollenin biosynthesis in *Arabidopsis thaliana*. *The Plant Cell*, **22:** 4045-4066.

Knight CD, Cuming AC, Quatrano RS. 2002. Moss gene technology. In: Gilmartin PM, Bowler C, eds. *Molecular Plant Biology*. Oxford: Oxford University Press, 285-299.

Krystyna Z. 1995. Ultrastructural features of secretory tapetum in the capsule of the moss *Ceratodon purpureus* Hedw Brid. *Phytomorphology*, **45:** 31-37.

Lallemand B, Erhardt M, Heitz T, Legrand M. 2013. Sporopollenin biosynthetic enzymes interact and constitute a metabolon localized to the endoplasmic reticulum of tapetum cells. *Plant Physiology*, doi: http://dx.doi.org/10.1.4/pp112.213124.

Li H, Zhang DB. 2010. Biosynthesis of anther cuticle and pollen exine in rice. *Plant Signaling and Behavior*, **5:** 1121-1123.

Li J, Yu MA, Geng LL, Zhao J. 2010. The fasciclin-like arabinogalactan protein gene, FLA3, is involved in microspore development of *Arabidopsis*. *The Plant Journal*, **64:** 482-497.

Li SF, Higginson T, Parish RW. 1999. A novel MYB-related gene from *Arabidopsis thaliana* expressed in development anthers. *Plant Cell Physiology*, **40:** 343-347.

Lugardon B. 1990. Pteridophyte sporogenesis: a survey of spore wall ontogeny and fine structure in a polyphyletic plant group. In: Blackmore S, Knox, RB, eds. *Microspores: Evolution and Ontogeny*. London: Academic Press, 95-120.

Lugardon B. 1994. Exine formation in *Chamaecyparis lawsoniana* (Cupressaceae) and a discussion on pteridophyte exospores and gymnosperm exine ontogeny. *Review of palaeobotany and palynology*, **85:** 35-51.

McClymont JW, Larson DA. 1964. An electron-microscope study of spore wall structure in the Musci. *American Journal of Botany*, **51(2):** 195-200.

Menand B, Yi K, Jouannic S, Hoffman L, Ryan E, Linstead P, Schaefer DG, Dolan L. 2007. An ancient mechanism controls the development of cells with a rooting function in land plants. *Science*, **316:** 1477-1480.

Meuter-Gerhards A, Riegart S, Wiermann R. 1999. Studies on sporopollenin biosynthesis in *Curcurbita maxima* (DUCH)-II: the involvement of aliphatic metabolism. *Journal of Plant Physiology*, **154:** 431-436.

Morant M, Bak S, Møller BL, Werck-Reichhart D. 2003. Plant cytochromes P450: tools for pharmacology, plant protection and photoremediation. *Current Opinion in Biotechnology*, **14:** 1-12.

Morant M, Jørgensen K, Schaller H, Pinot F, Møller BL, Werck-Reichhart D, Bak S. 2007. CYP703 is an ancient cytochrome P450 in land plants catalyzing in-chain hydroxylation of lauric acid to provide building blocks for sporopollenin synthesis in pollen. *Plant Cell*, **19:** 1473-1487.

Morbelli MA. 1995. Megaspore wall in Lycophyta – ultrastructure and function. *Review of Palaeobotany and Palynology*, **85:** 1-12.

Nakosteen PC, Hughes KW. 1978. Sexual life cycle of three species of Funariaceae in culture. *The Bryologist*, **81(2):** 307-314.

Nei M, Kumar S. 2000. *Molecular Evolution and Phylogenetics*. New York: Oxford University Press.

Nishikawa S, Zinkl GM, Swanson RJ, Maruyama D, Preuss D. 2005. Callose (beta-1,3 glucan) is essential for *Arabidopsis* pollen wall patterning, but not tube growth. *BMC Plant Biology*, **5:** 22.

Nishiyama T, Fujita T, Shin-I T, Seki M, Nishide H, Uchiyama I, Kamiya A, Carninci P, Hayashizaki Y, Shinozaki K, Kohara Y, Hasebe M. 2003. Comparative genomics of *Physcomitrella patens* gametophytic transcriptome and *Arabidopsis thaliana*: implication for land plant evolution. *Proceedings of the National Academy of Sciences*, **100 (13):** 8007-8012.

Owen HA, Makaroff CA. 1995. Ultrastructure of microsporogenesis and microgametogenesis in *Arabidopsis thaliana* (L.) Haynh. Ecotype Wassilewskija (Brassicaceae). *Protoplasma*, **185:** 7-21.

Pacini E, Franchi GG, Hesse M. 1985. The tapetum: Its form, function, and possible phylogeny in Embryophyta. *Plant Systematics and Evolution*, **149(3):** 155-185.

Paxson-Sowders DM, Dodrill CH, Owen HA, Makaroff CA. 2001. DEX1, a novel plant protein, is required for exine pattern formation during pollen development in *Arabidopsis*. *Plant Physiology*, **127:** 1739-1749.

Paxson-Sowders DM, Owen HA, Makaroff CA. 1997. A comparative ultrastructural analysis of exine pattern development in wild-type *Arabidopsis* and a mutant defective in pattern formation. *Protoplasma*, **198:** 53-65.

Pelloux J, Rustérucci C, Mellerowicz EJ. 2007. New insights into pectin methylesterase structure and function. *Trends in Plant Science*, **12(6):** 267-277.

Pérez-Muñoz CA, Jernstedt JA, Webster BD. 1993. Pollen wall development in *Vigna vexillata*: II. Ultrastructural studies. *American Journal of Botany*, **80(10):** 1193-1202.

Piffanelli P, Ross JHE, Murphy DJ. 1998. Biogenesis and function of the lipidic structures of pollen grains. *Sexual Plant reproduction*, **11:** 65-80.

Polevova SV. 2012. Sporoderm ultrastructure in *Anthoceros agrestis* Paton. *Arctoa*, **21:** 63-69.

Pouteau S, Ferret V, Gaudin V, Lefebvre D, Sabar M, Zhao G, Prunus F. 2004. Extensive phenotypic variation in early flowering mutants of Arabidopsis. *Plant Physiology*, **135:** 201-211.

Preuss D, Rhee SY, Davis RW. 1994. Tetrad Analysis possible in *Arabidopsis* with mutation of the QUARTET (QRT) genes. *Science*, **264:** 1458-1460.

Prigg MJ, Bezanilla M. 2010. Evolutionary crossroads in developmental biology: *Physcomitrella patens*. *Development*, **137:** 3535-3543.

Puchta H. 2003. Towards the ideal GMP: Homologous recombination and marker gene excision. *Journal of Plant Physiology*, **160:** 743-754.

Quatrano RS, McDaniel SF, Khandelwal A, Perroud P, Cove, DJ. 2007. *Physcomitrella patens*: mosses enter the genomic age. *Current Opinion in Plant Biology*, **10:** 182-189.

Qui YL, Li LB, Wang B, Chen ZD, Knoop V, Groth-Malonek M, Dombrovska, O, Lee J, Kent L, Rest J, Estabrook GF, Hendry TA, Taylor DW, Testa CM, Ambros M, Crandall-Stotler B, Duff RJ, Stech M, Frey W, Quandt D, Davis CC. 2006. The deepest divergences in land plants inferred from phylogenomic evidence. *Proceedings of the National Academy of Sciences of the United States of America*, **103:** 15511-15516.

Quilichini TD, Friedmann MC, Samuels AL, Douglas, CJ. 2010. ATP-binding cassette transporter G26 (ABCG26) is required for male fertility and pollen exine formation in *Arabidopsis thaliana*. *Plant Physiology*, **154:** 678-690.

Rensing SA, Ick J, Fawcett JA, Lang D, Zimmer A, Van De Peer Y, Reski R. 2007. An ancient genome duplication contribution to the abundance of metabolic genes in the moss *Physcomitrella patens*. *BMC Evolutionary Biology*, **7:** 130.

Rensing SA, Lang D, Zimmer A, *et al*. 2008. The *Physcomitrella* genome reveals evolutionary insights into the conquest of land by plants. *Science*, **319:** 64-69.

Renzaglia KS, Duff RJ, Nickrent DL, Garbary DJ. 2000. Vegetative and reproductive innovations of early land plants: implications for a unified phylogeny. *Philosophical Transactions of the Royal Society of London Series B-Biological Sciences*, **355:** 769-793.

Reski R, Cove DJ. 2004. *Physcomitrella patens*. *Current Biology*, **14(7):** 261-262.

Reski R, Frank W. 2005. Moss (*Physcomitrella* patens) functional genomics – gene discovery and tool development, with implications for crop plants and human health. *Briefings in Functional Genomics and Proteomics*, **4(1):** 48-57.

Rhee SY, Osborne E, Poindexter PD, Somerville CR. 2003. Microspore separation in the *quartet 3* mutants of *Arabidopsis* is impaired by a defect in a developmentally regulated polygalacturonase required for pollen mother cell wall degradation. *Plant Physiology*, **133:** 1170-1180.

Rhee SY, Somerville CR. 1998. Tetrad pollen formation in *quartet* mutants of *Arabidopsis thaliana* is associated with persistence of pectic polysaccharides of the pollen mother cell. *The Plant Journal*, **15(1):** 79-88.

Roland F. 1971. Characterization and extraction of the polysaccharides of the intine and of the generative cell wall in the pollen grains of some Ranunculaceae. *Grana*, **11(2):** 101-106.

Rowland O, Lee R, Franke R, Schreiber L, Kunst L. 2007. The CER3 wax biosynthetic gene from *Arabidopsis thaliana* is allelic to WAX2/YRE/FLP1, *Federation of European Biochemical Societies Letters*, **581:** 3538-3544.

Ruszala EM, Beerling DJ, Franks PJ, Chater C, Casson SA, Gray JE, Hetherington AM. 2011. Land plants acquired active stomatal control early in their evolutionary history. *Current biology*, **21:** 1030-1035.

Schaefer DG. 2002. A new moss genetics: targeted mutagenesis in *Physcomitrella patens*. *Annual Review of Plant Biology*, **53:** 477-501.

Schaefer DG, Zryd J. 1997. Efficient gene targeting in the moss *Physcomitrella patens*. *The Plant Journal*, **11(6):** 1195-1206.

Schaefer DG, Zrÿd J. 2001. The moss *Physcomitrella patens*, now and then. *Plant Physiology*, **127:** 1430-1438.

Schols HA, Voragen AGJ. 2002. The chemical structure of pectins. In: Seymour GB, Knox PG, eds. *Pectins and Their Manipulation*. Boca Raton: CRC Press, 1-29.

Schuette S, Renzaglia KS, Duckett JG. 2006. Exploring the biology of the model moss *Physcomitrella patens*: the forgotten frontier. In Botany 2006 (Chico, USA).

Schuette S, Wood AJ, Geisler M, Geisler-Lee J, Ligrone R, Renzaglia KS. 2009. Novel localization of callose in the spores of *Physcomitrella patens* and phylogenomics of the callose synthase gene family. *Annals of Botany*, **103(5):** 749-756.

Scott RJ, Hodge R, Paul W, Draper J. 1991. The molecular biology of anther differentiation. *Plant Science*, **80:** 167-191.

Scott RJ, Spielman M, Dickinson HG. 2004. Stamen structure and function. *Plant Cell*, **16:** S46-S60.

Session A, Burke E, Presting G, Aux G, McElver J, Patton D, Dietrich B, Ho P, Bacwaden J, Ko C *et al*. 2002. A high-throughput *Arabidopsis* reverse genetics system. *Plant Cell*, **14:** 2985-2994.

Shi J, Tan H, Yu X, Liu Y, Liang W, Ranathunge K, Franke RB, Schreiber L, Wang Y, Kai G, Shanklin J, Ma H, Zhang D. 2011. *Defective Pollen Wall* is required for anther and microspore development in rice and encodes a fatty acyl carrier protein reductase. *The Plant Cell*, **23:** 2225-2246.

Smyth GK. 2004. Linear models and empirical bayes methods for assessing differential expression in microarray experiments. *Statistical Applications in Genetics and Molecular Biology*, **3(1):** Article 3.

Smyth GK. 2005. Limma: linear models for microarray data. In: Gentleman VCR, Dudoit S, Irizarry R, Huber W, eds. *Bioinformatics and computational biology solutions using R and Bioconductor*. New York: Springer, 397-420.

Stetler DA, DeMaggio AE. 1976. Ultrastructural characteristics of spore germination in the moss *Dawsonia superba*. *American Journal of Botany*, **63(4):** 438-442.

Stieglitz H, Stern H. 1973. Regulation of β-1,3-glucanase activity in developing anthers of *Lilium*. *Developmental Biology*, **34:** 169-173.

Suárez-Cervera M, Arcalís E, Le Thomas A, Seoane-Camba JA. 2002. Pectin distribution pattern in the apertural intine of *Euphorbia peplus* L. (Euphorbiaceae) pollen. *Sexual Plant Reproduction*, **14:** 291-298.

Suzuki T, Masaoka K, Nishi M, Nakamura K, Ishiguro S. 2008. Identification of *kaonashi* mutants showing abnormal pollen exine structure in *Arabidopsis thaliana*. *Plant and Cell Physiology*, **49(10):** 1465-1477.

Tamura K, Peterson D, Peterson N, Stecher G, Nei M, Kumar S. 2011. MEGA5: molecular evolutionary genetics analysis using maximum likelihood, evolutionary distance, and maximum parsimony methods. *Molecular Biology and Evolution*, **28:** 2731-2739.

Tan H, Liang W, Hu J, Zhang D. 2012. *MTR1* encodes a secretory fasciclin glycoprotein required for male reproductive development in rice. *Developmental Cell*, **22:** 1127-1137.

Taylor WA. 1986. Ultrastructure of sphenophyllalean spores. *Review of Palaeobotany and Palynology*, **47:** 105-128.

Tryon AF, Lugardon B. 1991. Spores of the Pteridophyta. Surface, wall structure and diversity based on electron microscope studies. New York: Springer.

Tucker GA, Seymour GB. 2002. Modification and degradation of pectins. In: Seymour GB, Knox PG, eds. *Pectins and Their Manipulation*. Boca Raton, CRC Press, 150-173.

Uehara K, Kurita S. 1989. An ultrastructural study of spore wall morphogenesis in *Equisetum arvense*. *American Journal of Botany*, **76:** 939-951.

Uehara K, Kurita S. 1991. Ultrastructural study on spore wall morphogenesis in *Lycopodium clavatum* (Lycopodiaceae). *American Journal of Botany*, **78(1):** 24-36.

Uehara K, Kurita S, Sahashi N, Ohmoto T. 1991. Ultrastructural study of microspore wall morphogenesis in *Isoetes japonica* (Isoetaceae). *American Journal of Botany*, **78:** 1182-1190.

Updegraff DM. 1969. Semimicro determination of cellulose in biological materials. *Analytical Biochemistry*, **32(3):** 420-424.

Villarreal JC, Renzaglia KS. 2006. Sporophyte structure in the neotropical hornwort *Phaeomegaceros fimbriatus*: Implications for phylogeny, taxonomy, and character evolution. *International Journal of Plant science*, **167(3):** 413-427.

Vizcay-Barrena G, Wilson ZA. 2006. Altered tapetal PCD and pollen wall development in the *Arabidopsis ms1* mutant. *Journal of Experimental Botany*, **57(11):** 2709-2717.

Waterkeyn L, Bienfait A. 1971. Morphologie et nature des parois sporocytaires chez les pteridophytes. *La Cellule*, **69:** 7-23.

Waters ER. 2003. Molecular adaptation and the origin of land plants. *Molecular Phylogenetics and Evolution*, **29:** 456-463.

Wellman CH. 2004. Origin, function and development of the spore wall in early land plants. In: Hemsley AR, Poole I, eds. *Evolution of plant physiology*. London: Royal Botanic Gardens, Kew, 43-63.

Wellman CH. 2009. Ultrastructure of dispersed and *in situ* specimens of the Devonian spore *Rhabdosporites langii* (Eisenack) Richardson 1960: evidence for the evolutionary relationships of Progymnosperms. *Palaeontology*, **52:** 139-167.

Whelan S, Goldman N. 2001. A general empirical model of protein evolution derived from multiple protein families using a maximum-likelihood approach. *Molecular Biology and Evolution*, **18:** 691-699.

Wilson ZA, Zhang D. 2009. From *Arabidopsis* to rice: pathways in pollen development. *Journal of Experimental Botany*, **60(5):** 1479-1492.

Yang C, Vizcay-Barrena G, Conner K, Wilson ZA. 2007. MALE STERILITY1 is required for tapetal developmental and pollen wall biosynthesis. *The Plant Cell*, **19:** 3530-3548.

Yang ZN, Lou Y, Xu XF, Zhang C, Chang HS, Zhu J. 2012. Genetic pathways for pollen wall formation in Arabidopsis. In IPC XIII/IOPC IX 2012 (Tokyo, Japan).

Yi B, Zeng FQ, Lei SL, Chen YN, Yao XQ, Zhu Y, Wen J, Shen JX, Ma CZ, Tu JX, Fu TD. 2010. Two duplicate CYP704B1-homologous genes BnMs1 and BnMs2 are required for pollen exine formation and tapetal development in *Brassica napus*. *The Plant Journal*, **63:** 925-938.

Zavada MS. 1983. Comparative morphology of monocot pollen and evolutionary trends of apertures and wall structures. *Botanical Review*, **49:** 331-379.

Zavada MS, Gabarayeva N. 1991. Comparative pollen wall development of *Welwitschia mirabilis* angiosperms. *Bulletin of the Torrey Botanical Club*, **118(3):** 292-302.

Zhang DS, Liang WQ, Yin C, Zong J, Gu F, Zhang D. 2010. OsC6, encoding a lipid transfer protein, is required for postmeiotic anther development in rice. *Plant Physiology*, **154:** 149-162.

Zhang Z, Zhu J, Gao J, Wang C, Li H, Li H, Zhang H, Zhang S, Wang D, Wang Q, Huang H, Xia H, Yang Z. 2007. Transcription factor AtMYB103 is required for anther development by regulating tapetum development, callose dissolution and exine formation in *Arabidopsis*. *The Plant Journal*, **52:** 528-538

Appendix I. Expression profiles of *P. patens* genes, homologous to pollen wall associated genes in *A. thaliana*, derived from microarray analysis (gametophyte vs early sporophyte). Expression profiles for all *P. patens* homologues are shown. Genes ranked by log fold change expression. A number of the 31,000 genes were randomly selected and duplicated to fill out the 41,384 probe real estate and therefore were utilised as spot replicates which are included in the table below.

Gene name in *A. thaliana*	Homologous Gene Transcript ID	Log Fold Change Expression	P-Value
QRT1	Pp_121276_1	2.66	0.0052
QRT1	Pp_121276_2	2.47	0.0058
RPG1	Pp_146196_1	2.40	0.0001
QRT1	Pp_135225_2	2.37	0.0084
QRT1	Pp_14944_1	2.25	0.0051
QRT1	Pp_14944_2	2.11	0.0045
QRT1	Pp_135225_1	2.06	0.0129
CYP703A2	Pp_140533_2	1.96	0.0010
CYP704B1	Pp_148664_1	1.93	0.1092
CYP704B1	Pp_148664_2	1.88	0.1157
MS2	Pp_11916_2	1.83	0.0321
CYP703A2	Pp_140533_1	1.73	0.0022
QRT1	Pp_31639_1	1.66	0.0102
CYP704B1	Pp_183927_2	1.65	0.0624
CYP703A2	Pp_201018_1	1.58	0.0023
MS2	Pp_11916_1	1.57	0.0360
QRT2	Pp_116593_2	1.57	0.0409
CYP704B1	Pp_183927_1	1.56	0.0679
ACOS5	Pp_81614_1	1.47	0.0990
CYP703A2	Pp_186336_1	1.47	0.0173
ACOS5	Pp_104959_1	1.41	0.0230
CYP703A2	Pp_186336_2	1.40	0.0223
ACOS5	Pp_104959_2	1.39	0.0211
QRT2	Pp_116593_1	1.28	0.0542
ACOS5	Pp_89614_1	1.12	0.0244
RPG1	Pp_149962_2	0.92	0.0031
AtMYB103/MS188	Pp_118391_2	0.89	0.1143
CYP703A2	Pp_98753_1	0.88	0.1114
CYP704B1	Pp_98753_1	0.88	0.1114
CYP703A2	Pp_181978_1	0.86	0.0015
RPG1	Pp_163268_2	0.86	0.0375
CYP703A2	Pp_181978_2	0.83	0.0010
CER3	Pp_108743_2	0.82	0.0042
CER3	Pp_108743_1	0.82	0.0039
RPG1	Pp_163268_1	0.80	0.0399
QRT1	Pp_127795_1	0.80	0.0764
AtMYB103/MS188	Pp_118391_1	0.79	0.1335
QRT1	Pp_127795_2	0.76	0.0683
CYP703A2	Pp_133201_1	0.72	0.0263
CYP704B1	Pp_133201_1	0.72	0.0263
CER3	Pp_198498_1	0.72	0.0045
QRT1	Pp_15316_1	0.67	0.0315
QRT1	Pp_33289_1	0.64	0.0402
AtMYB103/MS188	Pp_16221_2	0.61	0.0024
AtMYB103/MS188	Pp_16221_1	0.61	0.0026
CYP703A2	Pp_133201_2	0.61	0.0304

CYP704B1	Pp_133201_2	0.61	0.0304
QRT1	Pp_15316_2	0.59	0.0460
CYP703A2	Pp_167379_2	0.59	0.0260
CYP704B1	Pp_128150_1	0.59	0.0644
ACOS5	Pp_140413_2	0.57	0.1427
CYP703A2	Pp_167379_1	0.57	0.0425
ACOS5	Pp_140413_1	0.53	0.1433
CYP704B1	Pp_128150_2	0.51	0.0793
CYP704B1	Pp_151187_1	0.47	0.0193
CYP704B1	Pp_151187_2	0.46	0.0240
TDE1/DET2	Pp_151601_2	0.44	0.0029
CYP703A2	Pp_220794_1	0.44	0.1110
CYP704B1	Pp_220794_1	0.44	0.1110
A6	Pp_99807_1	0.39	0.0958
TDE1/DET2	Pp_151601_1	0.38	0.0025
AtbZIP34	Pp_176895_1	0.37	0.0251
QRT1	Pp_44526_1	0.34	0.0722
NEF1	Pp_121066_1	0.34	0.1431
AtbZIP34	Pp_176895_2	0.34	0.0406
QRT1	Pp_16387_1	0.33	0.0431
QRT1	Pp_33184_1	0.32	0.0047
DEX1	Pp_172150_2	0.32	0.0095
CYP703A2	Pp_31920_1	0.31	0.0032
NEF1	Pp_121066_2	0.31	0.0337
MS1	Pp_148091_1	0.30	0.0100
AtbZIP34	Pp_162038_2	0.30	0.0262
A6	Pp_150189_2	0.30	0.0133
DEX1	Pp_172150_1	0.29	0.0092
AtbZIP34	Pp_162038_1	0.29	0.0232
CALS5/LAP1	Pp_143195_2	0.28	0.0481
CYP704B1	Pp_197900_1	0.28	0.0053
CYP703A2	Pp_31879_1	0.27	0.0191
CYP704B1	Pp_31879_1	0.27	0.0191
CYP703A2	Pp_152476_1	0.26	0.0606
CALS5/LAP1	Pp_143195_1	0.26	0.0424
QRT1	Pp_16387_2	0.26	0.0700
A6	Pp_150189_1	0.24	0.0443
CYP703A2	Pp_165869_2	0.24	0.0099
QRT2	Pp_149319_1	0.24	0.0444
AtbZIP34	Pp_45185_1	0.22	0.0063
CALS5/LAP1	Pp_190367_2	0.22	0.0142
CYP703A2	Pp_152476_2	0.22	0.0752
CYP703A2	Pp_165869_1	0.21	0.0239
CALS5/LAP1	Pp_139798_1	0.20	0.0033
CALS5/LAP1	Pp_190367_1	0.20	0.0201
QRT2	Pp_149319_2	0.20	0.0444
MS1	Pp_148091_2	0.20	0.0466
MS1	Pp_150355_2	0.19	0.0528
AtMYB103/MS188	Pp_8347_1	0.19	0.0482
CYP703A2	Pp_151293_2	0.19	0.1110
CYP704B1	Pp_151293_2	0.19	0.1110
MS1	Pp_150355_1	0.19	0.0564
CYP703A2	Pp_151293_1	0.18	0.0675
CYP704B1	Pp_151293_1	0.18	0.0675
QRT1	Pp_24242_1	0.18	0.0772
AtbZIP34	Pp_160508_2	0.18	0.1903
AtbZIP34	Pp_160508_1	0.18	0.1326
A6	Pp_214139_1	0.18	0.0959
CYP703A2	Pp_64513_1	0.17	0.0656
CYP704B1	Pp_64513_1	0.17	0.0656
KNS2	Pp_197679_1	0.17	0.0207
CER3	Pp_199329_1	0.17	0.0115
ACOS5	Pp_117032_2	0.17	0.3605

QRT2	Pp_199574_1	0.17	0.0978
CALS5/LAP1	Pp_199665_1	0.16	0.0732
CALS5/LAP1	Pp_139798_2	0.15	0.0091
CYP704B1	Pp_149913_1	0.15	0.0170
AtbZIP34	Pp_171242_2	0.15	0.0968
CALS5/LAP1	Pp_117054_1	0.15	0.0394
A6	Pp_60798_1	0.14	0.0207
ACOS5	Pp_117032_1	0.14	0.3257
QRT3	Pp_227125_1	0.14	0.0549
ACOS5	Pp_192148_1	0.14	0.1113
CYP704B1	Pp_139286_2	0.13	0.0486
CYP704B1	Pp_139286_1	0.13	0.1093
CALS5/LAP1	Pp_185944_2	0.12	0.3377
QRT1	Pp_145419_1	0.12	0.2801
A6	Pp_75622_1	0.12	0.1487
AtbZIP34	Pp_171242_1	0.11	0.2751
CALS5/LAP1	Pp_117054_2	0.11	0.1732
CYP704B1	Pp_119258_1	0.11	0.3154
CALS5/LAP1	Pp_185944_1	0.11	0.3956
QRT1	Pp_145419_2	0.11	0.2994
AtMYB103/MS188	Pp_8874_1	0.11	0.3123
QRT2	Pp_43415_1	0.10	0.3054
KNS2	Pp_186437_1	0.10	0.1208
CYP703A2	Pp_120688_2	0.10	0.0713
CYP703A2	Pp_120688_1	0.10	0.0614
RPG1	Pp_146546_2	0.10	0.0506
A6	Pp_19653_1	0.10	0.3368
TDE1/DET2	Pp_119780_2	0.10	0.0277
QRT2	Pp_163808_1	0.10	0.0495
QRT2	Pp_163808_2	0.10	0.0977
CYP704B1	Pp_149913_2	0.10	0.0898
CYP703A2	Pp_111667_1	0.09	0.0899
TDE1/DET2	Pp_166483_2	0.09	0.0819
KNS2	Pp_216637_1	0.08	0.2985
CALS5/LAP1	Pp_127776_2	0.08	0.0804
CALS5/LAP1	Pp_127776_1	0.08	0.1992
CYP704B1	Pp_119258_2	0.08	0.4065
A6	Pp_19653_2	0.08	0.3861
AtMYB103/MS188	Pp_150459_1	0.07	0.1933
QRT2	Pp_133517_1	0.07	0.1955
ACOS5	Pp_174501_2	0.07	0.2298
A6	Pp_25096_1	0.07	0.2124
AtMYB103/MS188	Pp_150459_2	0.07	0.2810
QRT3	Pp_198113_1	0.07	0.5625
ACOS5	Pp_192148_2	0.07	0.4863
TDE1/DET2	Pp_119780_1	0.06	0.1320
QRT2	Pp_133517_2	0.06	0.3832
CYP704B1	Pp_182724_1	0.06	0.1340
AtbZIP34	Pp_64165_1	0.06	0.3300
RPG1	Pp_146546_1	0.06	0.2038
AtbZIP34	Pp_201072_1	0.06	0.2115
QRT1	Pp_150987_1	0.06	0.2204
ACOS5	Pp_113172_1	0.06	0.3184
CYP703A2	Pp_110612_2	0.06	0.6475
CYP704B1	Pp_110612_2	0.06	0.6475
CYP704B1	Pp_182724_2	0.05	0.2491
CYP703A2	Pp_110612_1	0.05	0.6534
CYP704B1	Pp_110612_1	0.05	0.6534
AtMYB103/MS188	Pp_173907_2	0.05	0.6679
CYP703A2	Pp_167047_1	0.05	0.5366
CYP703A2	Pp_138465_2	0.04	0.4768
AtMYB103/MS188	Pp_135480_1	0.04	0.3822
ACOS5	Pp_122015_1	0.04	0.3758

ACOS5	Pp_174501_1	0.04	0.5066
AtbZIP34	Pp_64750_1	0.04	0.6003
CYP703A2	Pp_148103_2	0.04	0.5848
CYP704B1	Pp_148103_2	0.04	0.5848
AtMYB103/MS188	Pp_135480_2	0.04	0.4319
A6	Pp_105138_2	0.04	0.6471
AtbZIP34	Pp_163915_1	0.04	0.5360
AtMYB103/MS188	Pp_143587_2	0.04	0.4412
AtMYB103/MS188	Pp_143587_1	0.03	0.5934
QRT1	Pp_31656_1	0.03	0.5985
KNS2	Pp_210965_1	0.03	0.5089
CYP703A2	Pp_219188_1	0.03	0.4330
QRT1	Pp_94470_1	0.03	0.5350
ACOS5	Pp_113172_2	0.03	0.5936
ACOS5	Pp_122015_2	0.03	0.6083
CYP703A2	Pp_149501_2	0.03	0.6946
AtMYB103/MS188	Pp_173907_1	0.03	0.8254
A6	Pp_105138_1	0.02	0.7231
KNS2	Pp_186437_2	0.02	0.7239
A6	Pp_61200_1	0.02	0.5946
A6	Pp_65557_1	0.02	0.6386
QRT2	Pp_176513_2	0.02	0.8058
CYP703A2	Pp_167047_2	0.02	0.8350
QRT2	Pp_176513_1	0.02	0.8631
CYP703A2	Pp_148103_1	0.02	0.7747
CYP704B1	Pp_148103_1	0.02	0.7747
AtbZIP34	Pp_163915_2	0.02	0.8694
CYP703A2	Pp_204665_1	0.01	0.9220
CYP703A2	Pp_149501_1	0.01	0.8676
A6	Pp_189861_1	0.01	0.8056
CYP703A2	Pp_32062_1	0.01	0.7968
CYP703A2	Pp_111667_2	0.01	0.8134
AtMYB103/MS188	Pp_61394_1	0.01	0.8849
ACOS5	Pp_150981_2	0.01	0.9256
CYP703A2	Pp_138465_1	0.00	0.9492
TDE1/DET2	Pp_166483_1	0.00	0.9464
AtMYB103/MS188	Pp_126855_2	0.00	0.9628
CYP703A2	Pp_50846_1	0.00	0.9854
CYP703A2	Pp_189599_2	0.00	0.9771
AtMYB103/MS188	Pp_89855_1	0.00	0.9964
QRT1	Pp_118762_1	0.00	0.9744
RPG1	Pp_136254_2	0.00	0.9395
AtMYB103/MS188	Pp_153206_2	-0.01	0.9121
ACOS5	Pp_115006_2	-0.01	0.9021
QRT1	Pp_174093_2	-0.01	0.9340
CYP703A2	Pp_189599_1	-0.01	0.8790
QRT1	Pp_103704_1	-0.01	0.9561
QRT1	Pp_135307_2	-0.01	0.9474
ACOS5	Pp_233094_1	-0.01	0.8050
QRT1	Pp_118762_2	-0.01	0.8926
AtMYB103/MS188	Pp_148816_2	-0.01	0.7681
A6	Pp_189861_2	-0.01	0.7251
QRT1	Pp_134522_2	-0.02	0.8400
CYP703A2	Pp_200880_1	-0.02	0.7520
A6	Pp_56975_1	-0.02	0.8140
AtMYB103/MS188	Pp_34929_1	-0.02	0.7297
A6	Pp_167530_1	-0.02	0.8176
QRT1	Pp_174093_1	-0.02	0.8144
CYP703A2	Pp_133330_2	-0.02	0.6519
AtMYB103/MS188	Pp_123689_1	-0.02	0.7510
ACOS5	Pp_122068_2	-0.02	0.6137
QRT2	Pp_160263_1	-0.02	0.5864
AtMYB103/MS188	Pp_121437_1	-0.02	0.8544

ACOS5	Pp_150981_1	-0.02	0.7998
AtMYB103/MS188	Pp_153206_1	-0.02	0.6248
QRT1	Pp_152977_1	-0.02	0.8767
ACOS5	Pp_122068_1	-0.02	0.6049
CYP703A2	Pp_140101_2	-0.03	0.8024
CYP704B1	Pp_140101_2	-0.03	0.8024
CYP703A2	Pp_133330_1	-0.03	0.6200
A6	Pp_131016_1	-0.03	0.5836
A6	Pp_175736_2	-0.03	0.5382
CYP703A2	Pp_147541_2	-0.03	0.5915
AtMYB103/MS188	Pp_189472_2	-0.03	0.5432
A6	Pp_131016_2	-0.03	0.5506
QRT2	Pp_160263_2	-0.03	0.4995
A6	Pp_160804_1	-0.03	0.8314
A6	Pp_163193_2	-0.03	0.6318
CYP704B1	Pp_180507_2	-0.03	0.8017
QRT1	Pp_135307_1	-0.03	0.8278
QRT2	Pp_22776_1	-0.03	0.6805
ACOS5	Pp_152177_1	-0.03	0.5851
CYP703A2	Pp_140101_1	-0.03	0.7227
CYP704B1	Pp_140101_1	-0.03	0.7227
CYP703A2	Pp_147541_1	-0.03	0.4135
A6	Pp_175736_1	-0.03	0.4610
A6	Pp_160804_2	-0.03	0.8026
CYP703A2	Pp_106848_2	-0.03	0.4911
CYP704B1	Pp_106848_2	-0.03	0.4911
QRT1	Pp_103704_2	-0.04	0.7772
AtMYB103/MS188	Pp_189472_1	-0.04	0.5877
CALS5/LAP1	Pp_183682_2	-0.04	0.4666
CYP703A2	Pp_64909_1	-0.04	0.6796
CYP703A2	Pp_87503_1	-0.04	0.5291
QRT1	Pp_132301_1	-0.04	0.5682
QRT1	Pp_189145_2	-0.04	0.5582
ACOS5	Pp_115006_1	-0.04	0.4264
QRT1	Pp_189145_1	-0.04	0.4748
AtMYB103/MS188	Pp_126855_1	-0.04	0.4013
QRT1	Pp_121267_1	-0.04	0.6483
A6	Pp_147889_1	-0.04	0.4090
A6	Pp_163193_1	-0.04	0.4637
AtbZIP34	Pp_159871_2	-0.04	0.4696
A6	Pp_147889_2	-0.04	0.3737
CALS5/LAP1	Pp_175718_2	-0.05	0.4980
QRT1	Pp_134522_1	-0.05	0.5253
CER3	Pp_177243_2	-0.05	0.3710
A6	Pp_167530_2	-0.05	0.4489
CYP704B1	Pp_195286_2	-0.05	0.3010
CYP703A2	Pp_139150_1	-0.05	0.6112
QRT1	Pp_44780_1	-0.05	0.4767
NEF1	Pp_230745_1	-0.06	0.5766
QRT1	Pp_152977_2	-0.06	0.6512
ACOS5	Pp_152177_2	-0.06	0.4048
CYP703A2	Pp_106848_1	-0.06	0.3837
CYP704B1	Pp_106848_1	-0.06	0.3837
CALS5/LAP1	Pp_183682_1	-0.06	0.2126
A6	Pp_172885_2	-0.06	0.3501
ACOS5	Pp_124849_2	-0.06	0.3915
AtbZIP34	Pp_159871_1	-0.06	0.2711
ACOS5	Pp_124849_1	-0.06	0.3255
CYP703A2	Pp_110816_2	-0.06	0.1962
CYP704B1	Pp_110816_2	-0.06	0.1962
A6	Pp_110742_2	-0.07	0.2756
AtMYB103/MS188	Pp_123689_2	-0.07	0.2980
CYP703A2	Pp_139150_2	-0.07	0.6035

QRT1	Pp_31765_1	-0.07	0.3587
A6	Pp_113399_1	-0.07	0.2663
A6	Pp_107800_1	-0.07	0.4983
QRT1	Pp_132301_2	-0.07	0.3802
A6	Pp_172885_1	-0.07	0.2290
A6	Pp_91949_1	-0.07	0.2425
RPG1	Pp_122188_2	-0.07	0.2537
A6	Pp_110742_1	-0.07	0.3480
CYP704B1	Pp_195286_1	-0.07	0.2756
CER3	Pp_177243_1	-0.08	0.2053
A6	Pp_113399_2	-0.08	0.1808
CALS5/LAP1	Pp_175718_1	-0.08	0.1749
A6	Pp_59275_1	-0.08	0.1034
CYP703A2	Pp_110816_1	-0.08	0.1386
CYP704B1	Pp_110816_1	-0.08	0.1386
RPG1	Pp_122188_1	-0.08	0.2322
CYP703A2	Pp_211162_1	-0.09	0.3507
CYP703A2	Pp_22681_1	-0.09	0.4685
A6	Pp_107800_2	-0.09	0.4172
CYP704B1	Pp_180507_1	-0.09	0.4931
RPG1	Pp_136254_1	-0.09	0.0989
CALS5/LAP1	Pp_115455_1	-0.09	0.1105
A6	Pp_8713_1	-0.09	0.3264
CYP703A2	Pp_197852_1	-0.09	0.2043
CYP704B1	Pp_197852_1	-0.09	0.2043
A6	Pp_60671_1	-0.09	0.4272
AtMYB103/MS188	Pp_29378_1	-0.10	0.1990
CYP703A2	Pp_150408_2	-0.10	0.0671
CALS5/LAP1	Pp_115455_2	-0.10	0.1342
QRT1	Pp_121267_2	-0.10	0.1961
AtMYB103/MS188	Pp_148816_1	-0.10	0.0215
CALS5/LAP1	Pp_207622_1	-0.10	0.0592
ACOS5	Pp_209184_1	-0.11	0.5052
AtMYB103/MS188	Pp_113218_2	-0.11	0.3699
AtMYB103/MS188	Pp_184923_2	-0.11	0.2873
AtMYB103/MS188	Pp_123475_1	-0.12	0.4423
A6	Pp_61203_1	-0.12	0.3378
AtMYB103/MS188	Pp_19381_2	-0.12	0.1747
AtMYB103/MS188	Pp_123475_2	-0.12	0.4330
AtMYB103/MS188	Pp_113218_1	-0.12	0.1851
QRT1	Pp_108383_1	-0.12	0.3437
AtMYB103/MS188	Pp_153179_1	-0.12	0.2501
QRT1	Pp_208299_1	-0.13	0.5891
CALS5/LAP1	Pp_183499_1	-0.13	0.0112
AtMYB103/MS188	Pp_143649_1	-0.13	0.3657
CALS5/LAP1	Pp_183499_2	-0.13	0.0235
A6	Pp_14679_1	-0.13	0.1719
QRT1	Pp_108383_2	-0.13	0.3276
AtMYB103/MS188	Pp_143649_2	-0.14	0.3673
CYP703A2	Pp_150408_1	-0.14	0.0177
A6	Pp_196989_1	-0.14	0.0285
AtbZIP34	Pp_81285_1	-0.15	0.0204
QRT1	Pp_15518_1	-0.15	0.0620
AtMYB103/MS188	Pp_121437_2	-0.15	0.1818
AtMYB103/MS188	Pp_184923_1	-0.15	0.2028
A6	Pp_192933_2	-0.16	0.2402
CYP703A2	Pp_2770_1	-0.16	0.0128
AtMYB103/MS188	Pp_153179_2	-0.16	0.1720
A6	Pp_14679_2	-0.16	0.0628
AtMYB103/MS188	Pp_19381_1	-0.16	0.0807
A6	Pp_192933_1	-0.16	0.2962
CYP704B1	Pp_168494_2	-0.17	0.0117
QRT1	Pp_182229_1	-0.17	0.1453

KNS2	Pp_119166_1	-0.17	0.1184
QRT1	Pp_187864_1	-0.18	0.1390
QRT2	Pp_193100_2	-0.18	0.1153
QRT1	Pp_232357_1	-0.18	0.0932
QRT1	Pp_182229_2	-0.18	0.1517
CYP703A2	Pp_115760_1	-0.19	0.0666
CYP704B1	Pp_115760_1	-0.19	0.0666
CYP703A2	Pp_115760_2	-0.19	0.0831
CYP704B1	Pp_115760_2	-0.19	0.0831
KNS2	Pp_119166_2	-0.19	0.0876
QRT1	Pp_187864_2	-0.19	0.1303
A6	Pp_90481_1	-0.19	0.0112
AtMYB103/MS188	Pp_100368_2	-0.20	0.0618
A6	Pp_196989_2	-0.20	0.0189
A6	Pp_218702_1	-0.20	0.0133
QRT1	Pp_190734_2	-0.20	0.0048
CYP704B1	Pp_177185_1	-0.21	0.0023
AtMYB103/MS188	Pp_111064_1	-0.22	0.0196
AtMYB103/MS188	Pp_111064_2	-0.22	0.0128
AtMYB103/MS188	Pp_100368_1	-0.22	0.0477
CYP704B1	Pp_177185_2	-0.22	0.0030
QRT1	Pp_58226_1	-0.22	0.0011
CYP704B1	Pp_168494_1	-0.23	0.0012
A6	Pp_122478_1	-0.23	0.0016
A6	Pp_54237_1	-0.23	0.1052
QRT1	Pp_190734_1	-0.24	0.0016
KNS2	Pp_188513_2	-0.25	0.0405
CYP703A2	Pp_188189_1	-0.27	0.0026
CYP704B1	Pp_188189_1	-0.27	0.0026
A6	Pp_122478_2	-0.27	0.0089
QRT1	Pp_15518_2	-0.28	0.0028
KNS2	Pp_188513_1	-0.28	0.0054
CYP703A2	Pp_63679_1	-0.30	0.0486
QRT2	Pp_13931_2	-0.31	0.0115
QRT1	Pp_138756_1	-0.33	0.0419
CYP703A2	Pp_188189_2	-0.33	0.0009
CYP704B1	Pp_188189_2	-0.33	0.0009
AtMYB103/MS188	Pp_27442_1	-0.33	0.0470
AtMYB103/MS188	Pp_8210_1	-0.33	0.0117
QRT1	Pp_121141_1	-0.33	0.0056
QRT1	Pp_152856_1	-0.34	0.0021
CYP704B1	Pp_105982_2	-0.34	0.0120
QRT1	Pp_152856_2	-0.35	0.0035
CYP703A2	Pp_149034_1	-0.35	0.0054
CYP704B1	Pp_149034_1	-0.35	0.0054
A6	Pp_8710_1	-0.36	0.0072
CYP704B1	Pp_105982_1	-0.36	0.0053
QRT1	Pp_121141_2	-0.38	0.0049
AtbZIP34	Pp_128606_2	-0.38	0.0002
QRT2	Pp_193100_1	-0.39	0.0145
QRT1	Pp_138756_2	-0.40	0.0309
CYP703A2	Pp_149034_2	-0.41	0.0025
CYP704B1	Pp_149034_2	-0.41	0.0025
QRT1	Pp_45683_1	-0.43	0.0327
AtbZIP34	Pp_128606_1	-0.44	0.0003
QRT2	Pp_13931_1	-0.52	0.0017
CYP704B1	Pp_116547_1	-0.55	0.0011
CYP704B1	Pp_116547_2	-0.57	0.0005
CYP703A2	Pp_172320_2	-0.57	0.0004
QRT1	Pp_79815_1	-0.58	0.0011
CYP703A2	Pp_172320_1	-0.59	0.0004
ACOS5	Pp_92121_1	-0.65	0.0001
TDE1/DET2	Pp_181942_1	-0.70	0.0005

TDE1/DET2	Pp_181942_2	-0.71	0.0013
QRT1	Pp_145945_1	-0.87	0.0002
QRT1	Pp_145945_2	-0.97	0.0002
CYP703A2	Pp_102043_1	-1.10	0.0003
CYP703A2	Pp_102043_2	-1.13	0.0003
QRT1	Pp_4364_1	-1.40	0.0000
QRT1	Pp_15580_2	-1.74	0.0001
QRT1	Pp_15580_1	-1.83	0.0001
QRT1	Pp_222560_1	-1.92	0.0001
QRT1	Pp_155350_1	-2.13	0.0001
QRT1	Pp_155350_2	-2.22	0.0001

Appendix II. Expression profiles of *P. patens* genes, homologous to pollen wall associated genes in *A. thaliana*, derived from microarray analysis (gametophyte vs mid sporophyte). Expression profiles for all *P. patens* homologues are shown. Genes ranked by log fold change expression. A number of the 31,000 genes were randomly selected and duplicated to fill out the 41,384 probe real estate and therefore were utilised as spot replicates which are included in the table below.

Gene name in *A. thaliana*	**Homologous Gene Transcript ID**	**Log Fold Change Expression**	**P-Value**
RPG1	Pp_146196_1	3.40	2.67E-05
RPG1	Pp_146196_2	3.22	3.51E-05
QRT1	Pp_121276_1	3.05	0.0016
QRT1	Pp_121276_2	2.84	0.0018
QRT1	Pp_135225_2	2.63	0.0017
QRT1	Pp_14944_1	2.57	0.0016
QRT1	Pp_14944_2	2.43	0.0018
QRT1	Pp_135225_1	2.27	0.0028
CYP703A2	Pp_140533_2	2.17	0.0001
CYP704B1	Pp_148664_1	1.97	0.0898
CYP704B1	Pp_148664_2	1.91	0.0937
CYP703A2	Pp_140533_1	1.91	0.0003
QRT1	Pp_31639_1	1.90	0.0030
QRT2	Pp_116593_2	1.84	0.0178
RPG1	Pp_163268_2	1.81	0.0017
CYP703A2	Pp_201018_1	1.74	0.0004
CYP704B1	Pp_183927_2	1.72	0.0409
RPG1	Pp_163268_1	1.71	0.0018
CYP703A2	Pp_186336_1	1.62	0.0043
CYP704B1	Pp_183927_1	1.61	0.0458
CYP703A2	Pp_186336_2	1.54	0.0061
ACOS5	Pp_104959_1	1.53	0.0071
MS2	Pp_11916_2	1.52	0.0662
ACOS5	Pp_104959_2	1.51	0.0062
QRT2	Pp_116593_1	1.50	0.0237
ACOS5	Pp_81614_1	1.50	0.0830
RPG1	Pp_149962_1	1.36	0.0012
RPG1	Pp_149962_2	1.31	0.0007
MS2	Pp_11916_1	1.30	0.0730
ACOS5	Pp_89614_1	1.20	0.0109
CYP703A2	Pp_181978_1	0.97	0.0003

CYP703A2	Pp_181978_2	0.93	0.0003
AtMYB103/MS188	Pp_118391_2	0.91	0.0893
CYP703A2	Pp_98753_1	0.89	0.0957
CYP704B1	Pp_98753_1	0.89	0.0957
QRT1	Pp_127795_1	0.84	0.0409
AtMYB103/MS188	Pp_118391_1	0.80	0.1041
QRT1	Pp_127795_2	0.80	0.0346
CYP703A2	Pp_133201_1	0.77	0.0134
CYP704B1	Pp_133201_1	0.77	0.0134
CYP703A2	Pp_167379_2	0.72	0.0207
QRT1	Pp_15316_1	0.71	0.0145
CYP703A2	Pp_167379_1	0.69	0.0325
QRT1	Pp_33289_1	0.67	0.0270
AtMYB103/MS188	Pp_16221_2	0.67	0.0007
AtMYB103/MS188	Pp_16221_1	0.67	0.0007
CYP703A2	Pp_133201_2	0.64	0.0167
CYP704B1	Pp_133201_2	0.64	0.0167
QRT1	Pp_15316_2	0.62	0.0259
CYP704B1	Pp_128150_1	0.62	0.0355
ACOS5	Pp_140413_2	0.58	0.1146
ACOS5	Pp_140413_1	0.54	0.1135
CYP704B1	Pp_128150_2	0.53	0.0456
CYP704B1	Pp_151187_1	0.50	0.0080
CYP704B1	Pp_151187_2	0.49	0.0112
CYP703A2	Pp_220794_1	0.46	0.0743
CYP704B1	Pp_220794_1	0.46	0.0743
NEF1	Pp_121066_1	0.41	0.0912
QRT1	Pp_16387_1	0.40	0.0352
A6	Pp_99807_1	0.40	0.0691
AtbZIP34	Pp_176895_1	0.39	0.0135
QRT1	Pp_33184_1	0.38	0.0046
AtbZIP34	Pp_176895_2	0.36	0.0241
QRT1	Pp_44526_1	0.36	0.0566
KNS2	Pp_197679_1	0.35	0.0009
CYP703A2	Pp_31920_1	0.34	0.0007
AtbZIP34	Pp_162038_2	0.33	0.0094
A6	Pp_150189_2	0.33	0.0042
AtbZIP34	Pp_162038_1	0.31	0.0079
CYP704B1	Pp_197900_1	0.31	0.0025
QRT1	Pp_16387_2	0.31	0.0538
CYP703A2	Pp_31879_1	0.30	0.0057
CYP704B1	Pp_31879_1	0.30	0.0057
CALS5/LAP1	Pp_143195_2	0.30	0.0311
TDE1/DET2	Pp_151601_2	0.29	0.0197
CALS5/LAP1	Pp_143195_1	0.28	0.0291
CYP703A2	Pp_165869_2	0.28	0.0061
TDE1/DET2	Pp_151601_1	0.28	0.0118
CER3	Pp_199329_1	0.27	0.0014
CYP703A2	Pp_152476_1	0.27	0.0436
DEX1	Pp_172150_1	0.27	0.0145
A6	Pp_150189_1	0.26	0.0247
QRT2	Pp_149319_1	0.25	0.0193
AtbZIP34	Pp_45185_1	0.25	0.0013
DEX1	Pp_172150_2	0.25	0.0316
NEF1	Pp_121066_2	0.24	0.0830
CYP703A2	Pp_165869_1	0.24	0.0150
CALS5/LAP1	Pp_190367_2	0.24	0.0064
CYP703A2	Pp_151293_2	0.23	0.0609
CYP704B1	Pp_151293_2	0.23	0.0609
CYP703A2	Pp_152476_2	0.23	0.0581
CALS5/LAP1	Pp_139798_1	0.22	0.0012

CALS5/LAP1	Pp_190367_1	0.22	0.0107
CYP703A2	Pp_151293_1	0.21	0.0346
CYP704B1	Pp_151293_1	0.21	0.0346
AtMYB103/MS188	Pp_8347_1	0.21	0.0305
QRT2	Pp_149319_2	0.21	0.0221
MS2	Pp_120173_2	0.21	0.3410
CYP703A2	Pp_64513_1	0.21	0.0661
CYP704B1	Pp_64513_1	0.21	0.0661
A6	Pp_214139_1	0.19	0.0482
AtbZIP34	Pp_160508_1	0.18	0.0968
QRT1	Pp_24242_1	0.18	0.0594
AtbZIP34	Pp_160508_2	0.18	0.1424
MS2	Pp_120173_1	0.18	0.4064
ACOS5	Pp_117032_2	0.18	0.3049
QRT2	Pp_199574_1	0.18	0.0735
CYP704B1	Pp_149913_1	0.17	0.0081
CALS5/LAP1	Pp_139798_2	0.17	0.0030
CALS5/LAP1	Pp_199665_1	0.17	0.0310
QRT3	Pp_227125_1	0.17	0.0447
A6	Pp_60798_1	0.16	0.0087
CALS5/LAP1	Pp_117054_1	0.16	0.0182
AtbZIP34	Pp_171242_2	0.16	0.0491
ACOS5	Pp_117032_1	0.16	0.2754
TDE1/DET2	Pp_166483_2	0.15	0.0121
CER3	Pp_108743_1	0.15	0.4902
CER3	Pp_108743_2	0.15	0.5074
CYP704B1	Pp_139286_2	0.14	0.0422
ACOS5	Pp_192148_1	0.14	0.0796
CYP704B1	Pp_139286_1	0.13	0.0916
A6	Pp_75622_1	0.13	0.1411
CALS5/LAP1	Pp_117054_2	0.12	0.1375
QRT1	Pp_145419_1	0.12	0.2956
CALS5/LAP1	Pp_185944_2	0.12	0.3023
AtbZIP34	Pp_171242_1	0.12	0.2553
CYP704B1	Pp_119258_1	0.12	0.2817
AtMYB103/MS188	Pp_8874_1	0.12	0.2584
CYP703A2	Pp_120688_1	0.12	0.0275
CYP703A2	Pp_120688_2	0.12	0.0383
QRT2	Pp_43415_1	0.11	0.2126
QRT1	Pp_145419_2	0.11	0.2967
CYP704B1	Pp_149913_2	0.11	0.0620
CYP703A2	Pp_111667_1	0.11	0.0610
CALS5/LAP1	Pp_185944_1	0.11	0.3626
QRT2	Pp_163808_1	0.11	0.0253
QRT2	Pp_163808_2	0.11	0.0545
A6	Pp_19653_1	0.09	0.3424
CALS5/LAP1	Pp_127776_2	0.09	0.0472
CALS5/LAP1	Pp_127776_1	0.09	0.1713
A6	Pp_25096_1	0.08	0.1375
TDE1/DET2	Pp_166483_1	0.08	0.0800
KNS2	Pp_216637_1	0.08	0.3322
CYP704B1	Pp_119258_2	0.08	0.3726
KNS2	Pp_210965_1	0.08	0.1565
AtMYB103/MS188	Pp_150459_1	0.08	0.1826
QRT2	Pp_133517_1	0.08	0.1382
ACOS5	Pp_174501_2	0.07	0.2037
CYP704B1	Pp_182724_1	0.07	0.0852
A6	Pp_19653_2	0.07	0.4052
AtbZIP34	Pp_201072_1	0.07	0.1850
AtbZIP34	Pp_64165_1	0.07	0.2457
AtMYB103/MS188	Pp_150459_2	0.07	0.3006

QRT1	Pp_150987_1	0.07	0.1630
TDE1/DET2	Pp_119780_1	0.07	0.1332
TDE1/DET2	Pp_119780_2	0.07	0.1122
QRT2	Pp_133517_2	0.06	0.3341
ACOS5	Pp_192148_2	0.06	0.5035
ACOS5	Pp_113172_1	0.06	0.2320
CYP703A2	Pp_138465_2	0.06	0.3837
CYP704B1	Pp_182724_2	0.06	0.1908
QRT3	Pp_198113_1	0.06	0.6156
CYP703A2	Pp_167047_1	0.06	0.4302
ACOS5	Pp_122015_1	0.05	0.3440
KNS2	Pp_186437_1	0.05	0.4978
AtbZIP34	Pp_64750_1	0.05	0.5543
ACOS5	Pp_174501_1	0.05	0.5056
AtMYB103/MS188	Pp_135480_1	0.04	0.3834
MS1	Pp_148091_2	0.04	0.6435
MS1	Pp_148091_1	0.04	0.6641
AtbZIP34	Pp_163915_1	0.04	0.4868
CYP703A2	Pp_148103_2	0.04	0.5731
CYP704B1	Pp_148103_2	0.04	0.5731
AtMYB103/MS188	Pp_143587_1	0.04	0.5246
AtMYB103/MS188	Pp_135480_2	0.04	0.4376
AtMYB103/MS188	Pp_143587_2	0.04	0.3882
A6	Pp_105138_2	0.04	0.6111
CYP703A2	Pp_110612_2	0.04	0.7747
CYP704B1	Pp_110612_2	0.04	0.7747
AtMYB103/MS188	Pp_173907_2	0.04	0.7515
QRT1	Pp_94470_1	0.04	0.4821
RPG1	Pp_146546_2	0.04	0.4757
CYP703A2	Pp_110612_1	0.03	0.7628
CYP704B1	Pp_110612_1	0.03	0.7628
CYP703A2	Pp_219188_1	0.03	0.4212
ACOS5	Pp_122015_2	0.03	0.5787
ACOS5	Pp_113172_2	0.03	0.5404
QRT1	Pp_31656_1	0.03	0.6719
KNS2	Pp_186437_2	0.03	0.6816
QRT2	Pp_176513_2	0.03	0.7486
A6	Pp_105138_1	0.03	0.6542
A6	Pp_61200_1	0.03	0.5519
A6	Pp_65557_1	0.03	0.5809
CYP703A2	Pp_167047_2	0.03	0.7445
CER3	Pp_198498_1	0.02	0.9099
QRT2	Pp_176513_1	0.02	0.8107
AtbZIP34	Pp_163915_2	0.02	0.8230
CYP703A2	Pp_149501_2	0.02	0.7837
CER3	Pp_177243_1	0.02	0.7642
CYP703A2	Pp_148103_1	0.02	0.7344
CYP704B1	Pp_148103_1	0.02	0.7344
AtMYB103/MS188	Pp_173907_1	0.02	0.9000
RPG1	Pp_146546_1	0.01	0.7787
CYP703A2	Pp_149501_1	0.01	0.8596
A6	Pp_189861_1	0.01	0.7817
CYP703A2	Pp_204665_1	0.01	0.9155
AtMYB103/MS188	Pp_61394_1	0.01	0.8174
CYP703A2	Pp_32062_1	0.01	0.7655
QRT1	Pp_103704_1	0.01	0.9406
ACOS5	Pp_150981_2	0.01	0.8517
CYP703A2	Pp_111667_2	0.01	0.7647
CYP703A2	Pp_138465_1	0.01	0.8346
CYP703A2	Pp_189599_2	0.01	0.9259
AtMYB103/MS188	Pp_126855_2	0.00	0.9680

QRT1	Pp_118762_1	0.00	0.9843
AtMYB103/MS188	Pp_89855_1	0.00	0.9678
CYP703A2	Pp_50846_1	0.00	0.9783
CYP703A2	Pp_189599_1	0.00	0.9271
AtMYB103/MS188	Pp_153206_2	0.00	0.9205
QRT1	Pp_174093_2	0.00	0.9526
QRT1	Pp_118762_2	-0.01	0.9556
QRT1	Pp_135307_2	-0.01	0.9600
ACOS5	Pp_233094_1	-0.01	0.8274
ACOS5	Pp_115006_2	-0.01	0.8349
AtMYB103/MS188	Pp_123689_1	-0.01	0.8512
A6	Pp_56975_1	-0.01	0.8556
A6	Pp_160804_1	-0.01	0.9344
AtMYB103/MS188	Pp_34929_1	-0.02	0.7624
AtMYB103/MS188	Pp_148816_2	-0.02	0.7458
CYP703A2	Pp_200880_1	-0.02	0.7226
A6	Pp_189861_2	-0.02	0.6809
ACOS5	Pp_150981_1	-0.02	0.8221
QRT1	Pp_174093_1	-0.02	0.7957
CYP703A2	Pp_133330_2	-0.02	0.6477
A6	Pp_160804_2	-0.02	0.8959
ACOS5	Pp_122068_2	-0.02	0.6204
CYP704B1	Pp_180507_2	-0.02	0.8755
QRT1	Pp_134522_2	-0.02	0.7536
QRT2	Pp_160263_1	-0.02	0.5616
CYP703A2	Pp_140101_2	-0.02	0.8341
CYP704B1	Pp_140101_2	-0.02	0.8341
QRT1	Pp_103704_2	-0.02	0.8677
CYP703A2	Pp_133330_1	-0.02	0.6684
ACOS5	Pp_122068_1	-0.02	0.6079
RPG1	Pp_136254_1	-0.02	0.6687
QRT1	Pp_152977_1	-0.03	0.8529
A6	Pp_163193_2	-0.03	0.7131
CYP703A2	Pp_140101_1	-0.03	0.7947
CYP704B1	Pp_140101_1	-0.03	0.7947
A6	Pp_131016_1	-0.03	0.6241
ACOS5	Pp_152177_1	-0.03	0.6620
AtMYB103/MS188	Pp_153206_1	-0.03	0.5510
QRT2	Pp_22776_1	-0.03	0.7549
AtMYB103/MS188	Pp_189472_2	-0.03	0.5611
A6	Pp_131016_2	-0.03	0.5667
CYP703A2	Pp_147541_2	-0.03	0.5712
A6	Pp_167530_1	-0.03	0.7127
QRT1	Pp_135307_1	-0.03	0.8057
RPG1	Pp_136254_2	-0.03	0.5748
QRT2	Pp_160263_2	-0.03	0.4559
A6	Pp_175736_2	-0.03	0.4459
CYP703A2	Pp_87503_1	-0.03	0.5901
MS1	Pp_150355_1	-0.03	0.7297
AtMYB103/MS188	Pp_189472_1	-0.03	0.6181
CYP703A2	Pp_147541_1	-0.04	0.3981
CALS5/LAP1	Pp_183682_2	-0.04	0.4814
QRT1	Pp_121267_1	-0.04	0.7139
QRT1	Pp_189145_2	-0.04	0.6083
CYP703A2	Pp_64909_1	-0.04	0.6869
QRT1	Pp_189145_1	-0.04	0.5098
A6	Pp_175736_1	-0.04	0.3876
A6	Pp_163193_1	-0.04	0.5097
AtbZIP34	Pp_159871_2	-0.04	0.5069
QRT1	Pp_132301_1	-0.04	0.5295
CYP703A2	Pp_106848_2	-0.04	0.4236

CYP704B1	Pp_106848_2	-0.04	0.4236
A6	Pp_147889_1	-0.04	0.4266
CYP703A2	Pp_139150_1	-0.04	0.6800
A6	Pp_147889_2	-0.04	0.3791
ACOS5	Pp_115006_1	-0.05	0.3299
AtMYB103/MS188	Pp_121437_1	-0.05	0.7156
AtMYB103/MS188	Pp_126855_1	-0.05	0.3127
CALS5/LAP1	Pp_175718_2	-0.05	0.4084
CER3	Pp_177243_2	-0.06	0.3476
ACOS5	Pp_152177_2	-0.06	0.4350
QRT1	Pp_134522_1	-0.06	0.4205
QRT1	Pp_152977_2	-0.06	0.5916
CYP703A2	Pp_139150_2	-0.06	0.6477
A6	Pp_172885_2	-0.06	0.3840
CYP704B1	Pp_195286_2	-0.06	0.2773
A6	Pp_167530_2	-0.06	0.3509
CALS5/LAP1	Pp_183682_1	-0.06	0.1670
AtbZIP34	Pp_159871_1	-0.06	0.2239
QRT1	Pp_31765_1	-0.07	0.3872
A6	Pp_110742_2	-0.07	0.2550
QRT1	Pp_44780_1	-0.07	0.3778
A6	Pp_110742_1	-0.07	0.3761
AtMYB103/MS188	Pp_123689_2	-0.07	0.2574
MS1	Pp_150355_2	-0.07	0.4604
A6	Pp_172885_1	-0.07	0.2268
A6	Pp_107800_1	-0.07	0.4541
ACOS5	Pp_124849_1	-0.07	0.2555
ACOS5	Pp_124849_2	-0.07	0.3237
CYP703A2	Pp_106848_1	-0.07	0.3168
CYP704B1	Pp_106848_1	-0.07	0.3168
CYP703A2	Pp_110816_2	-0.08	0.1469
CYP704B1	Pp_110816_2	-0.08	0.1469
QRT1	Pp_132301_2	-0.08	0.2810
A6	Pp_91949_1	-0.08	0.1605
A6	Pp_113399_1	-0.08	0.2031
CYP703A2	Pp_22681_1	-0.08	0.5199
CYP704B1	Pp_195286_1	-0.08	0.2553
A6	Pp_107800_2	-0.09	0.4221
CYP704B1	Pp_180507_1	-0.09	0.5467
CYP703A2	Pp_211162_1	-0.09	0.3468
A6	Pp_59275_1	-0.09	0.0719
A6	Pp_113399_2	-0.09	0.1421
A6	Pp_60671_1	-0.09	0.4277
CALS5/LAP1	Pp_175718_1	-0.09	0.0982
CYP703A2	Pp_110816_1	-0.10	0.0901
CYP704B1	Pp_110816_1	-0.10	0.0901
AtMYB103/MS188	Pp_29378_1	-0.10	0.1128
CYP703A2	Pp_197852_1	-0.10	0.1408
CYP704B1	Pp_197852_1	-0.10	0.1408
CYP703A2	Pp_150408_2	-0.10	0.0297
A6	Pp_8713_1	-0.11	0.2022
QRT1	Pp_121267_2	-0.11	0.1814
ACOS5	Pp_209184_1	-0.11	0.4688
AtMYB103/MS188	Pp_123475_1	-0.11	0.4975
CALS5/LAP1	Pp_115455_1	-0.11	0.0834
AtMYB103/MS188	Pp_113218_2	-0.11	0.3456
QRT1	Pp_208299_1	-0.11	0.6418
CALS5/LAP1	Pp_207622_1	-0.12	0.0272
AtMYB103/MS188	Pp_123475_2	-0.12	0.4603
A6	Pp_61203_1	-0.12	0.3671
CALS5/LAP1	Pp_115455_2	-0.12	0.0847

AtMYB103/MS188	Pp_148816_1	-0.12	0.0124
AtMYB103/MS188	Pp_184923_2	-0.12	0.1743
AtMYB103/MS188	Pp_153179_1	-0.12	0.2593
QRT1	Pp_108383_1	-0.12	0.3383
AtMYB103/MS188	Pp_113218_1	-0.13	0.1504
AtMYB103/MS188	Pp_19381_2	-0.13	0.1309
AtMYB103/MS188	Pp_143649_1	-0.13	0.3784
AtMYB103/MS188	Pp_143649_2	-0.13	0.3938
RPG1	Pp_122188_2	-0.13	0.0488
QRT1	Pp_108383_2	-0.14	0.3059
A6	Pp_14679_1	-0.14	0.1454
CALS5/LAP1	Pp_183499_1	-0.14	0.0044
CYP703A2	Pp_150408_1	-0.15	0.0051
CALS5/LAP1	Pp_183499_2	-0.15	0.0089
A6	Pp_192933_2	-0.16	0.2465
A6	Pp_196989_1	-0.16	0.0117
RPG1	Pp_122188_1	-0.16	0.0392
A6	Pp_192933_1	-0.16	0.3009
AtMYB103/MS188	Pp_153179_2	-0.16	0.1446
AtMYB103/MS188	Pp_184923_1	-0.17	0.1375
CYP703A2	Pp_2770_1	-0.17	0.0049
A6	Pp_14679_2	-0.17	0.0427
AtMYB103/MS188	Pp_19381_1	-0.17	0.0635
AtbZIP34	Pp_81285_1	-0.17	0.0164
QRT1	Pp_15518_1	-0.18	0.0478
QRT1	Pp_182229_1	-0.18	0.0903
CYP704B1	Pp_168494_2	-0.19	0.0032
AtMYB103/MS188	Pp_121437_2	-0.19	0.1393
CYP703A2	Pp_115760_1	-0.20	0.0254
CYP704B1	Pp_115760_1	-0.20	0.0254
QRT1	Pp_182229_2	-0.20	0.0941
QRT1	Pp_232357_1	-0.20	0.0327
QRT1	Pp_187864_1	-0.20	0.0595
CYP703A2	Pp_115760_2	-0.20	0.0306
CYP704B1	Pp_115760_2	-0.20	0.0306
KNS2	Pp_119166_1	-0.21	0.0696
A6	Pp_90481_1	-0.21	0.0070
AtMYB103/MS188	Pp_100368_2	-0.21	0.0323
A6	Pp_196989_2	-0.22	0.0125
QRT1	Pp_187864_2	-0.22	0.0539
QRT2	Pp_193100_2	-0.22	0.1127
A6	Pp_218702_1	-0.23	0.0042
QRT1	Pp_190734_2	-0.23	0.0013
KNS2	Pp_119166_2	-0.23	0.0527
AtMYB103/MS188	Pp_111064_2	-0.24	0.0022
AtMYB103/MS188	Pp_111064_1	-0.24	0.0043
AtMYB103/MS188	Pp_100368_1	-0.24	0.0234
CYP704B1	Pp_177185_1	-0.24	0.0019
A6	Pp_54237_1	-0.25	0.0798
CYP704B1	Pp_177185_2	-0.25	0.0026
QRT1	Pp_58226_1	-0.25	0.0004
A6	Pp_122478_1	-0.26	0.0007
CYP704B1	Pp_168494_1	-0.26	0.0007
QRT1	Pp_190734_1	-0.27	0.0005
CYP703A2	Pp_188189_1	-0.30	0.0015
CYP704B1	Pp_188189_1	-0.30	0.0015
A6	Pp_122478_2	-0.30	0.0036
KNS2	Pp_188513_2	-0.32	0.0182
CYP703A2	Pp_63679_1	-0.32	0.0246
QRT1	Pp_15518_2	-0.33	0.0022
QRT2	Pp_13931_2	-0.34	0.0063

QRT1	Pp_138756_1	-0.35	0.0218
AtMYB103/MS188	Pp_27442_1	-0.36	0.0240
AtMYB103/MS188	Pp_8210_1	-0.37	0.0026
QRT1	Pp_121141_1	-0.37	0.0013
QRT1	Pp_152856_1	-0.37	0.0005
CYP703A2	Pp_188189_2	-0.37	0.0003
CYP704B1	Pp_188189_2	-0.37	0.0003
CYP704B1	Pp_105982_2	-0.37	0.0042
CYP703A2	Pp_149034_1	-0.38	0.0030
CYP704B1	Pp_149034_1	-0.38	0.0030
QRT1	Pp_152856_2	-0.38	0.0011
CYP704B1	Pp_105982_1	-0.39	0.0021
A6	Pp_8710_1	-0.40	0.0034
KNS2	Pp_188513_1	-0.42	0.0011
QRT1	Pp_121141_2	-0.42	0.0009
QRT1	Pp_138756_2	-0.43	0.0171
AtbZIP34	Pp_128606_2	-0.43	0.0001
CYP703A2	Pp_149034_2	-0.45	0.0013
CYP704B1	Pp_149034_2	-0.45	0.0013
QRT2	Pp_193100_1	-0.46	0.0181
QRT1	Pp_45683_1	-0.49	0.0086
AtbZIP34	Pp_128606_1	-0.51	0.0004
QRT2	Pp_13931_1	-0.57	0.0007
CYP704B1	Pp_116547_1	-0.61	0.0004
CYP704B1	Pp_116547_2	-0.63	0.0001
CYP703A2	Pp_172320_2	-0.65	0.0002
QRT1	Pp_79815_1	-0.65	0.0010
CYP703A2	Pp_172320_1	-0.67	0.0001
ACOS5	Pp_92121_1	-0.74	0.0000
QRT1	Pp_145945_1	-0.99	0.0002
TDE1/DET2	Pp_181942_1	-1.03	0.0001
TDE1/DET2	Pp_181942_2	-1.07	0.0002
QRT1	Pp_145945_2	-1.10	0.0002
CYP703A2	Pp_102043_1	-1.24	0.0002
CYP703A2	Pp_102043_2	-1.27	0.0002
QRT1	Pp_4364_1	-1.58	0.0000
QRT1	Pp_15580_2	-1.97	0.0001
QRT1	Pp_15580_1	-2.05	0.0001
QRT1	Pp_222560_1	-2.16	0.0001
QRT1	Pp_155350_1	-2.40	0.0001
QRT1	Pp_155350_2	-2.49	0.0001